CORRELATION OF SUSTAINABLE FLY ASH CONCRETE WITH GRADE 35 MPA COMPRESSIVE STRENGTH FOR WATER-RETAINING STRUCTURE

JESTER WONG YIE SIONG

UNIVERSITI TUNKU ABDUL RAHMAN

CORRELATION OF SUSTAINABLE FLY ASH CONCRETE WITH GRADE 35 MPA COMPRESSIVE STRENGTH FOR WATER-RETAINING STRUCTURE

JESTER WONG YIE SIONG

A project report submitted in partial fulfilment of the requirements for the award of Bachelor of Civil Engineering with Honours

Lee Kong Chian Faculty of Engineering and Science
Universiti Tunku Abdul Rahman

May 2025

DECLARATION

I hereby declare that this project report is based on my original work except for citations and quotations which have been duly acknowledged. I also declare that it has not been previously and concurrently submitted for any other degree or award at UTAR or other institutions.

Name : Jester Wong Yie Siong

ID No. : 21UEB01956

Date : 22/6/2024

COPYRIGHT STATEMENT

This final year project report is submitted in partial fulfilment of the requirements for the Bachelor of Civil Engineering with Honours at Universiti Tunku Abdul Rahman (UTAR). This final year project report represents the work of the author, except where due acknowledgement has been made in the text. No part of this final year project report may be reproduced, stored, or transmitted in any form or by any means, whether electronic, mechanical, photocopying, recording, or otherwise, without the prior written permission of the author or UTAR, in accordance with UTAR's Intellectual Property Policy.

ACKNOWLEDGEMENTS

First and foremost, I would like to express my deepest gratitude to my research supervisor, Ir. Ts. Dr. Yip Chun Chieh, for his invaluable guidance, encouragement, and constructive feedback throughout the course of this study. Their expertise and commitment were instrumental in shaping the direction and quality of this research.

I would also like to extend my sincere thanks to the technical staff from Lee Kong Chian Faculty of Engineering and Science for their assistance, particularly in providing access to laboratory equipment and resources necessary to complete the experimental work.

I am also grateful to my seniors and friends for their support, collaboration, and encouragement throughout the course of this project.

ABSTRACT

With growing global emphasis on sustainable construction practices, this study explored the use of Class F fly ash as a partial replacement for Ordinary Portland Cement (OPC) in concrete, particularly for water-retaining structures. The research investigated the compressive strength and durability performance of fly ash concrete, with and without the inclusion of a crystalline waterproofing admixture (Sika WT-220 PMY). A concrete mix design targeting 35 MPa compressive strength was first developed using the British Method prepared by Building Research Development, with a ratio of 1:0.45:1.18:2.51 (cement : water : fine aggregate : coarse aggregate). Class F fly ash sourced from Sultan Abdul Aziz Power Plant was substituted at 5 %, 10 %, 15 %, and 20 % by weight of cement in the design mix. Compression test results showed decreasing trend with increasing fly ash replacement, with 5 % being the optimal replacement which achieved the highest compressive strength of 35.86 MPa among all substitution levels. The Sika WT-220 PMY was incorporated into the concrete mix with 5 % fly ash replacement. A total of 4 different concrete mixes were prepared, which were control mix, control mix with Sika, 5 % FA mix and 5 % FA + Sika mix. Durability was assessed through initial surface absorption test (ISAT), sorptivity test, and water absorption test. All three tests showed similar results in which the incorporation of fly ash and Sika WT-220 PMY demonstrated better durability performance than plain OPC control mix. Concrete mix with 5 % Fly ash and Sika WT-220 PMY outperformed the other mix. Compared to the control mix, the optimized 5 % fly ash and Sika WT-220 PMY mix demonstrated a 26.09 % reduction in Initial Surface Absorption Test (ISAT) values, a 13.86 % decrease in the sorptivity coefficient, and a 24.56 % reduction in overall water absorption. These findings confirm the beneficial effects of fly ash and crystalline waterproofing admixtures in improving the durability performance and sustainability of concrete.

Key Words: Fly Ash Concrete, Waterproofing, Compressive Strength, Durability Performance, Sustainable Construction

Subject Area: TA401-492 (Materials of engineering and construction)

TABLE OF CONTENTS

LIST OF TABLES

LIST OF FIGURES

LIST OF SYMBOLS / ABBREVIATIONS

F	Flow Rate (ml/s)
m_c	Mass of Cement per m^3 in Trial Mix (kg)
R	Optimum Fly Ash Replacement Level (%)
Θ	Area Under Cap (m^2)
W_w	Weight of Concrete After Immersed
W_d	Weight of Concrete Before Immersed
f_m	Target Mean Strength
f_c	Characteristic Strength
s	Standard Deviation
I	Water Absorption per Unit Area
M	Mass of Absorbed Water
A	Exposed Surface Area
ρ	Density of Water
t	Time
ACI	American Concrete Institute
ASTM	American Society for Testing and Materials
BRE	Building Research Establishment
BS	British Standard
CREAM	Construction Research Institute of Malaysia
EN	European Standards
FA	Fly Ash
GHGs	Green House Gaseous
IS	India Standard
ISA	Initial Surface Absorption $(ml/\mathrm{m}^2/\mathrm{s})$
ISAT	Initial Surface Absorption Test
ITZ	Interfacial Transition Zone
MoA	Memorandum of Agreement
OD	Outer diameter
OPC	Ordinary Portland Cement
PRAH	Permeability-Reducing Admixtures for Hydrostatic
PRAN	Permeability-Reducing Admixtures for Non-Hydrostatic

SSD	Saturated Surface-Dry
SP	Superplasticizer

CHAPTER 1

INTRODUCTION

1.1 General Introduction

The development of water-resisting concrete is an outcome of human constant efforts to advance construction methods and water management, and it is a monument to human innovation and technical advancement. The concrete industry as we know it nowadays was influenced by the major developments in materials and technologies that have developed throughout the journey from ancient civilizations to the modern day.

Tracing back to ancient Greece, cementitious materials such as lime and volcanic ash had already been utilized by Greeks to produce pozzolanic binders, which were used to build infrastructure and structures at that time. They discovered that the Santorin earth found on Santorini Island, was rich in silica-alumina and could produce mortar with hydraulic characteristics when mixed with lime that allows concrete to harden both underwater and in the air (Zitzman, 2020). This mix composition was used by the Greeks as a protective layer for structures made of unburned bricks as it could sustain wet conditions and have greater durability. This can be proved by Archaic Cistern shown in Figure 1.1, which is the water storage reservoir built by Greeks in Ancient Kamiros that has remained a good physical structure and still yields a compressive strength of about 13.5 MPa (Koui & Ftikos, 1998). This makes Greeks the founder of the concrete that can set underwater.

Figure 1.1: Archaic Cistern Built by Greeks (Limited, 2010).

Nevertheless, it was the Roman people who truly pioneered the application of concrete in water-retaining structures. When the Roman Empire conquered Greek Empire, they improvised the Greeks' cement mix composition by replacing sand with pozzolana (Zitzman, 2020), producing a more durable and water-resisting concrete known as "opus caementicium" or "roman concrete" (Lymm Construction, 2023) as shown in Figure 1.2. Not only was the roman concrete being utilized in the building of the famous Pantheon Dome (Figure 1.3), it was also used in the building of Sebastos harbour at Caesarea Maritima (Figure 1.4), the first ever harbour that was built directly out into the sea (Bergin, 2018). Even though the Roman concrete had proved to be a success, but with the fall of Roman Empire, most of the concrete technology and knowledge at that time had been forgotten and vanished through time. However, the Roman's principle of substituting the sand with pozzolans significantly impacted concrete technology and revolutionized the modern concrete industry.

Figure 1.2: Opus Caementicium (Camarasa, 2014).

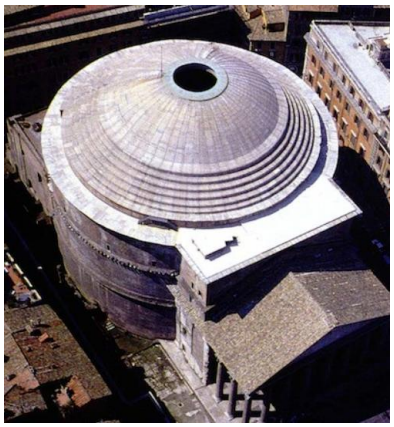

Figure 1.3: Pantheon Dome (Gromicko and Shepard, 2011).

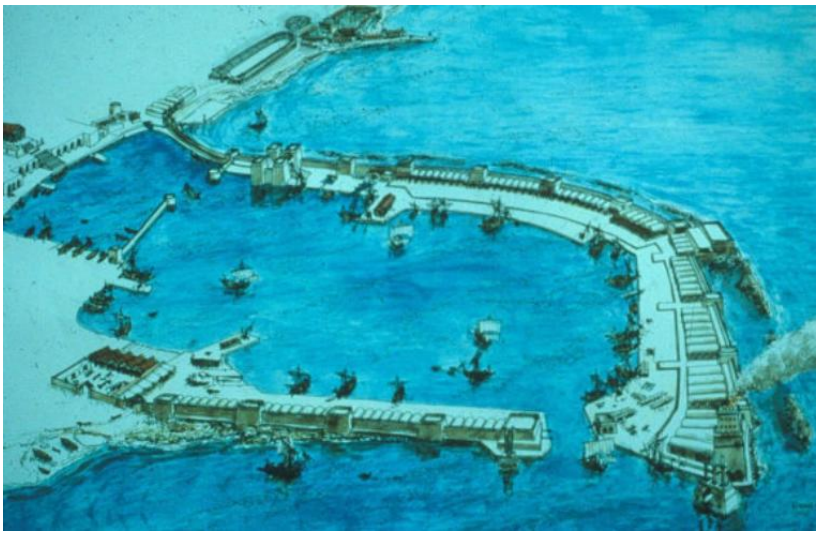

Figure 1.4: Sebastos Harbour at Caesarea Maritima (Bergin, 2018).

In the mid-1900s, inspired by the Romans' principle of substituting materials in mix compositions, researchers at the University of California pioneered the utilisation of fly ash (Figure 1.5) as a cement replacement (E. Davis et al., 1937). Since then, fly ash has gradually become an essential component in concrete, contributing to improved durability and sustainability. Its significance is evident in large-scale construction projects, such as the Burj Khalifa in Dubai (Figure 1.6), where a fly ash replacement level of 13–20 % was used in the building's concrete mixes (Aldred, 2010).

Figure 1.5: Fly Ash (Dale, 2023).

Figure 1.6: Burj Khalifa (Aldred, 2010).

Now in the 21st century, as the world population has reached its new peak of more than 8.1 billion population (Macrotrends, 2024), the rising demand for residential, non-residential building and urbanization is expected to increase the need of Portland cement. According to the statistics done by Madhumitha Jaganmohan (2024), the world's cement production was projected to reach 4.1 billion tons whereby the overall amount of cement manufactured globally in 1995 was only 1.39 billion tons, reflecting how rapidly the cement industry has expanded since then as shown in Figure 1.7. However, large-scale production of cement raises major environmental concerns, including high energy consumption, CO_2 emissions as well as global warming. To mitigate these impacts, the industry has increasingly explored alternative materials such as fly ash which can reduce cement consumption while maintaining concrete performance.

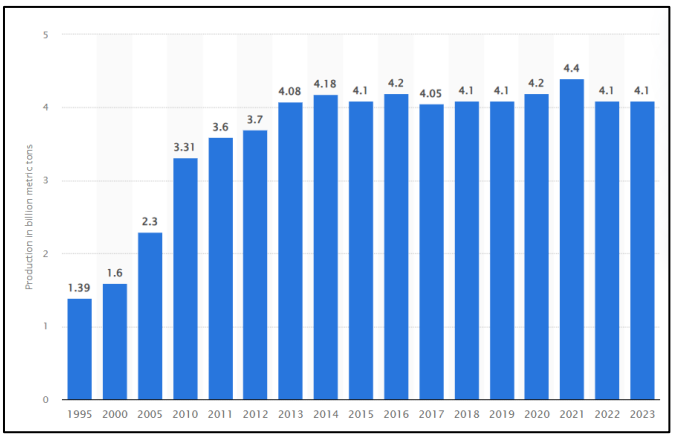

Figure 1.7: Global Cement Production from 1995 to 2023 (Madhumitha Jaganmohan, 2024).

1.2 Importance of the Study

This study examines the optimum quantity of fly ash replacement in cement with water-resisting admixture that can obtain compressive strength of 35 MPa as well as the surface absorption and durability of the concrete. The data acquired from this lab experiment could serve as an important reference for the industry designers and engineers, especially in marine concrete industry. The carbon footprint of these projects could be significantly lowered by using fly ash, a by-product produced from coal combustion, in part as a replacement for cement. This methodology further improves ecological sustainability and capitalizes on fly ash's advantageous characteristics to increase the strength and durability of concrete in marine constructions. Thus, this study has the potential to significantly contribute to the advancement of environmentally friendly building techniques in the maritime sector.

On top of that, partial substitution of cement with fly ash is also significant to the construction industry as Malaysia government has been emphasizing and promoting the concept of sustainable construction through the implementation of the Twelfth Malaysia Plan in which Malaysia aims to attain net-zero emissions of greenhouse gases (GHGs) by 2050 (Devan, 2023). The importance of fly ash concrete could be seen through the Memorandum of Agreement (MoA) signed between the Construction Research Institute of Malaysia (CREAM) and ACE Greencemt Venture (M) Sdn. Bhd, the largest fly ash supplier in Malaysia, that aims to examine the microstructural characteristics and long-term durability of fly ash concrete (Adlina, 2024). Therefore, the usage of fly ash in concrete is crucial for cement manufacturers and developers to correspond with the government policy and seize the early opportunities in the green building market.

1.3 Problem Statement

As 35.51 % of the global electricity generator power plants are still relying on coal combustion to provide energy (Our World in Data, 2024), a high amount of coal combustion waste such as fly ash is produced. Even though fly ash which is the by-product of coal combustion has been incorporated into the construction of massive buildings such as Burj Khalifa, however it is rarely been used in the building of modern water-retaining structures. As water-retaining structures

expect higher durability and strength requirements than normal buildings, design mix proportion of fly ash concrete must be carefully designed to achieve a certain level of strength in order to meet the requirement stated in the code of construction to ensure the integrity and strength of the water-retaining structure.

Furthermore, carbon dioxide produced from the manufacturing of Portland cement is accounted for approximately 7 % of global CO_2 emissions, making this sector one of the major emitters of greenhouse gaseous (Belaid, 2022). To account for this issue, University of California has done research regarding the utilization of fly ash as a partial replacement of cement. However, the suitable amount of fly ash replacement is specific and varies according to the fly ash's physical and chemical properties. This is important especially in the construction of water-retaining structures as the fly ash will be mixed with other chemical admixtures to produce water-resisting properties. An inappropriate amount of fly ash can produce unwanted chemical reactions which might end up with undesired strength and durability of the fly ash concrete.

A significant challenge faced by Malaysia and other developing countries is the gradual yet persistent increase in the price of cement, driven by factors such as rising energy costs, limited availability of raw materials, increasing global market demand, and stricter environmental regulations on carbon emissions. This economic trend is placing financial strain on the construction industry and threatens the feasibility of large-scale water-retaining structures such as dams and reservoirs that demand high-performance and durable concrete. As cement prices continue to rise, there is a growing need to identify and evaluate sustainable alternatives such as fly ash to partially replace OPC without compromising the structural integrity, strength, and durability of concrete.

Other than that, due to its location around the equator, Malaysia experiences consistent and high-intensity rainfall throughout the year with a high mean annual precipitation of 2540 millimetres in Peninsular Malaysia (Lockard and Zakaria Bin Ahmad, 2019). This subsequently increases the volume as well as the flow velocity of river water which compromises the durability of the water-retaining structure, especially those made with conventional plain OPC concrete. Even though fly ash has been used as cement replacement to increase the strength of the water-retaining structures, however

there is a lack of comprehensive performance data concerning the behaviour of Grade 35 fly ash concrete in constantly water-exposed environments.Other than that, due to the location around equator, Malaysia experiences consistent and high-intensity rainfall throughout the year with a high mean annual precipitation of 2540 millimetres in Peninsular Malaysia (Lockard and Zakaria Bin Ahmad, 2019). This subsequently increase the volume as well as the flow velocity of river water which compromise the durability of the water-retaining structure, especially those made with conventional plain OPC concrete. Even though fly ash had been used as cement replacement to increase the strength of the water-retaining structures, however there is a lack of comprehensive performance data concerning the behaviour of Grade 35 fly ash concrete in constantly water-exposed environments.

1.4 Aim and Objectives

This study aims to innovate and obtain the mix proportion for sustainable fly ash concrete with replacement of cement to obtain the desired compressive strength. The main objectives that will achieve the aim are as follows:

(i) To design mix proportion of grade 35 MPa concrete compressive strength.

(ii) To determine the ideal amount of the fly ash replacement in cement with water resisting admixture to achieve grade 35 MPa compressive strength.

(iii) To examine the waterproofing and surface absorption of the concrete.

1.5 Scope and Limitation of the Study

A trial mix should first be designed to obtain trial mix concrete with a compressive strength of 35 MPa (Grade C35/42). Then, ISAT, Water Absorption Test and Sorptivity Test are to be conducted to determine the surface water resistance of concrete that has been partially substituted with fly ash for cement and has water-resistant admixture added to it. Nevertheless, the optimum amount of fly ash substitution for cement is to be determined before the start of every test.

One of the limitations of this study is that the resources and period available are insufficient. The curing process of concrete is known to consume most of the time, ranging from 7 days to 28 days for the concrete to cure to develop strength. However, since trial and error processes are unavoidable in designing a trial mix of grade 35 MPa, much time is needed for the repetitive process of raw material mixing, moulding, demoulding, and concrete curing until concrete with desired strength is produced. The plastic concrete mould that is easier to demould concrete compared to steel concrete mould is also limited, making no choice but to proceed with the steel concrete mould that requires a longer time to demould.

In terms of data and information, even though fly ash concrete has a well-known reputation for long durability, there is limited data and evidence of the performance of Grade 35 fly ash concrete in water-retaining structures over decades. More in-depth research would have to be done to comprehend the complete performance of the fly ash concrete that was exposed in the wet environment over many years.

In addition, as all the test is carried out under controlled conditions, it may not be the actual representation of the real environment. Factors such as water purity, humidity and temperature are all constant throughout the test. The fly ash concrete samples are also made on a smaller scale for laboratory testing which may neglect the possible variation of fly ash properties when it is used in an extremely high amount in real-world construction.

Lastly, there is absence of steel reinforcement in this study of fly ash concrete which could lead to different results when compared to the real construction situation whereby fly ash concrete normally consists of steel reinforcement that provides tensile strength.

1.6 Contribution of the Study

This study provides a comprehensive understanding on the physical, chemical, and pozzolanic reaction of fly ash, highlighting its potential as a partial cement substitution in concrete mix design for water-retaining structures. By analysing the effects of fly ash in both fresh and hardened states of concrete, the research sheds light on the function of fly ash in the construction of water-retaining structures. This knowledge not only supports the optimization of mix

proportions for improved performance but also opens new avenues for the development of innovative and sustainable construction materials. These materials have the potential to achieve higher quality, greater durability, and lower environmental impact at a reduced cost, aligning with global efforts to promote greener and more cost-effective building practices.

The experiments conducted in this research provide critical data on the suitability of fly ash as a cement substitute specifically for water-retaining structures, where durability and impermeability are of paramount importance. Key performance indicators such as surface durability, capillary performance, overall permeability, and compressive strength of fly ash concrete are evaluated. The findings serve as a reference point for identifying the optimum replacement percentage and could contribute to the development of guidelines or standards for the safe and effective use of fly ash in such applications.

Beyond water-retaining structures, the results of this study can also be extended to other infrastructure projects that demand high-performance and durable concrete, such as bridges, tunnels, and retaining walls. Widespread adoption of these findings not only broadens the practical application of fly ash in various structural contexts but also promotes more economical and environmentally responsible practices within the construction industry.

1.7 Outline of the Report

There will be a total of 5 chapters in this report which are introduction, literature review, methodology, results and conclusion. The end of the report will be the references.

Chapter 1 is the introduction of this study, which includes the evolution of the cement used in water-retaining structures, how traditional construction knowledge impacts modern cement technology and the growth of cement production. The next subchapter covered the importance of this study in how this study can help the construction industry nowadays to move towards sustainable development by integrating useful waste material in the construction of water-retaining structures. Aims and objectives as well as problem statements are included to clearly specify the direction, goal, and extent of this study. The contribution of the study is also included in this chapter describes how this study

can provide valuable insights to the industry and other researchers regarding the use of sustainable material in water-retaining structures.

Chapter 2 is the literature review on the specific topic related to this study, including properties of fly ash, effect of fly ash, optimum fly ash replacement, waterproofing approaches, effect of hydrostatic pressure, etc. The numerous studies and strategies employed in these fields by various authors will also be reviewed in this chapter, particularly the testing techniques, mix design methods and compositions, and the application of water-resistant admixtures.

Chapter 3 is the methodology and work plan of this study. Operational workflow is provided to organise the steps and procedures of each experiment process. The trial mix is designed according to Grade 35 and the proportion of each material is calculated. Each material used in this study is discussed to ensure the material specification complies to the respective standard. The casting operation and curing process are explained in detail to ensure the consistency of the results. Ultimately, standard testing is conducted according to the ASTM and BS standards to ensure the validity of the results obtained. The testing includes compressive strength test, water absorption test, sorptivity test and initial surface absorption test (ISAT).

Chapter 4 presented and analysed the data obtained throughout the experiment. It began by examining the workability and density of concrete with varying amounts of fly ash substitution. Following this, the compressive strength of both the trial mix and the concrete samples with different levels of fly ash substitution was analysed. The optimum fly ash content was determined as the percentage that produced the highest compressive strength among the tested substitutions. Additionally, the results of Initial Surface Absorption Test (ISAT) were discussed, focusing on the combined effects of fly ash and waterproofing admixture on concrete permeability. Finally, the outcomes of the water absorption test and sorptivity test were presented, comparing the mass of water ingress across different concrete samples.

Chapter 5 presented a comprehensive summary of the research findings, demonstrating that the collected data met the study's aims and objectives. It also provided recommendations for future studies, offering guidance for researchers exploring similar topics or seeking to expand on the results of this work.

CHAPTER 2

LITERATURE REVIEW

2.1 Introduction

Concrete, primarily consisting of cement, water, aggregates (gravel and sand), and occasionally admixtures, is one of the most extensively utilized building materials worldwide. For many different construction applications ranging from large-scale infrastructure projects to residential structures, this conventional concrete composition has proven to be reliable and adaptable. However, conventional concrete has some vital limitations in the construction of water-retaining structures, such as low surface durability, insufficient strength and vulnerability to water penetration.

Therefore, as the construction industry searched for more durable and stronger materials for water-retaining structures, fly ash was discovered and incorporated into the conventional concrete along with waterproofing admixture to modify the properties of the conventional concrete for water-retaining structures construction.

In this chapter, research journal articles regarding the concrete materials used in water-retaining structures are studied to investigate the impacts of fly ash substitution and the addition of waterproofing admixtures. Experiments done by other researchers are studied and the result obtained is analysed to further discover the properties of the materials used in fly ash concrete. Various standard tests are also to be reviewed to understand the methodology used in conducting the standard test.

2.2 Cement

2.2.1 Production of Cement

The wet process and the dry process are the two primary methods used in the manufacture of cement. Raw materials including clay and limestone are combined with water to produce a slurry in the wet process. This slurry is subsequently ground finely and heated in a rotary kiln to evaporate the water in the slurry. On the other hand, the dry method grinds raw materials into a fine powder, which removes the need for water. Prior to being calcined in a rotary

kiln, this powder is heated using kiln gases. In contemporary cement factories, the dry process is the preferred approach since it eliminates the requirement to evaporate water, making it significantly more economical and energy efficient. Additionally, it emits fewer emissions, which better satisfies the environmental pollution concerns. Cement manufacturing generally consists of four major stages which are quarrying, preparation of raw material, clinkering and cement preparation which can be seen in Figure 2.1.

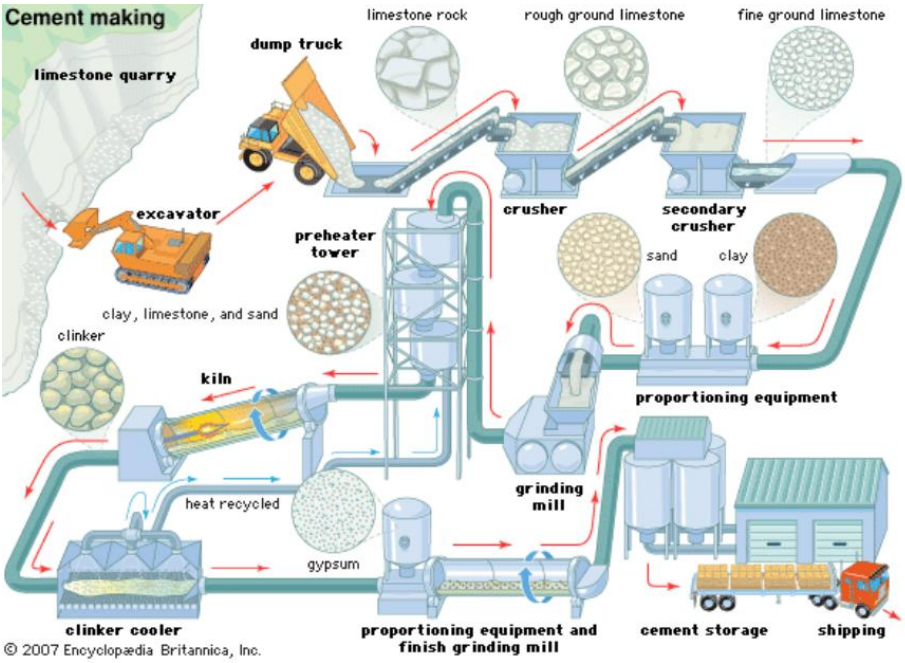

Figure 2.1: Cement Manufacturing Process (CivilDigital, 2013).

After extraction, the raw materials such as limestone and clay are crushed, ground, and mixed together inside the grinding mill. The ground raw meal is fed into a preheater tower where the material is heated by exhaust gases from the kiln. Then, the heated materials are transferred into rotary cement kiln to be burnt at a temperature of 1,450 degrees Celsius and cooled. During this heating and cooling process, the materials undergo calcination process and clinkering process that aims to reshape the raw materials into fine grey spherical shaped nodules with a diameter of 5 to 25 mm (Lavagna and Nisticò, 2022). The cement clinker produced contains four important minerals which are Tricalcium Aluminate (C_3A), Alite (C_3S), Belite (C_2S), and Tetracalcium alumino-ferrite (C_4AF) (Schumacher and Juniper, 2013). Lastly, the cooled cement clinker (Figure 2.2) is added with gypsum and grind to produce Portland cement.

Figure 2.2: Cement Clinker (Anahita D'Souza, 2020).

In Malaysia, the cement produced is separated into 7 types according to the ASTM C150 standard. Type I cement is the most common type of Portland cement and mainly used in construction where no specific requirement is needed. Type II cement has moderate sulphate resistance and Type III cement has high early strength. Type IV cement has low heat of hydration and is used to minimize thermal cracking. Similar to Type II cement, Type V cement is of high sulphate resistance which provides the highest sulphate resistance among all types due to low C_3A content. Among all the types of cement mentioned, Type I cement is the most common cement used in Malaysian construction. Table 2.1 shows the chemical composition of typical Type I OPC.

Table 2.1: Chemical Composition of Type I OPC (Xie, Cheng and Wan, 2019).

Compound	Weight (%)
$\mathbf{CaO}$	63.82
$\mathbf{SiO_2}$	20.09
$\mathbf{Al_2O_3}$	3.87
$\mathbf{SO_3}$	3.50
$\mathbf{Fe_2O_3}$	1.69
$\mathbf{MgO}$	2.22
$\mathbf{K_2O}$	0.39
$\mathbf{Na_2O}$	0.30
$\mathbf{TiO_3}$	0.16
$\mathbf{MnO}$	0.05

2.2.2 Carbon Dioxide Emission from Cement Production

The cement industry has long been recognized as one of the largest sources of global CO_2 emissions, largely due to its energy-intensive processes and reliance on carbonate-rich raw materials. On average, approximately 900 kg of carbon dioxide (CO_2) is emitted for every ton of cement produced (Bakhtyar, Kacemi and Nawaz, 2017). The high carbon footprint of cement production stems from the combination of two of the three primary sources of anthropogenic CO_2 emissions which are carbonate decomposition and oxidation of fossil fuels.

Approximately 60 % of the raw material used in cement production is composed of carbonate minerals which are predominantly limestone ($CaCO_3$). When limestone is subjected to a high temperature of 900 °C during calcination, it chemically decomposes into lime (CaO) and carbon dioxide (CO_2). This reaction is necessary for producing clinker, the principal ingredient in Portland cement. The CO_2 released during this process is classified as process emissions, which are inherent and unavoidable in traditional cement chemistry (Sousa and Bogas, 2021). These emissions alone are responsible for an estimated 5 to 8 % of total global anthropogenic CO_2 emissions, excluding those related to land-use change.

The second major contributor to CO_2emissions is the combustion of fossil fuels required to generate the extremely high temperatures (up to 1450 °C) needed to form clinker. Fuels such as coal, petroleum coke, and natural gas are commonly used in the kiln to maintain these temperatures. The direct combustion of these fuels produces significant CO_2 emissions, commonly referred to as energy emissions (Sousa and Bogas, 2021). While advancements in energy efficiency can reduce the quantity of fuel needed per tonne of cement, the industry remains heavily dependent on fossil fuels, making this source a persistent challenge.

In addition to these major sources, a smaller share of CO_2 emissions comes from indirect activities. These include the electricity used to power equipment for grinding, raw material handling, conveying, as well as transportation emissions related to moving raw materials from quarries to the plant (Sousa and Bogas, 2021). Though relatively minor in comparison, these

indirect emissions still contribute to the overall carbon footprint of cement manufacturing.

In conclusion, the cement industry faces growing pressure to address its significant contribution to global CO_2 emissions, which stem largely from the calcination of limestone and the combustion of fossil fuels during clinker production. The shift toward low-carbon cement is not only a technical innovation but also a vital step toward achieving international climate goals and sustainable construction practices. Adopting partial substitution of OPC with supplementary cementitious materials such as fly ash is one of the most effective strategies as fly ash not only reduces the need for cement but likewise enhances certain properties of concrete. Moreover, the use of fly ash also supports a circular economy by repurposing industrial by-products that would otherwise contribute to waste streams.

2.2.3 Hydration of Ordinary Portland Cement

Ordinary Portland Cement hydration refers to the exothermic chemical reaction that occurs when cement is mixed with water. By understanding the hydration of cement, engineers can manage setting periods, optimize mix designs for desired strength, and guarantee appropriate curing to improve durability. Furthermore, it likewise aids in controlling the heat produced during hydration, which is important to avoid thermal cracking in the construction of large water-retaining structures.

This process involves multiple concurrent single chemical reactions between water and the key minerals of the cement and is important to concrete as it determines the strength and durability of the concrete. According to the research done by Nelson (1990), the cement hydration period is separated into 5 phases based on the heat of hydration which are phase I (pre-induction period), phase II (induction period), phase III (acceleration period), phase IV (deceleration period) and phase V (diffusion period). Figure 2.3 shows the separation of phase of the cement hydration according to heat of hydration.

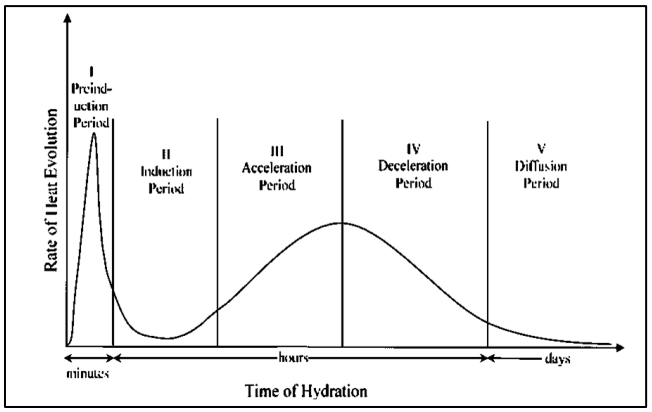

Figure 2.3: Phases of Hydration Process (Nelson, 1990).

When the cement is mixed with water, Alite (C_3S) undergoes dissolution at the surface area and releases silicate and hydroxyl ions that will react with calcium ions. As the dissolution of the C_3S is greater than the diffusion of ion, the liquid phase becomes saturated and the precipitation of this phase forms a low-density layer of calcium silicate hydrate ($C_3S_2H_3$ or $C-S-H$) as shown in Figure 2.4 around the cement grain along with calcium hydroxide ($Ca(OH)_2$) (Lavagna and Nisticò, 2022). The rapid chemical reaction of Alite is responsible for the initial strength of the concrete and this reaction can be written as $2C_3S + 6H_2O \rightarrow C_3S_2H_3 + 3Ca(OH)_2$. Meanwhile, a small amount of Belite (C_2S) likewise interacts with water, but at a slower speed, and this contributes to the concrete's long-term strength. Gypsum that is added into the cement will react with Tricalcium Aluminate (C_3A) to produce Ettringite and subsequently Monosulphate. All these reactions produce heat that makes up phase I.

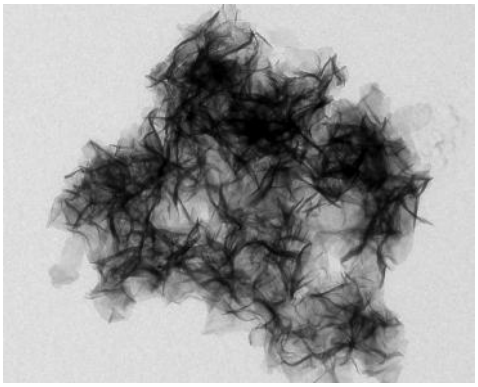

Figure 2.4: Transmission Electron Microscopy (TEM) images of C-S-H (Kumar et al., 2017).

After the rapid hydration of cement at phase I, the rate of heat of hydration becomes significantly slower in phase II (induction period). There are two major theories that can explain this scenario. The first one is Protective Membrane Theory. It suggested that the metastable C-S-H layers covered the surface of dissolving C_3S, preventing the dissolution of C_3S (Lavagna and Nisticò, 2022). Another theory which is the Theory of Dissolution states the solution is over-saturated with calcium hydroxide ($Ca(OH)_2$), thus reducing the dissolution rate of silicate species and subsequently lowers the heat of hydration (MacLaren and White, 2003). This induction period is important as it allows the fresh cement paste to remain workable for a period of time before setting and enables fresh concrete to be transported from factory to the construction site (Vipin Kant Singh, 2023). However, although these two theories are mainly used to explain this situation, there are insufficient experimental data that can further prove the validity of these two theories.

In phase III, the heat of hydration rises again as the hydration of C_3S accelerates again. C_2S also undergoes hydration but at a slower rate. According to the model done by Tennis and Jennings (2000), two layers of C-S-H are formed, and each layer has a different density in which the low-density layer formed the outer C-S-H layer while high-density layer forms the inner C-S-H layer which can be seen in Figure 2.5. The outer C-S-H layer is formed during the early hydration process whereas the inner C-S-H layer is formed during late hydration process. When compared to outer C-S-H layer, inner layer has low porosity and increases when the water-to-cement ratio decreases.

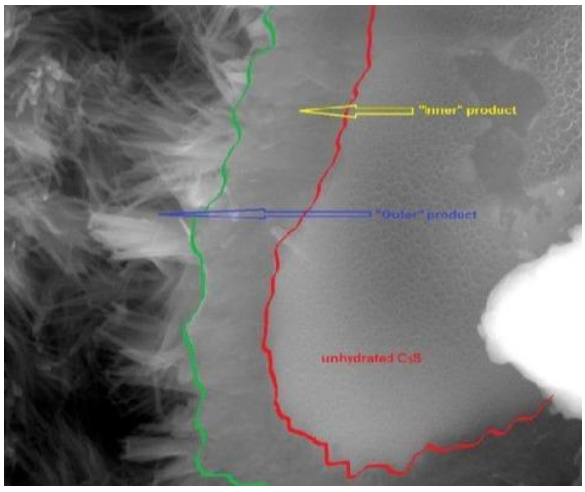

Figure 2.5: Inner and Outer C-S-H layer (Lavagna and Nisticò, 2022).

In addition, calcium hydroxide reached its maximum concentration and started to precipitate into crystalline calcium hydroxide, which is also known as Portlandite as shown in Figure 2.6 (MacLaren and White, 2003). Portlandite is one of the major products of cement hydration that occupies 27 % of the paste volume and is responsible for maintaining the alkalinity of the cement and resisting carbonated-induced corrosion (Salah et al., 2022). Nevertheless, the dissolution of Portlandite would facilitate the degradation of concrete which may cause significant safety issues, especially to the water-retaining structures that contact with water (Ruiz-Agudo et al., 2013).

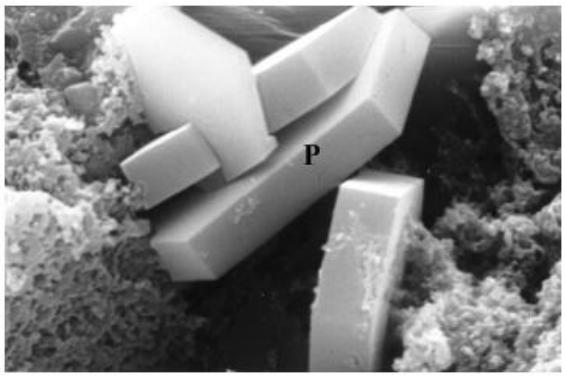

Figure 2.6: Portlandite (Aïtcin, 2016).

Lastly at phase IV and V, which is also known as post-acceleration period, the liquid phase becomes saturated with C-S-H and eventually covers up all the surface area of the cement grain, causing the reduction of hydration heat. Figure 2.7 shows the cement component after 7 days of hydration.

Figure 2.7: Cement After 7 days of Hydration (Lavagna and Nisticò, 2022).

2.2.4 Curing of Concrete

The curing of concrete is the process of maintaining adequate moisture, temperature, and time conditions to allow the cement in the concrete to properly hydrate and gain strength. Proper curing is essential for achieving the desired properties of concrete, such as strength, durability, and resistance to shrinkage and cracking. Not only that, the curing process also improves the water resistance, abrasion resistance and volumetric stability of the concrete (Akinwumi and Gbadamosi, 2014).

There are several curing methods used in the industry such as membrane curing, polythene sheet curing and steam curing. Nonetheless, water submerged curing (Figure 2.8) is the most popular curing method as it is cheap, abundant, and easy to conduct. The curing period varies depending on the type of cement used. As per the standard set by American Concrete Institute (ACI) Committee 301, the minimum curing period should be a period of time when the concrete can achieve a minimum of 70 % of the specified compressive strength, which is usually 7 days (Zemajtis, 2018). A longer curing period generally produces concrete with higher compressive strength compared to shorter curing periods. This phenomenon is attributed to the continuous hydration process of the cement, which generates more calcium silicate hydrate (C-S-H) gel, the primary binding agent responsible for concrete's strength.

Figure 2.8: Water Submerged Curing (Rahimi et al., 2023).

According to the concrete compressive strength test done by Rahimi et al. (2023) using the Type I cement, the concrete was able to attain 19.03 MPa

which was 70 % of the 27 MPa required compressive strength after 7 days of curing. The concrete took 28 days curing to achieve the compressive strength of 28.29 MPa which was higher than the required compressive strength of 27 MPa as shown in Table 2.2. This result indicates that the minimum curing period for concrete using Type I cement is 7 days. However, the compressive strength results of this experiment were only applicable to Qayen cement produced in Iran. Another experiment may have different results despite same curing time due to different chemical compositions of cement and experimental conditions.

Table 2.2: Results of Compressive Strength (Rahimi et al., 2023).

Specimen	Curing Time (day)	Compressive Strength (MPa)	Mean Strength (MPa)	Required Design Strength (MPa)
$S_{1,1}$	7	18.84	19.03	17.55
$S_{1,2}$	7	19.92		
$S_{1,3}$	7	18.33		
$S_{1,10}$	28	29.20	28.29	27.00
$S_{1,11}$	28	28.46		
$S_{1,12}$	28	27.22		

2.3 Coal Fly Ash

2.3.1 Production of Coal Fly Ash

Fly ash, which is also known as coal fly ash, is a heterogenous byproduct produced from the coal combustion process in thermal power plants. The general process of coal-powered electrical generation stations can be seen in Figure 2.9.

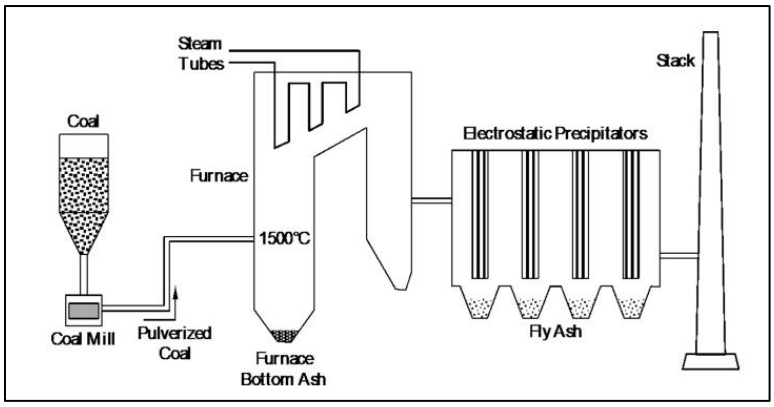

Figure 2.9: Coal-fired Electrical Generating Station (Thomas, 2013).

At first, the pulverized coal is blown into the furnace and burned at a high temperature of 1500 ℃. During this process, the non-combustible components of coal such as calcium oxide, iron oxide, alumina and silica are melted and form molten mineral residue (Nayak et al., 2022). When cooled, the molten residue hardens, and ash is produced. Due to gravity, the heavier and coarser ash falls to the bottom of the furnace and is known as bottom ash. Meanwhile, the lighter and finer ash is carried away by the flue gas into the electrical precipitators where the ash is filtered (Yousuf et al. 2020). Therefore, it is known as fly ash since it 'fly' away from the furnace. Figure 2.10 shows the images of typical fly ash and bottom ash. Due to the lightweight and fine size, fly ash can be easily transmitted through air and may cause respiratory diseases such as asthma, inflammation and immunological reactions when inhaled.

Figure 2.10: Fly Ash and Bottom Ash (The Constructor, 2022).

2.3.2 Physical Properties of Coal Fly Ash

Understanding the properties of coal fly ash is crucial as they directly influence the quality and performance of concrete with fly ash replacement. Fly ash typically appears as a silty material made up of fine spherical particles, with sizes ranging from 0.01 to 100 μm. This spherical morphology contributes to improved workability in concrete mixes. The bulk density of fly ash ranges from 0.54 to 0.86 g/cm^3, classifying it as low to medium density, while its specific gravity ranges between 1.3 and 2.9, indicating its relatively lightweight nature (Nele De Belie et al., 2018).

Additionally, fly ash has a high specific surface area of 300-500 m^2/kg, as measured by Blaine's Air Permeability Method nature (Nele De Belie et al., 2018). This large surface area enhances its reactivity, particularly in pozzolanic reactions, where fly ash combines with calcium hydroxide to form additional

calcium silicate hydrate (C-S-H), thereby improving the concrete's strength and durability over time. These unique properties make fly ash a valuable supplementary cementitious material in concrete production, contributing to both performance enhancement and environmental sustainability. The physical properties of fly ash summarised in Table 2.3.

Table 2.3: Summarized Typical Physical Properties of Fly Ash.

Physical Properties	Value
Particle Shape	Spherical
Particle Size	$0.01 - 100$ μm
Bulk Density	$0.54 - 0.86$ g/cm^3
Specific Gravity	$1.3 - 2.9$
Surface Area	$300 - 500$ m^3/kg

2.3.3 Chemical Properties of Coal Fly Ash

In terms of chemical properties, fly ash mainly consists of SiO_2, Fe_2O_3, Al_2O_3 and CaO and the amount of each chemical composition changes according to the type of coal used in combustion. Fly ash pH value ranges from 1.2 to 12.5 with most of the fly ash being alkaline (Yao et al., 2015). Fly ash pH value is mainly based on the ratio of Ca to S whereby a higher Ca/S ratio results in higher pH value. When compared to low-pH fly ash, alkaline fly ash tends to have higher electrical conductivity as it contains greater amount of dissolved salt.

According to the standard set by American Society for Testing Materials (ASTM C618), fly ash is classified into 2 classes which are Class C and Class F based on the amount of oxide present. Class C fly ash is the byproduct generated from the combustion of sub-bituminous or lignite coal which contains 50 % to 70 % of SiO_2, Al_2O_3 and Fe_2O_3 and over 10 % of CaO. The surface of Class C fly ash appears to be cellular and irregular which can be seen in Figure 2.11 (a). Class F fly ash, on the other side, is produced from either bituminous or anthracite coal combustion which has over 70 % of SiO_2, Al_2O_3 and Fe_2O_3 and less than 10 % of CaO. Class F fly ash has a smooth surface texture and spherical morphology as shown in Figure 2.11 (b) (Jiao et al., 2017).

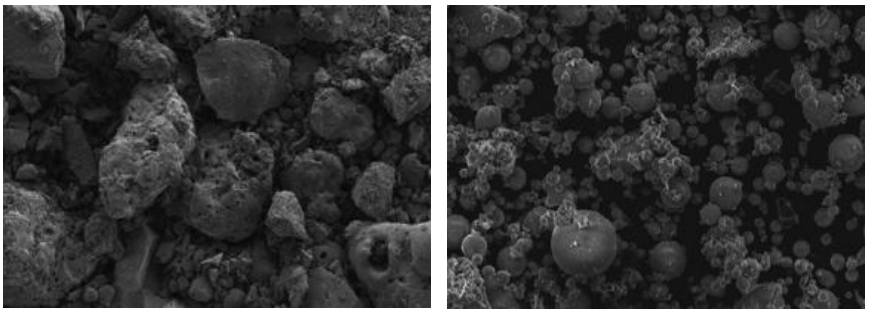

(a) (b)

Figure 2.11: (a) Surface of Class C Fly Ash Particle, (b) Surface of Class F Fly Ash Particle (Jiao et al., 2017).

Another difference between Class C and Class F fly ash is the colour as shown in Figure 12. Class C fly ash is lighter in colour due to its lower unburned carbon content, while Class F fly ash is darker, reflecting its higher carbon residue. This difference in composition and appearance is also evident in their chemical composition, as shown in Table 2.4.

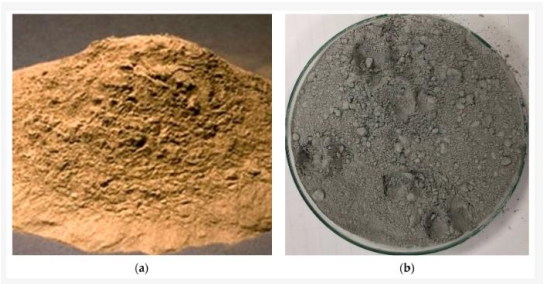

Figure 2.12: (a) Class C Fly Ash, (b) Class F Fly Ash (Akbulutet al., 2024).

Table 2.4: Typical Chemical Composition of Class C and Class F Fly Ash (Wang et al.,2024).

Compound	Class C (Wt %)	Class F (Wt %)
$\mathbf{SiO_2}$	$33.00 - 43.65$	$41.60 - 60.00$
$\mathbf{Al_2O_3}$	$19.39 - 23.14$	$17.74 - 29.45$
$\mathbf{Fe_2O_3}$	$1.46 - 5.91$	$4.88 - 25.40$
$\mathbf{CaO}$	$21.80 - 27.66$	$1.25 - 9.30$
$\mathbf{MgO}$	$4.86 - 5.64$	$0.20 - 0.90$
$\mathbf{K_2O}$	$0.47 - 2.08$	$1.90 - 2.79$
$\mathbf{Na_2O}$	$1.38 - 3.70$	$0.36 - 0.88$

2.3.4 Application of Class C and Class F Fly Ash

The performance and application of Class C and Class F fly ash in concrete differ due to their chemical compositions, pozzolanic reactivity, and cementitious properties. These differences make each type of fly ash suitable for specific construction requirements.

Class C fly ash is characterized by its high calcium oxide (CaO) content, which gives it both pozzolanic and self-cementitious properties. This means it can react with water independently, without relying entirely on calcium hydroxide ($Ca(OH)_2$) from cement hydration. As a result, Class C fly ash is known for its ability to promote rapid early strength development (McCarthy and Dryer, 2019). This feature makes it particularly useful in time-sensitive applications such as road pavements, airport runways, and repair works where quick setting and strength gain are crucial.

In terms of durability, Class C fly ash provides moderate resistance to chemical attacks. However, it is less effective than Class F fly ash in mitigating sulphate attack and alkali-silica reactions due to its lower silica content and higher calcium oxide levels. As a result, Class C fly ash is typically used in environments with less aggressive chemical exposure, such as residential and commercial building construction.

Moreover, Class F fly ash is predominantly pozzolanic, as it contains lower calcium oxide levels but a higher percentage of silica (SiO_2). Unlike Class C fly ash, it cannot react with water independently but relies on calcium hydroxide produced during cement hydration to activate its pozzolanic reaction (Hemalatha and Ramaswamy, 2017). This slower reaction leads to a gradual but more robust development of strength and durability over time. Results from Uysal and Akyuncu (2012) showed that concrete with Class C fly ash generally has higher 28-day strength but lower 90-day strength than concrete with Class F fly ash.

The high silica content of Class F fly ash also improves the microstructure of concrete by forming additional calcium silicate hydrate (C-S-H) over time, which reduces porosity and enhances both strength and durability. This characteristic makes it highly effective in reducing the permeability of concrete, thus minimizing the ingress of harmful substances like chloride ions.

Consequently, Class F fly ash is widely utilised in marine and coastal structures, bridges, and infrastructure exposed to salts or seawater.

Another key advantage of Class F fly ash is its low heat of hydration, which makes it suitable for mass concrete applications. Large structures like dams and thick foundations benefit from the controlled temperature rise during curing, which reduces the risk of thermal cracking. Consequently, Class F fly ash is favoured in maritime projects where long-term performance and resistance to degradation are critical. Therefore, Class F fly ash is to be used in this study.

2.4 Effect of Fly Ash

2.4.1 Workability

According to Wang, Zhang, and Sun (2003), fly ash enhances the workability of concrete through two primary physical mechanisms, which are the filling effect and the lubrication effect. The filling effect improves workability by refining the particle size distribution within the concrete mix. When fine fly ash particles are introduced, they occupy the microscopic voids between the larger cement and aggregate particles. As a result, less water is trapped in these voids, and more free water remains available in the mix. This increased amount of unbound water contributes to a more fluid and workable concrete. The lubrication effect comes from the spherical shape of fly ash particles. Unlike the angular and irregular shapes of cement or crushed aggregates, the spherical particles roll easily over one another when the mix is stirred or compacted. This "ball bearing" effect (Figure 2.13) reduces internal friction among the solid components in the fresh concrete. As a result, less energy is required to move and compact the mix, making it feel smoother, more cohesive, and easier to pour or pump. This is particularly advantageous in mixes with low water-to-cement ratios, where maintaining good workability is often a challenge.

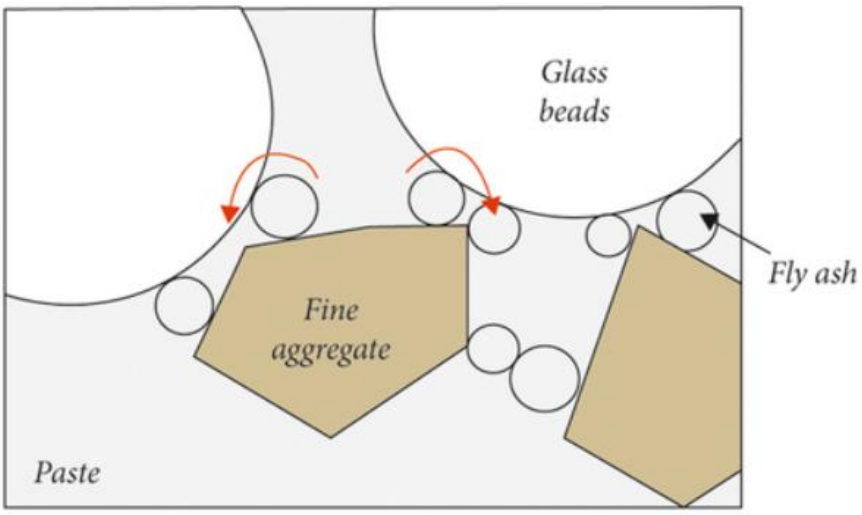

Figure 2.13: Fly Ash Particle as Ball Bearing (Du, Zhao, and Shi, 2021).

The research conducted by Yurdakul et al. (2014) determining the effect of replacing cement with Class F fly ash on the workability of fly ash concrete mixtures, specifically focusing on mixtures at a given water-to-binder ratio. The findings from their research revealed that increasing the dosage of Class F fly ash as a partial replacement for cement resulted in improved workability of the concrete mixtures. Similar findings were also obtained by Nath and Sarker (2011). In the experiment conducted with a constant water/cement ratio of 0.29 and superplasticizer, concrete mixture with 30 % and 40 % of fly ash substitution had resulted in 16.67 % and 6.67 % increase in slump height respectively when compared to 0 % fly ash substitution. The slump value of each percentage of fly ash substitution is presented in Table 2.5.

Table 2.5: Slump Value of 0%, 30% and 40% Fly Ash Substitution (Nath and Sarker, 2011).

Fly Ash Substitution (%)	**Substituted Fly Ash Density (kg/m^3)**	**Superplasticizer (kg/m^3)**	**Slump Value (mm)**
0	0	6.77	150
30	155	4.80	175
40	207	4.24	160

The study done by Fantu et al. (2021) explored the function of superplasticizers (SP), which are chemical admixtures utilised to improve the concrete's workability without altering its water content. The results in Figure

2.14 and Figure 2.15 show that SP greatly enhanced the slump values at constant water/cement ratio, even with higher FA substitution rates (up to 15 %). This is because the molecules of superplasticizer are typically anionic (negatively charged) and attach to the surfaces of cement particles. Superplasticizer alters the surface charge on the cement particles and the negative charge causes the cement particles to repel each other, reducing the clumping and helping the particles to disperse more evenly.

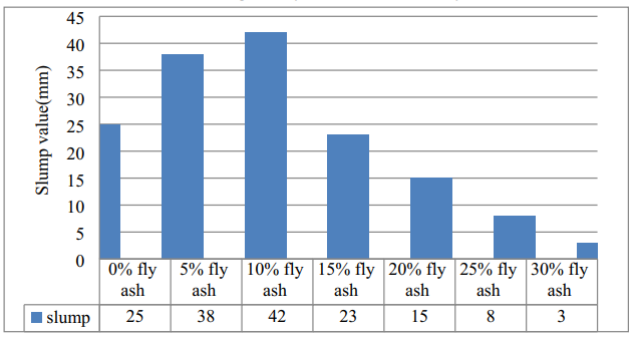

Figure 2.14: Slump Value without Superplasticizer (Fantu et al., 2021).

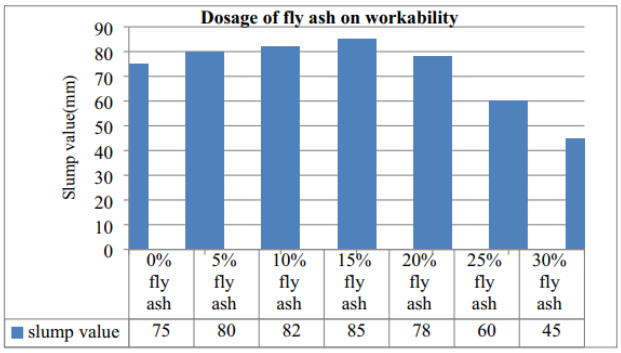

Figure 2.15: Slump Value with Superplasticizer (Fantu et al., 2021).

2.4.2 Microstructure

According to Elrahman and Hillemeier (2014), one of the fundamental mechanisms through which fly ash affects the concrete matrix and microstructure is its packing ability to fill the voids created by irregularly shaped cement particles and aggregates. Cement particles tend to have angular and rough surfaces, leading to inefficient packing that results in larger voids and increased permeability. Fly ash particles which are significantly smaller and predominantly spherical are able to fit into these vacant spaces, filling the gaps

and allowing a more compact arrangement of materials within the concrete matrix. This micro-filling effect reduces permeability and capillary pore volume, making concrete denser and more resistant to moisture ingress and chemical attack. Moghaddam, Sirivivatnanon and Vessalas (2019) as well as Jamkar, Ghugal and Patankar (2013) confirmed that finer fly ash enhanced concrete density more effectively than coarser fly ash as shown in Figure 2.16. However, only the unreacted fly ash particles contribute to the refinement and packing density of the concrete matrix, as the reacted portion participates in the pozzolanic reaction (Chindaprasirt, Jaturapitakkul and Sinsiri, 2007).

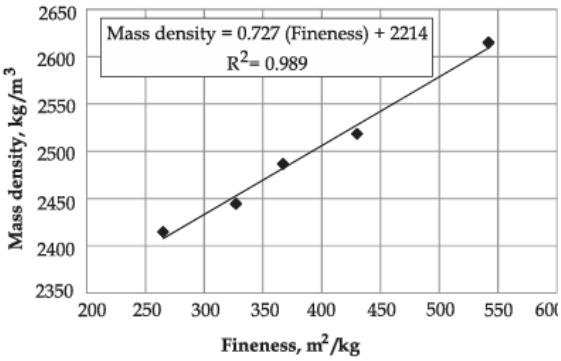

Figure 2.16: Graph of Fly Ash Fineness vs Concrete Mass Density (Jamkar, Ghugal and Patankar, 2013).

Another crucial mechanism in the enhancement of concrete microstructure by fly ash is its pozzolanic reaction. In traditional concrete, the interfacial transition zone (ITZ) between aggregate particles and the cement paste often contains more voids and weaker cement paste due to the deposition of calcium hydroxide (CH) produced from the cement hydration process, leading to a weaker bond between the aggregate and matrix. Fly ash which is rich in silica and alumina consumes the CH and produces secondary C-S-H gel in the void, leading to a denser ITZ with improved bonding. SEM analysis done by Saha (2018) demonstrated the microstructure of the fly ash concrete at 28-day curing and 180-day curing in Figure 2.17 (a) and (b). The voids of fly ash concrete matrix at 180-day curing is observed to be filled with C-S-H due to the pozzolanic reaction and this creates a denser concrete matrix with less porosity.

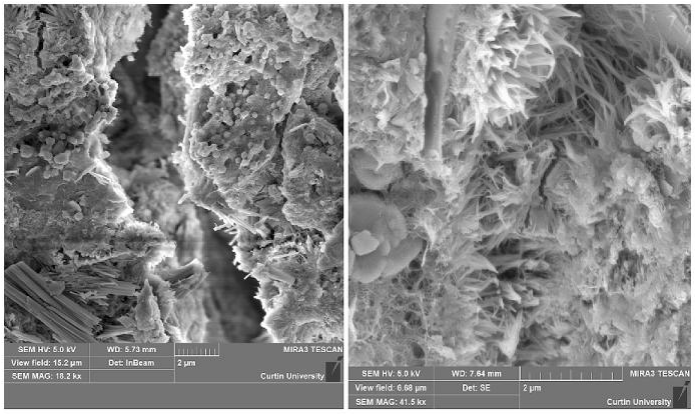

(a) (b)

Figure 2.17: SEM of Fly Ash Concrete at (a) 28-day, (b) 180-day (Saha, 2018).

However, despite the improvements in packing density and porosity reduction, fly ash concrete does not always exhibit higher compressive strength compared to control concrete. Saha (2018) observed that fly ash concrete, although denser than conventional concrete, showed lower compressive strength. This outcome is attributed to the fact that strength development in concrete is primarily governed by the content and quality of C-S-H gel rather than density and porosity. The filler effect of fly ash particles alone is insufficient to offset the reduction in compressive strength caused by decreased cement hydration, particularly at higher replacement levels (Tasdemir, 2003). Therefore, while increased density can contribute to durability and reduce permeability, the formation of secondary C-S-H gel through pozzolanic reaction that required a longer curing period plays a more significant role in determining the compressive strength of fly ash concrete.

2.4.3 Bleeding

Bleeding is the moving of free water to the surface of the cement paste which forms a layer laitance due to the settlement of heavier aggregates. This will reduce the concrete strength and durability as it produces a less dense and porous surface layer. Generally, utilization of fly ash can reduce the bleeding of concrete as fly ash can lower the water demand of the concrete mixture. Due to much smaller size than cement particle, fly ash particle helps fill the voids in concrete and minimize the movement of water to the surface. Besides, since fly ash reduces the water demand of concrete, low water content in concrete

naturally results in less bleeding as there is less excess water to migrate to the surface. This is supported by the experiment done by Ravindrarajah (2023) in which the bleeding reduced when Class F fly ash amount increased from 0 %, 10 %, 20 %, 30 % and 40 %. The addition of fly ash also significantly reduces the initial bleeding amount of concrete as shown in Figure 2.18.

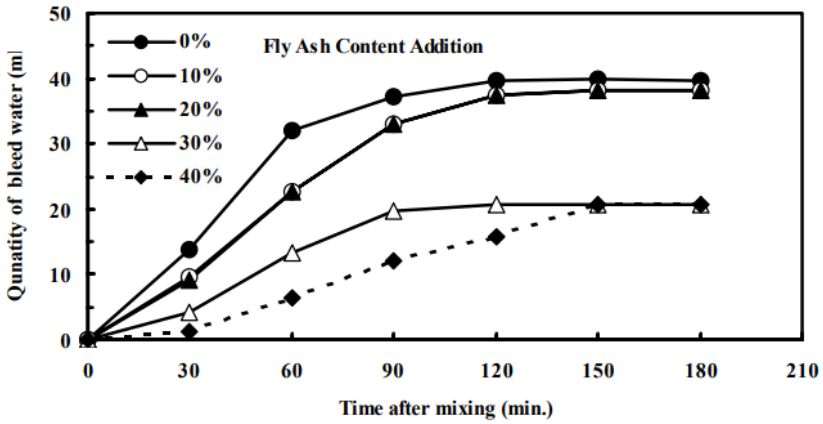

Figure 2.18: Chart of Bleed Water Quantity Over Time (Ravindrarajah, 2023).

Theoretically, the capability of fly ash to reduce concrete bleeding is said to be dependent on the ability to reduce the water demand of concrete mixture at a given slump. This is not always true as the experiment of Kosmatka (2006) proved that certain types of fly ash appeared to reduce bleeding even though it increases the water demand of the concrete. However, there is a direct correlation between bleeding and the water requirement of the fly ash.

2.4.4 Heat of Hydration

Heat of hydration is a release of energy in the form of heat during the exothermic chemical reaction when cement is mixed with water. It is an important factor that needs to be considered especially in the construction of massive projects such as water dams and bridges. Excessive heat produced will result in the existence of a temperature gradient (De Schutter, 2002), producing compressive and tensile force inside the concrete which gives rise to the occurring of thermal cracking and reduction of concrete durability.

Since fly ash needs a longer time to react with water than OPC, Class F fly ash concrete hydrates at a slower rate and produces less hydration heat.

The aluminosilicate components in the fly ash, which take part in a more gradual hydration process, are the reason for this slower reaction. Instead of the abrupt temperature increase observed during the hydration of conventional Portland cement (OPC), this slower reaction distributes the heat release over a longer time. This is proven by the experiment done by Langan, Weng and Ward (2002) which concluded that the addition of fly ash increased the heat of hydration released for the first few minutes but retarded the hydration heat for dormant and acceleration periods. Similar results were also obtained by Kim (2021) using fly ash replacement of 0 %, 10 %, 20 %, 30 %, 40 % with Type I cement originating from Korea. The result showed that when the fly ash replacement increased, the maximum heat of hydration was reduced, and the period of occurrence was retarded because of the slower pozzolanic reaction. Figure 2.19 shows the rate of hydration heat over time.

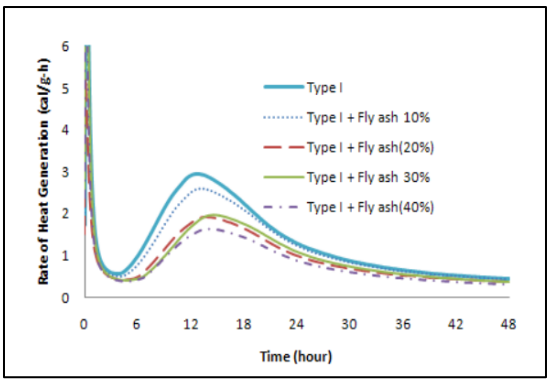

Figure 2.19: Rate of Hydration Heat Over Time (Kim, 2021).

2.4.5 Compressive Strength

The effects of Class F fly ash on compressive strength are primarily attributed to its chemical composition, which consists mainly of silicon dioxide (SiO_2), aluminium oxide (Al_2O_3), and iron oxide (Fe_2O_3). The high silicon dioxide content of Class F fly ash plays a crucial role in the pozzolanic reaction which is responsible for increasing compressive strength over time. When cement hydrates, it produces calcium silicate hydrate (C-S-H) gel and calcium hydroxide ($Ca(OH)_2$). While C-S-H gel provides strength, calcium hydroxide is a weak and porous byproduct that does not contribute to strength. However, the silicon dioxide in fly ash can react with this calcium hydroxide to produce secondary C-S-H gel, filling voids in the concrete matrix and making it stronger.

The pozzolanic reaction between silicon dioxide in fly ash and calcium hydroxide from cement hydration is a slow process. As a result, the early-age strength development of fly ash concrete particularly within the first seven days is much lower than that of conventional Ordinary Portland Cement (OPC) concrete. This is because OPC concrete can undergo rapid hydration and form a significant amount of calcium silicate hydrate (C-S-H) gel early on, which contributes to its initial strength gain. In contrast, fly ash concrete relies on the gradual pozzolanic reaction that requires calcium hydroxide from cement hydration, which takes longer to develop additional C-S-H gel. Consequently, at seven days of curing, OPC concrete typically exhibits a higher compressive strength compared to fly ash concrete (Xu et al., 2020).

Beyond 28 days, the strength development of fly ash concrete often surpasses that of OPC concrete due to the continued formation of C-S-H gel. As the pozzolanic reaction progresses, more calcium hydroxide is consumed, leading to the formation of additional binding material which enhances the overall strength and durability of the concrete. Research done by Misra, Ramteke, and Bairwa (2007) demonstrates that the 7-day (Figure 2.20) and 28-day (Figure 2.21) compressive strength of concrete with fly ash replacement is initially lower than that of control concrete with 0 % fly ash. Nevertheless, fly ash concrete continues to gain strength over time and eventually exceeds the strength of control concrete after 90 days of curing (Figure 2.22). This result highlights that fly ash concrete may require a longer curing period of up to 90 days or more to complete the pozzolanic reaction and fully develop its compressive strength.

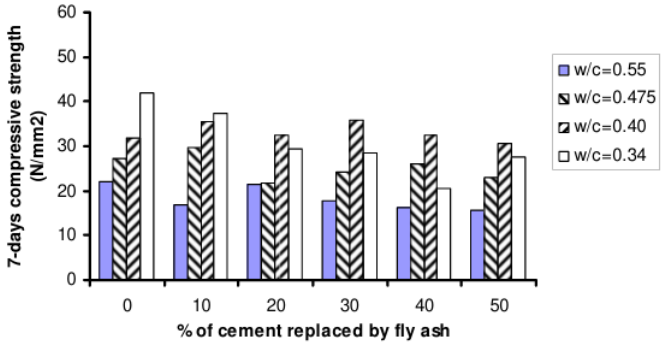

Figure 2.20: 7-day Compressive Strength (Misra, Ramteke, and Bairwa, 2007).

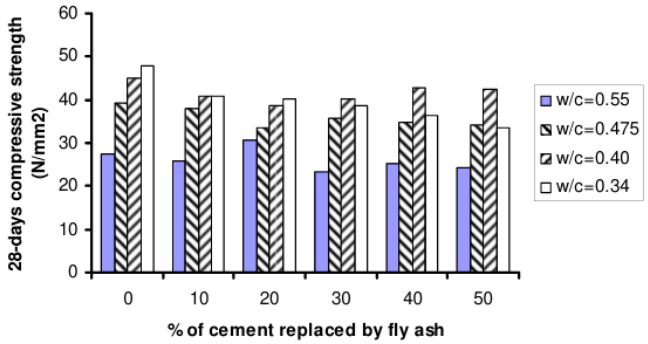

Figure 2.21: 28-day Compressive Strength (Misra, Ramteke, and Bairwa, 2007).

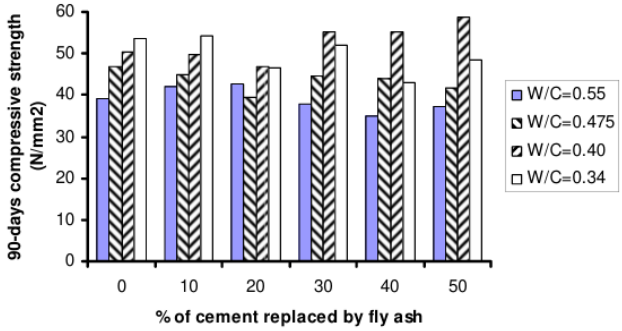

Figure 2.22: 90-day Compressive Strength (Misra, Ramteke, and Bairwa, 2007).

Similar findings were also reported by Chindaprasirt, Jaturapitakkul and Sinsiri (2007), stating that some fly ash particles remained inactive even after 28 days of curing. They identified three primary forms of fly ash particles in the hardened paste after 28 days of curing. The first form included fly ash particles with dissolved surfaces, indicating that these particles had undergone partial dissolution due to the pozzolanic reaction. This reaction led to the formation of secondary calcium silicate hydrate (C-S-H) gel, which enhances the strength and durability of concrete. Some particles showed evidence of etching and precipitation, confirming their active participation in hydration. The second form consisted of fly ash particles with smooth surfaces, suggesting that they remained unreacted or had minimal interaction with the surrounding cement matrix. These particles only acted as inert fillers which improved the packing density of the paste but had minimum contribution to the development of compressive strength. Their presence contributed to the refinement of pore structure, reducing the overall porosity of the cement matrix. The third form of

fly ash particles observed under SEM was those covered with hydration and pozzolanic reaction products. These particles were surrounded by C-S-H and other reaction compounds, indicating that the hydration process was progressing around them. SEM of the three forms of fly ash particle is illustrated in Figure 2.23 (a) and (b).

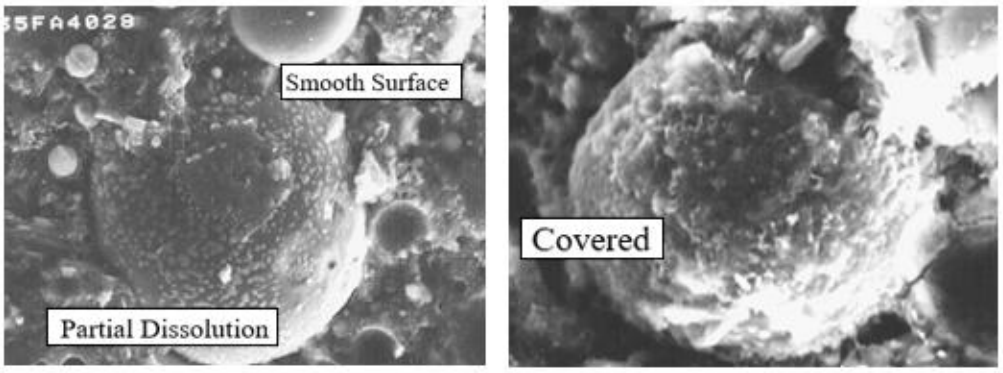

Figure 2.23: Fly Ash with (a) Partial Dissolution and Smooth Surface, (b) Hydration Product (Chindaprasirt, Jaturapitakkul and Sinsiri, 2007).

The particle size of fly ash significantly influences both the strength and durability of concrete. The effectiveness of the pozzolanic reaction is largely determined by the surface area of the fly ash particles. Finer fly ash particles offer a greater surface area which allows for more extensive contact with calcium hydroxide and water, leading to a more efficient pozzolanic reaction. This aligns with the SEM analysis done by Moghaddam, Sirivivatnanon and Vessalas (2019) on three types of fly ash, which are Classified fly ash (CFA), Run-of-station fly ash (RFA) and Grounded run-of-station fly ash (GRFA). The Grounded run-of-station fly ash particles with the largest surface area are observed to be covered with greater calcium silicate hydrate gel than the other two fly ash, as shown in Figure 2.24. This enhanced reactivity accelerates the formation of C-S-H, which contributes to a denser concrete matrix and results in improved compressive strength. Moreover, finer fly ash particles also facilitate a faster pozzolanic reaction, which not only

improves early-age strength but also promotes more consistent strength development over time (Jamkar, Ghugal and Patankar, 2013).

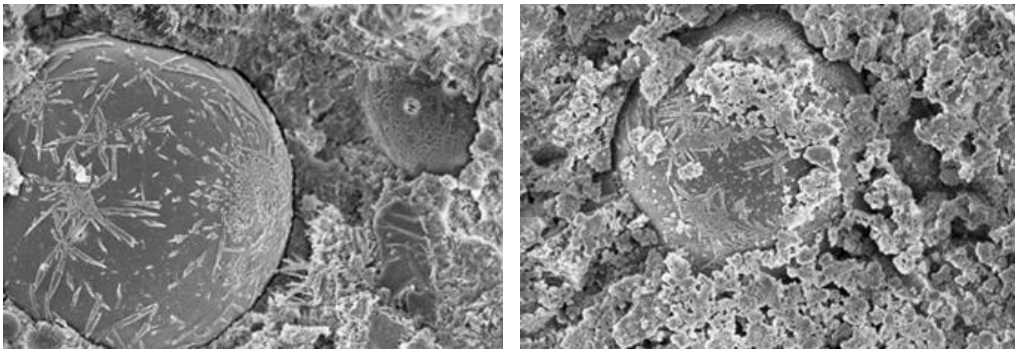

(a) RFA (b) CFA

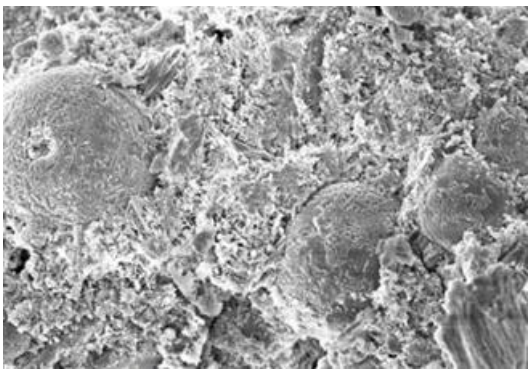

(c) GRFA

Figure 2.24: SEM Image of (a) RFA, (b) CFA, (c) GRFA (Moghaddam, Sirivivatnanon and Vessalas, 2019).

2.5 Optimum Amount of Fly Ash Replacement

While the use of fly ash offers significant advantages in enhancing the compressive strength and durability properties of concrete, the amount of fly ash replacement plays a pivotal role. At optimal replacement, the pozzolanic reaction from fly ash can contribute additional calcium silicate hydrate (C-S-H) over time when reacts with all the calcium hydroxide produced during cement hydration, leading to improved strength and density. However, beyond optimal level, the reduction in cement content can hinder the development of early strength, and the excess fly ash will only act as additional microfiller due to the shortage of calcium hydroxide (Oner, Akyuz and Yildix, 2005).

From the experiment conducted by Kiran and Ratnam (2014), 0 %, 5 %, 10 %, 15 %, 20 % of India-produced fly ash were used to test the strength of M35 grade concrete. Highest compressive strength was obtained when 10 % fly ash replacement was used. When 10 to 25 mm coarse aggregate size and 1.18 to 2.36 mm of fine aggregate as well as a water/binder ratio of 0.533 were used, similar optimum fly ash replacement of 10 % was also obtained from Mardiaman and Dewita (2022) for M35 grade concrete. 10 % of Class F fly ash replacement was also concluded as the optimum substitution by Ankesh, Malla, and Gowda (2016) when using water/binder ratio of 0.41 for M30 grade concrete.

As for the experiment done by Gull, Wani, and Amin (2020), India-produced Class F fly ash was used along with constant water/binder ratio of 0.38 for M20 grade concrete. The results (Figure 2.25 and Figure 2.26) showed that highest compressive and splitting tensile strength at 7 days and 28 days was obtained when 5 to 10 % fly ash was utilised to replace cement and further increase of fly ash have decreasing trend results. Since the fly ash was sieved and pulverized into finer size in this experiment, the large surface area of fly ash particle enhanced the pozzolanic reaction with calcium hydroxide, hence producing concrete with denser structure and higher early strength when compared to unpulverized fly ash.

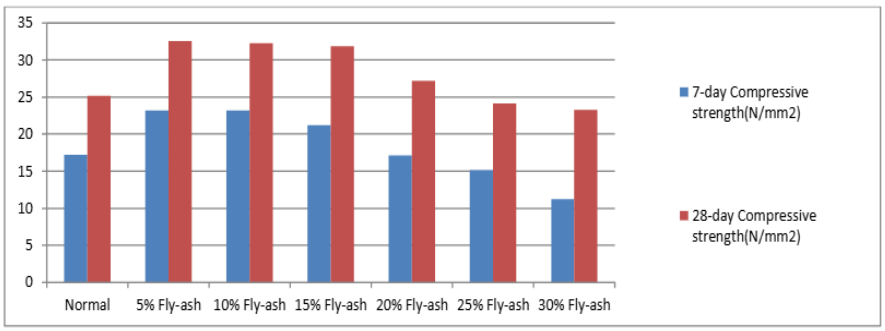

Figure 2.25: Compressive Strength Result at 7 days and 28 days (Gull, Wani, and Amin, 2020).

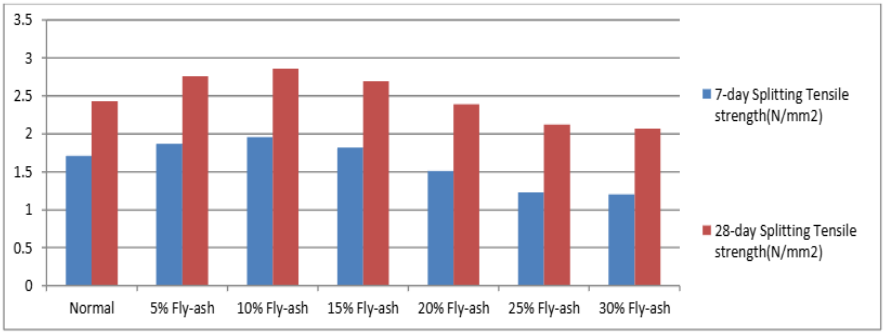

Figure 2.26: Splitting Tensile Strength Result at 7 days and 28 days (Gull, Wani, and Amin, 2020).

When 10 % of Vietnam-produced fly ash replacement was used in 450 kg/m^3 of cement with a water/binder ratio of 0.5, the concrete produced showed highest 28-days and 91-days compressive strength (Trong Lam, 2020). Another experiment was done by Haque and Kayali (1998) to investigate the optimum of Class F fly ash replacement when 400 kg/m^3 and 500 kg/m^3 of Type I cement were used. Superplasticizer was used in this experiment at a dosage of 1.51 kg per 100 kg of cementitious material. Table 2.6 shows the results of the experiment, indicating that the highest compressive strength was achieved at 10 % fly ash replacement for both 400 kg/m^3 and 500 kg/m^3 of cement.

Table 2.6: Compressive Strength at Different Fly Ash Replacements (Haque and Kayali, 1998).

Mix	**W/C**	**Compressive Strength (MPa)**				**2-h Water Penetration (mm)**
		7 days	**14 days**	**28 days**	**56 days**	
400-0	0.38	62.0	70.5	77.5	-	15
400-10	0.35	70.0	77.5	94.0	99.5	11
400-15	0.36	58.0	65.0	73.5	-	12
500-0	0.37	69.0	75.0	92.5	106.0	18
500-10	0.25	84.0	93.5	111.0	121.5	13
500-15	0.28	75.5	89.0	102.0	106.0	15

However, it is also noted that the optimum amount of fly ash varies when there is addition of other mineral admixtures. Another experiment was conducted by Chandini and Nusari (2021) to determine the optimum amount of India-produced Class C fly ash replacement with the addition of silica fume for

M40 grade concrete. The results obtained indicated that, at a water/binder ratio of 0.5, the concrete made using 15 % fly ash and 5 % silica fume produced the highest compressive strength results. This is because the finer particle size of silica fume has enhanced the pozzolanic reaction with calcium hydroxide, hence affecting the optimum fly ash replacement.

After conducting extensive research and analysis, it has been concluded that a Class F fly ash replacement level of 5 to 15 % appears to be the most feasible and practical range. This recommendation is based on the general performance trends observed in existing literature, where such replacement levels have shown the highest compressive strength. However, it is crucial to acknowledge that these findings are not universally applicable, as the optimal fly ash replacement is sensitive to a variety of factors such as different cement manufacturers, proportion of cement, origin of fly ash, admixtures, fineness of fly ash particle and water/cement ratio. Therefore, the recommendation of 5 to 15 % fly ash replacement only serves as a useful starting point, while the actual optimum fly ash replacement for this study should be validated through various standard tests tailored to the specific materials and conditions of this study.

2.6 Mix Proportion Design

Concrete mix proportion design is a crucial process to identify the appropriate amounts of cement, water, fine and coarse aggregates, and sometimes admixtures to create a cost-effective concrete mix with both the required hardened and fresh qualities. To design the concrete mix proportion, designer can either refer directly to the existing data from other similar work or conduct trial mix if statistical data from comparable projects is not available. Before the design of concrete mix proportion, important design parameters such as maximum aggregate size, maximum water/binder ratio, cement strength class and type of admixture must first be clarified so that the concrete can achieve the required 28 days compressive strength. The three existing mix proportion design methods that are widely used in the construction industry are the American Concrete Institute Method (ACI), Indian Standards Method (IS) and British Standard Method (BS).

According to the ACI technique, the workability of the concrete mix with a specific maximum size of well-graded aggregates depends on the water content, air-entrained volume, and specific chemical admixture, and is mostly independent of the concrete mix proportion, especially the amount of cementing material. Additionally, ACI method implies that the maximum size, represented as the fineness modulus, is the single factor that determines the ideal ratio of the bulk volume of coarse particles to the entire volume of concrete. The required strength and durability are taken into consideration when choosing the water/cement ratio. The amount of fine aggregates needed is calculated using the absolute volume approach, which accounts for the amount of air entrained in the mix, given the volumes of water, coarse aggregates, and cement (Santhosh and Shivananda, 2017). Different from BS and IS method, ACI method does not determine the fresh concrete density based on the specific gravity of the materials. Besides, ACI method does not classify aggregates as crushed or uncrushed nor does it consider the impact of aggregate flakiness and surface texture on sand and water content (Demissew, 2022).

The Indian Standard Method provides separate guidance for designing the high-strength concrete mix (M40 and above) and normal concrete mix (up to M35). The key assumption of the mix design is that the water/cement ratio mostly determines the compressive strength of workable concrete. The concrete grade and exposure type are taken into consideration while choosing the water/cement ratio in this procedure. The selection of water content is based on slump and nominal coarse size aggregate. Additionally, the IS 383 fine aggregate zone and the aggregate's nominal maximum size determine the volume of coarse aggregate. The material's batch weight per unit volume is determined using the absolute volume method (Santhosh and Shivananda, 2017).

The conventional road note No. 4 method is replaced with the most recent British Standard method prepared by Building Research Establishment in United Kingdom and is published with the title of “Design of Normal Concrete Mixes”. The new method eliminates the specific grading curves and overall grading curves of mixed aggregates as well as removing the mix design table that relates the ratio of water/cement, aggregate/cement ratio, aggregate type, maximum aggregate size and level of workability. The two types of aggregates that are recognized in this new method are crushed and uncrushed.

For both the crushed and uncrushed aggregate types, with maximum sizes ranging from 10 to 40 mm, the water content needed to provide a particular slump and vebe time can be calculated based on Table 3 in the Design of Normal Concrete Mixes as shown in Figure 2.27. The cement content is determined by dividing the free water content by the water/cement ratio while the concrete density can be found using the graph shown in Figure 2.28. The aggregate content of concrete is then obtained by deducting cement and water content from the total concrete density. Following that, fine aggregate proportion can be determined by using the chart shown in Figure 2.29 (Nwakire, 2013). Similar with ACI method, the concrete mix proportion is expressed in terms of the amount of material per unit volume of concrete (Santhosh and Shivananda, 2017).

Table 3 Approximate free-water contents (kg/ m^3) required to give various levels of workability

Slump (mm)		0–10	10–30	30–60	60–180
Vebe time (s)		>12	6–12	3–6	0–3
Maximum size of aggregate (mm)	Type of aggregate				
10	Uncrushed	150	180	205	225
	Crushed	180	205	230	250
20	Uncrushed	135	160	180	195
	Crushed	170	190	210	225
40	Uncrushed	115	140	160	175
	Crushed	155	175	190	205

Figure 2.27: Water Content for Different Aggregate Size (Marsh, 1988).

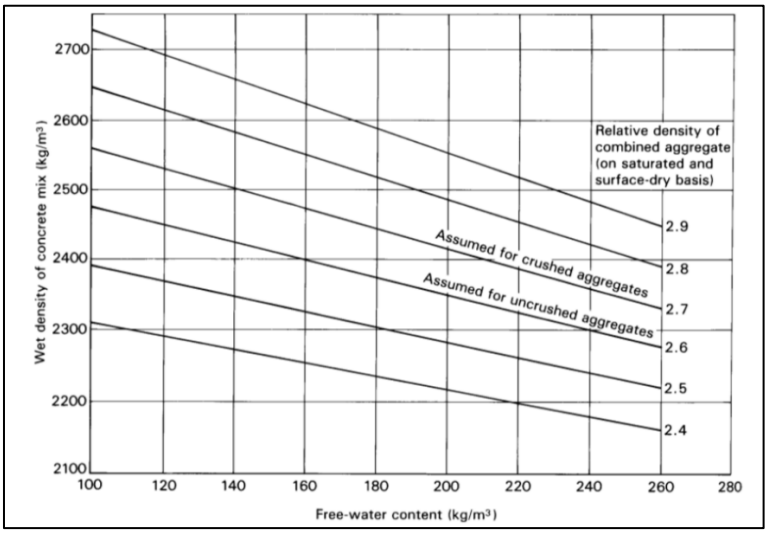

Figure 2.28: Wet Concrete Density Chart (Marsh, 1988).

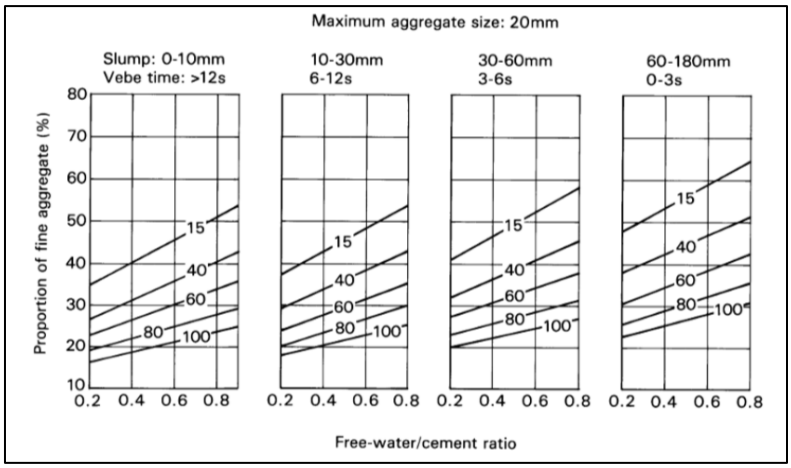

Figure 2.29 Chart of Fine Aggregate Content (Marsh, 1988).

Consideration taken in each of the methods can be seen in Table 2.7. However, final mix proportion should be determined and verified based on the actual trial mix instead of just relying on the theoretically designed mix proportion. Adjustment should be made to the mix proportion design if the performance of the concrete does not satisfy the design strength requirement.

Table 2.7: Consideration of IS, ACI and BS Method (Santhosh and Shivananda, 2017).

Consideration	IS Method	ACI Method	BS Method
28-day Compressive Strength	Yes	Yes	Yes
Compressive Strength Standard Deviation	Yes	No	Yes
Workability	Yes	Yes	Yes
Maximum Size and Types of Aggregate	Yes	Yes	Yes
Dry Rodded Unit Weight of Coarse Aggregates	No	Yes	No
Specific Gravity of Cement, Coarse and Fine Aggregates	Yes	Yes	Yes
Water Absorption and Moisture Content Adjustment	Yes	Yes	No
Type of construction	No	Yes	No
Exposure condition	Yes	Yes	Yes
Air/non-air entrainment	Yes	Yes	Yes

Based on the concrete mix proportion designed by Santhosh and Shivananda (2017) using ACI, IS and BS methods, the water and cement content of the respective method was obtained and shown in Figure 2.30 and Figure 2.31. The result showed that the overall water content is minimum for BS method and maximum for ACI method. For M15 and M30 concrete, the cement content is highest in ACI method and lowest in BS method. Since cement is the most expensive material in concrete, mix proportion designed using ACI method will require higher budget whereas the BS method with the lowest cement content is the cheapest method to design the mix proportion. Since there is limited resource, BS method is chosen to be used in this study.

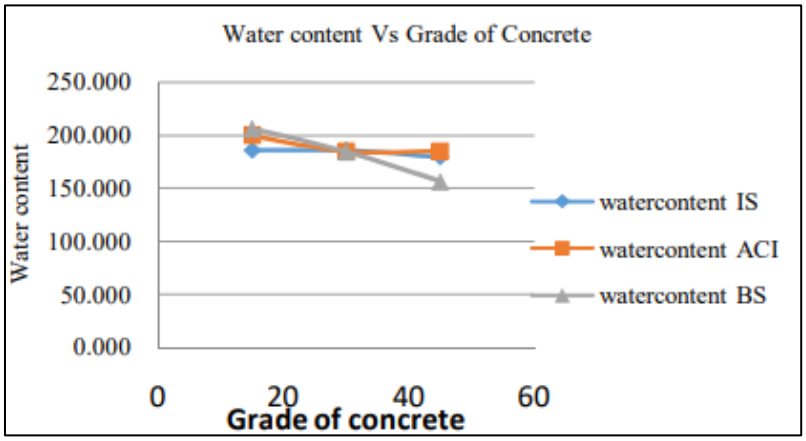

Figure 2.30: Graph of Water Content Over Concrete Grade (Santhosh and Shivananda, 2017).

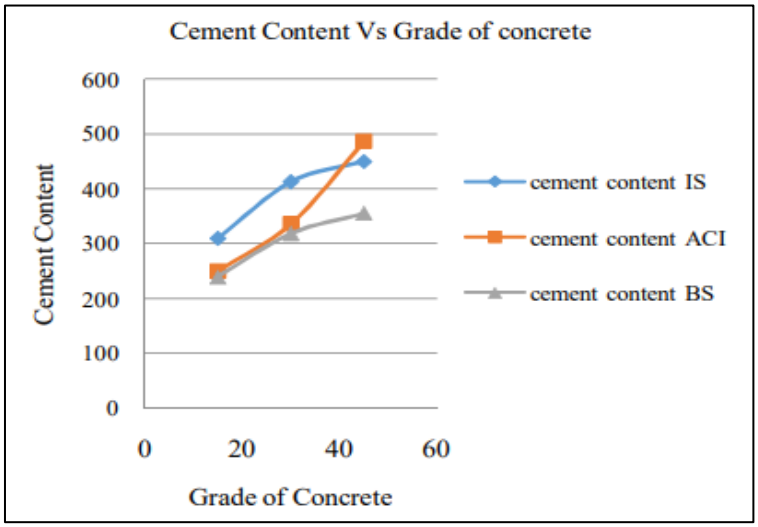

Figure 2.31: Graph of Cement Content Over Concrete Grade (Santhosh and Shivananda, 2017).

2.7 Waterproofing of Concrete

2.7.1 Waterproofing Method

Waterproofing concrete plays a significant role in water-retaining structures as it is crucial for maintaining long-term durability, avoiding water leakage, and preserving structural integrity. Therefore, waterproofing method of concrete is of importance, and it is classified into 3 major methods which are sheet membrane liquid membrane method and integral method.

The sheet membrane method involves applying a layer of pre-formed waterproofing sheet onto the surface of concrete to prevent water ingress, as illustrated in Figure 2.32. Common materials used in this method include butyl-rubber sheets, semi-rigid asbestos asphalt sheeting, and torch-on sheeting. These membranes can be applied as either bonded (adhered directly to the concrete surface) or unbonded systems. Regardless of the bonding method, it is essential that each membrane sheet overlaps the adjacent one by approximately 100 mm to ensure a continuous waterproofing barrier. The seams at these overlaps are sealed using adhesives or heat welding techniques to maintain watertight integrity. However, the seams represent the most vulnerable points in the system. If not sealed properly, they are susceptible to water penetration which can compromise the overall effectiveness of the waterproofing layer (Borle and Ghadge, 2016). This reliance on precise installation techniques and the potential for seam failure make the sheet membrane method less ideal for large-scale or submerged structures that require long-term resistance to hydrostatic pressure.

Figure 2.32: Sheet Membrane Method (Constro Facilitator, 2020).

The liquid membrane method involves the application of a waterproofing liquid onto the surface of hardened concrete, typically through spraying, trowelling, or brushing, as illustrated in Figure 2.33. Once applied, the liquid forms a continuous and flexible waterproof coating that serves as a protective barrier against water ingress. Commonly used materials for this method include acrylic coatings, polyurethane coatings, and epoxy coatings, each offering different levels of elasticity, durability, and chemical resistance depending on the application requirements. Unlike the sheet membrane method, which involves joints and overlaps that can potentially become weak points, the liquid membrane method creates a seamless and joint-free barrier that can conform easily to the contours and intricate details of the concrete surface. This ability to form a uniform layer significantly reduces the risk of leakage through seams or poor adhesion areas (Borle and Ghadge, 2016). However, despite its advantages in flexibility and surface adaptability, the liquid membrane method still faces limitations in large-scale applications, especially under constant hydrostatic pressure.

Figure 2.33: Liquid Membrane Method (Constro Facilitator, 2020).

The following method is the integral mixing method where the addition of waterproofing admixture is required at the time of material mixing as shown in Figure 2.34. According to the guidelines established by ACI Committee 212 (2016), integral waterproofing admixtures designed to reduce water penetration into concrete are broadly categorized into two functional subgroups based on the type of water exposure which are Permeability-Reducing Admixtures for Non-Hydrostatic Conditions (PRAN) and Permeability-Reducing Admixtures

for Hydrostatic Conditions (PRAH). PRAN admixtures, previously known as “moisture-repellent admixtures”, are typically hydrophobic in nature. They work by lining the capillary pores of the hardened concrete with water-repelling substances such as fatty acids, soaps, or silane/siloxane derivatives. PRAN products are useful for reducing dampness or minimizing water absorption in elements such as concrete facades, floors, walls, and slabs exposed to rain or humidity, but they are not recommended for structures exposed to standing water or constant water pressure as their effectiveness under hydrostatic conditions is limited. In contrast, PRAH admixtures are formulated to perform under hydrostatic pressure conditions where water actively exerts pressure on concrete, such as in tanks, retaining walls, underground basements, swimming pools, and wastewater treatment plants.

Figure 2.34: Integral Mixing Method (The Constructor, 2018).

Among PRAH admixtures, Crystalline Waterproofing Admixtures stand out due to their chemical reactivity and self-sealing capability. Crystalline waterproofing admixtures are composed of Portland cement, specially processed quartz sand and a proprietary blend of active chemicals. Upon contact with water and calcium hydroxide in freshly placed or hardened concrete, the active chemicals in the admixture trigger a chemical reaction that results in the formation of insoluble needle-like crystalline, primarily consists of calcium silicate hydrate and other stable mineral formations that can withstand water pressure (Gojević et al., 2021). Over time, this crystalline growth integrates with the cementitious matrix, enhancing the concrete's density, impermeability and durability (Gojević et al., 2021). However, García-Vera et al. (2018) reported

that the inclusion of crystalline waterproofing admixtures does not significantly influence compressive strength.

Although various waterproofing methods are available, not all are suitable for water-retaining structures. Techniques such as sheet membrane and liquid membrane waterproofing are often impractical for structures like dams, water reservoirs, and bridges, particularly those involved in maritime and large-scale infrastructure projects. These structures are typically subjected to high hydrostatic pressure, and the application of external membranes on such massive surfaces is not only technically challenging but also results in increased project costs and extended construction timelines. Due to these limitations, the integral mixing method emerges as a more practical, economical, and efficient solution. By incorporating crystalline waterproofing admixtures directly into the concrete mix, this method provides uniform protection throughout the concrete matrix and eliminates the need for additional surface treatments. For this study, the integral mixing method is adopted to produce waterproof concrete.

2.7.2 Waterproofing Evaluation Test

There are various types of tests or assessments that are used to evaluate the waterproofing quality of the concrete such as water absorption test, soprtivity test, initial surface absorption test and static water contact angle test. Based on the survey done by Muhammad et al. (2015), water absorption test was the most used test by the authors of published journal articles to determine the permeability and porosity of concrete, comprising 38 out of 40 authors. In water absorption test, the concrete samples must be immersed in the water for a considerable amount of time to ensure the concrete absorbs water fully, hence this test will likely take hours or even days to complete. After that, the concrete samples are dried into saturated surface dry condition to ensure that the weight represents only the water absorbed by the concrete and not the surface water. This test is important as it provides an understanding regarding the bulk porosity and the overall water resistance of concrete to predict the concrete's durability in wet environment. Higher water absorption indicates that concrete is permeable, which is likely to absorb water and therefore vulnerable under wet environment. The percentage of water absorption can be found using Equation 2.1.

$$\text{Water Absorption } (\%) = \frac{W_w - W_d}{W_d} \times 100\ \% \qquad (2.1)$$

where

W_w = Weight of Concrete After Immersed

W_d = Weight of Concrete Before Immersed

The sorptivity test, also known as capillary absorption test, has become an essential tool in modern construction due to its ability to accurately assess concrete's water absorption properties through capillary action. Unlike conventional water absorption tests, which measure the total amount of water a concrete specimen absorbs when fully submerged, the sorptivity test evaluates how water moves through the pore system from only one exposed surface. Since sorptivity test is highly sensitive to microstructural changes within the concrete, it can effectively detect the influence of supplementary cementitious materials such as fly ash, silica fume, and ground granulated blast furnace slag on concrete performance. This makes it a more precise indicator of the rate at which unsaturated concrete absorbs moisture, helping engineers and researchers better understand the permeability and durability of concrete.

Other than that, Initial Surface Absorption Test (ISAT) is also one of the most commonly used methods to examine the permeability of the concrete surface. According to Claisse, Elsayad and Shaaban (1997), initial surface absorption is defined as the rate of water flow, under a fixed temperature and applied pressure, into concrete per unit area at predetermined intervals from the beginning of the test. This test analyses the rate of water being absorbed by the concrete's surface, offering an understanding of the material's surface resistance to water penetration. Lower ISAT values signify a less permeable surface and consequently a more durable and water-resistant concrete mix. This is especially crucial in comprehending how vulnerable the concrete is to external factors like moisture infiltration, which may cause problems like reinforcing corrosion and weakened structural integrity over time. Initial surface absorption can be calculated from the mathematical formula developed by Levit (1970) which is shown in Equation 2.2.

$$\text{ISA} = \frac{F}{\Theta} \tag{2.2}$$

where

$ISA = \text{Initial Surface Absorption } (ml/m^2/\text{s})$

$F = \text{Flow Rate } (ml/\text{s})$

$\Theta = \text{Area Under Cap } (m^2)$

Another famous method to examine the water resistance is the static water contact angle test. The primary purpose of this test is to determine the contact angle that forms between a solid surface and a water liquid droplet. The surface wettability is indicated by this angle, which is commonly represented by 'θ'. The resistance of a material to water penetration is largely determined by its wettability, which has an immediate effect on the material's performance and durability. In this test, the water droplet is carefully placed on the surface. The water droplet is recorded from the side using a camera with a high resolution or a specialized tool called the contact angle goniometer to find the contact angle between the droplet's tangent at its edge and baseline, or the line where it touches the surface. The equilibrium between cohesive forces (inside the water itself) and adhesive forces (between the water and the surface) is reflected in this angle. The concrete surface is considered as hydrophilic for static contact angle of less than 90° whereas static contact angle greater than 90° shows that the surface is hydrophobic (Figure 2.35). There are also cases where the static contact angle is greater than 150°, indicating that the concrete has a superhydrophobic surface (Lößlein et al., 2022). In construction, materials with higher static contact angle are preferable as it has higher water resistance.

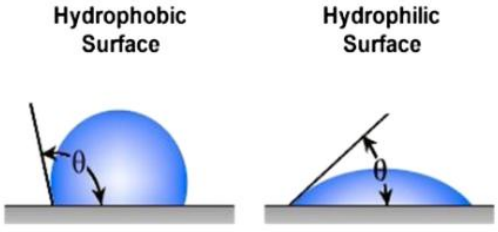

Figure 2.35: Static Water Angle For Hydrophobic and Hydrophilic Surface (Zhao et al., 2021).

Even though static water contact angle test is useful to determine the water resistance of the surface of concrete and is easy to operate, however this test is only limited to sheet and liquid membrane waterproofing methods but is not suitable for integral mixing method. It may provide varying results especially if the concrete surface is chemically heterogeneous. The water contact angle can be easily affected by the surface roughness, which means that the angle may not be the actual represent of the true wetting ability. Moreover, purchasing the costly high-resolution camera or contact angle goniometer that is needed for this static water contact angle test seems impractical in this study as the budget and time are limited. Therefore, water absorption test, sorptivity test and initial surface absorption test can be used to determine the water resistance of the concrete as they are feasible and non-destructive methods.

2.7.3 Water Absorption Test

The experiment conducted by Kurda, de Brito and Silvestre (2019) showed the impact of varying levels of fly ash replacement on the water absorption properties of concrete. The results as shown in Figure 2.36 demonstrate a clear trend at which the water absorption decreases when the percentage of Class F fly ash replacement increases.

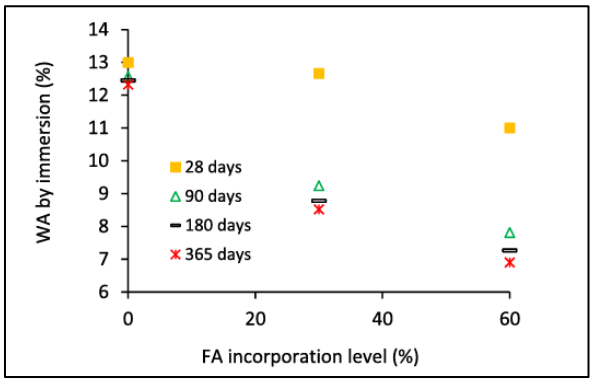

Figure 2.36: Water Absorption at Different Fly Ash Replacement (Kurda, de Brito and Silvestre, 2019).

At 28 days, incorporating 30 % and 60 % fly ash reduces water absorption by 3 % and 15 % respectively. This reduction can be attributed to the texture and particle size of the fly ash, which is able to fill the void, improve the packing density of the mix and reduce the water absorption.

At longer curing ages, the decrease in water absorption becomes more significant. For example, water absorption decreases by approximately 27 to 31 % with 30 % fly ash, and 38 to 44 % with 60 % fly ash between 90 and 365 days (Kurda, de Brito and Silvestre, 2019). This significant reduction is due to the increasing pozzolanic activity of fly ash over time. Fly ash reacts with calcium hydroxide ($Ca(OH)_2$), a byproduct of cement hydration, to form secondary calcium silicate hydrate (C-S-H) and this reaction reduces the interconnectivity of the pore structure, thereby decreasing the permeability of the concrete. This refinement minimizes the movement of water through the matrix, enhancing the concrete matrix's resistance to moisture ingress (Filho et al., 2013).

In addition, Zhuang, Wang, and Zhang (2022) conducted water absorption tests on fly ash concrete at varying water-cement ratios. The results as presented in Figure 2.37 revealed a trend consistent with the findings of Kurda, de Brito, and Silvestre (2019). Concrete with fly ash replacement exhibited lower water absorption compared to concrete without fly ash, particularly at lower water-binder ratios. This was observed at both 28-day and 56-day curing periods.

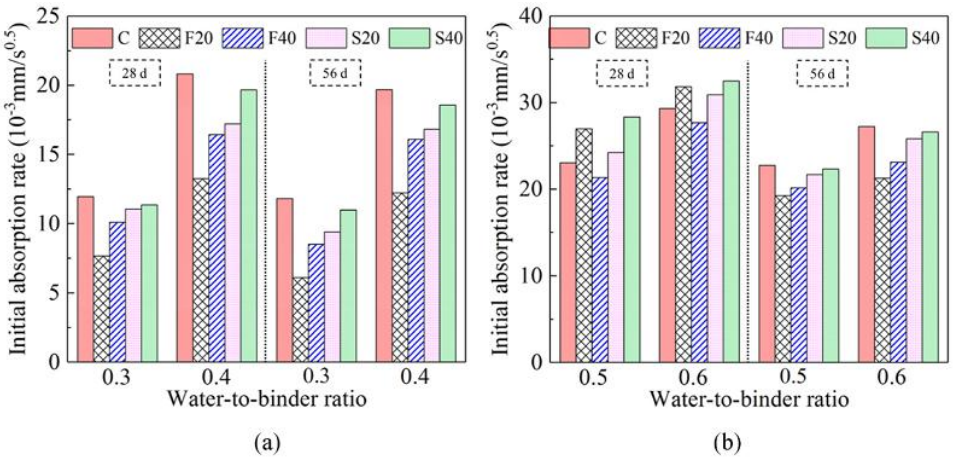

Figure 2.37: Water Absorption at Water-Binder Ratio of (a) 0.3 and 0.4 (b) 0.5 and 0.6 (Zhuang, Wang, and Zhang, 2022).

At high water-binder ratios of 0.5 and 0.6, the absorption rate of fly ash concrete at 28 days is generally higher than that of plain cement concrete. This is primarily due to the reduced cement content in the mix and the lower initial pozzolanic activity of fly ash compared to cement. These factors result in a less

refined pore structure at early ages, where the adverse impact of the reduced cement content outweighs the pore-refining effects of fly ash.

However, when the replacement level is sufficiently high, the significant refinement of the pore structure by fly ash compensates for the reduced cement hydration. Fly ash's ability to fill voids and react with calcium hydroxide forms additional calcium silicate hydrate (C-S-H) which effectively reduces the interconnectivity of pores. This explains why the absorption rate of concrete with higher fly ash replacement at 28 days is lower than that of plain cement concrete, despite the high water-binder ratio (Zhuang, Wang, and Zhang, 2022). This highlights the importance of optimizing fly ash content to achieve the desired balance between workability and durability.

2.7.4 Initial Surface Absorption Test

Based on Balakrishna et al. (2018), Initial Surface Absorption Test was conducted on concrete cubes with different strength grade using the mix proportion and instruments as shown in Table 2.8 and Figure 2.38.

Table 2.8: Mix Proportion of 3 Concrete Cube Samples for Each Concrete Grade (Balakrishna et al., 2018).

Grade/Mean Target Strength (N/mm^2)	Slump (mm)	W/C	Cement (kg)	Fine Aggregate (kg)	Coarse Aggregate (kg)
25/32.84	**10-30**	**0.50**	**3.84**	**5.98**	**17.04**
30/37.84	**10-30**	**0.45**	**4.27**	**6.09**	**16.50**
40/47.84	**10-30**	**0.44**	**4.35**	**5.62**	**16.88**

Figure 2.38: ISAT Instrument Setup (Balakrishna et al., 2018).

Concrete grade and surface absorption have a direct correlation, according to the results of the Initial Surface Absorption Test (ISAT) as shown in Table 2.9. In particular, the average ISAT value decreased with increasing concrete grade. Given that higher-grade concretes are usually denser and contain more cement binder, this implies that the concrete surface porosity is smaller which results in less surface water absorption. During the experiment, the ISAT values were recorded and a declining trend was observed as the test progressed. Due to the dry concrete surface and the rapid water absorption, this decreasing trend was typical for ISAT measurements where the initial rate of surface water absorption was highest at the start of the test (Balakrishna et al., 2018). Nevertheless, the rate of surface absorption dramatically decreases when the surface becomes saturated with water. Once the concrete has absorbed most of the water, the rate of water intrusion was reduced, resulting in the lowest average ISAT value at 60 minutes.

Table 2.9: ISAT for Different Strength Grade (Balakrishna et al., 2018).

Grade/Mean Target Strength (N/mm^2)	**Average ISAT values ($ml/m^2/s$)**		
	10 minutes	30 minutes	60 minutes
25/32.84	2.90	2.27	1.90
30/37.84	2.83	2.13	1.76
40/47.84	2.70	2.50	2.08

The Initial Surface Absorption Test (ISAT) was also conducted by Fonseka and Nanayakkara (2022) on fly ash concrete with the use of superplasticizer (SP). The results as shown in Figure 2.39 demonstrate that increasing the amount of fly ash in a concrete mix leads to a reduction in ISAT values for fly ash binary cement concretes. When Ordinary Portland Cement (OPC) is partially replaced with fly ash, the surface resistivity of the concrete increases significantly. For instance, water-cured concrete specimens with a w/c ratio of 0.3 and 35 % fly ash replacement showed a fourfold increase in surface resistivity compared to OPC concrete. This enhancement can be attributed to the pozzolanic reaction of fly ash, which refines the pore structure of the concrete and contributes to the densification of the concrete matrix.

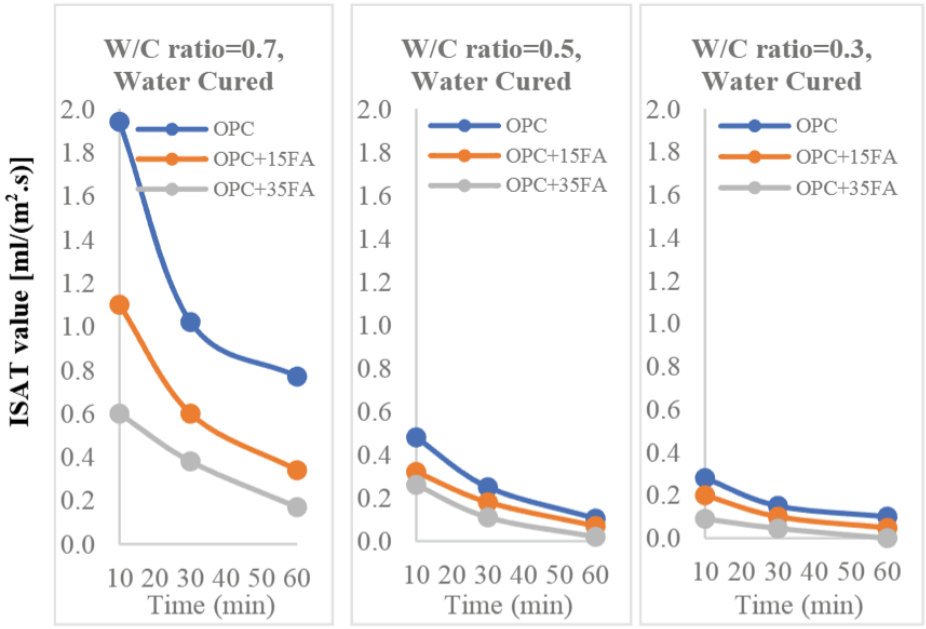

Figure 2.39: ISAT of 0 %, 15 % and 35 % Fly Ash Replacement at Different W/C ratio with SP (Fonseka and Nanayakkara, 2022).

The experiment also showed that concrete with a lower w/c ratio consistently exhibits higher surface resistivity compared to concrete with a higher w/c ratio (Fonseka and Nanayakkara, 2022). This is because a lower w/c ratio reduces the number of interconnected pores within the concrete matrix, thereby enhancing its resistance to water absorption. The reduction in pore connectivity effectively limits pathways for water infiltration, resulting in better performance in the ISAT.

Therefore, in this study, the application of waterproofing admixtures in Grade 35 concrete is expected to considerably lower the Initial Surface Absorption Test (ISAT) values in comparison to the outcomes of previous experiments carried out by Balakrishna et al. (2018) that did not use any waterproofing admixtures or SP.

2.7.5 Sorptivity Test

Saha (2018) conducted an experiment to investigate the effect of fly ash substitution on the sorptivity (capillary water absorption) of concrete over time. In the experiment, concrete mixes were prepared with varying fly ash replacement levels such as 0 % (FA0), 10 % (FA10), 20 % (FA20), 30 % (FA30), and 40 % (FA40) by weight of cement. The mix proportion of each fly ash

replacement is presented in Table 2.10. Sorptivity test is performed at two different curing periods (28-d and 180-d) and the results are shown in Figure 2.40.

Table 2.10: Mix Proportion of Different Fly Ash Replacement (Saha, 2018).

Mix ID	OPC (kg/m^3)	Fly Ash (kg/m^3)	Fine Aggregate (kg/m^3)	Coarse Aggregate (kg/m^3)	W/C Ratio
FA0	400	0	700	1200	0.35
FA10	360	40	700	1200	0.35
FA20	320	80	700	1200	0.35
FA30	280	120	700	1200	0.35
FA40	240	160	700	1200	0.35

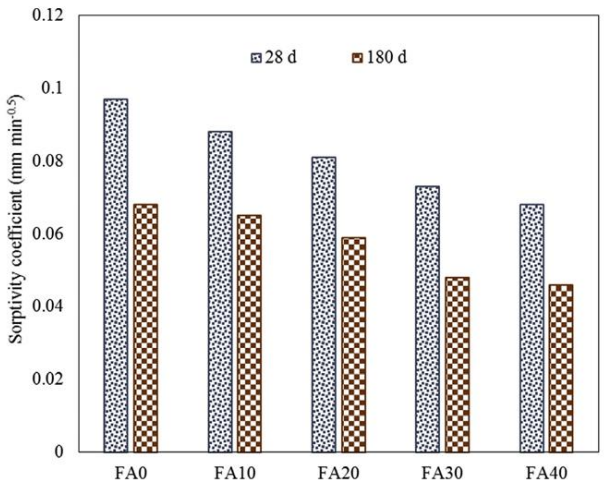

Figure 2.40: Sorptivity Coefficient of Different Fly Ash Replacement (Saha, 2018).

At 28 days, the highest sorptivity coefficient is observed in FA0 (0 % fly ash), indicating that plain concrete absorbs the most water. This is expected because OPC concrete alone results in a more porous microstructure with interconnected capillary pores, allowing greater water penetration. As the fly ash content increases from FA10 to FA40, the sorptivity coefficient gradually decreases. This indicates that fly ash enhances the concrete's resistance to capillary absorption due to both packing effect and pozzolanic reaction which

refines the pore structure by producing additional calcium silicate hydrate gel (Saha, 2018). At 180 days, the sorptivity coefficient is significantly lower across all mixes compared to their respective 28-day values. This reduction indicates that the hydration of cement and pozzolanic reactions of fly ash continue to refine the microstructure over time, making the concrete denser and less permeable. The FA0 mix still exhibits the highest sorptivity, confirming that concrete without fly ash remains the most susceptible to water absorption even after prolonged curing.

A comparison between 28-day and 180-day sorptivity values reveals that the reduction in water absorption is more pronounced in higher fly ash content mixes (FA20, FA30, FA40). This result supports the previous findings done by Misra, Ramteke, and Bairwa (2007) and Xu et al. (2020) which stated that fly ash concrete requires longer curing periods to fully develop its compressive strength and durability benefits.

2.8 Hydrostatic Pressure

2.8.1 Effect of Hydrostatic Pressure

For water-retaining structures, longevity and durability are the major design criteria with the ultimate aim of ensuring the structures are able to retain water without leaking. Hydrostatic pressure is the pressure exerted by a stationary (static) column of water due to its weight. When retaining a large volume of water, the flow of pressurized water through concrete microcracks (Figure 2.41) can deliver an extensive surface force to the crack walls, creating an effect similar to driving a wedge into the substance. Due to the splitting action created by this strain, the existing fractures not only expand wider but also spread faster and penetrate deeper into the concrete matrix. Many studies have been conducted on this phenomenon, which is commonly known as a “wedging” effect. As the microcrack opening width increases, the resistance to outside water permeating into the concrete via the surface crack drops, and this enables penetration of water and more fracture propagation. As a result, concrete will experience a vicious cycle as a result of the spread of fractures, which also raises the permeability coefficient and speeds up the water penetration through concrete (Slowik and Saouma, 2000).

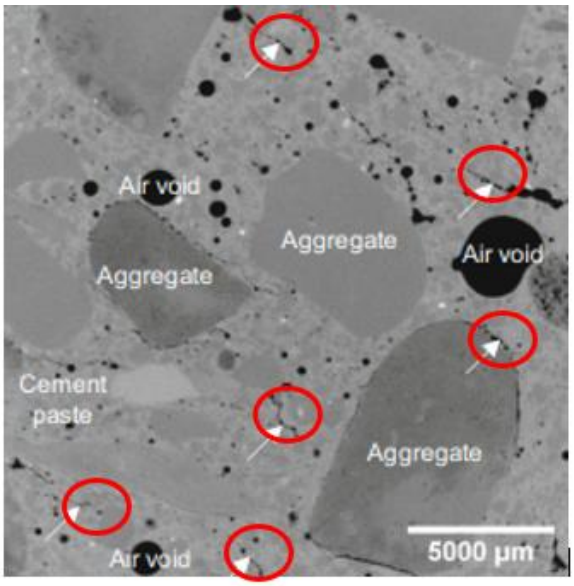

Figure 2.41: Microcracks in Concrete Pointed by Arrow (Mac et al., 2021).

Therefore, the practice of hydrostatic flow testing is crucial for evaluating the reliability and durability of water-retaining constructions, such as swimming pools, reservoirs, dams, and water tanks. In the hydrostatic load test, the concrete is filled with pressurized water and left to be observed over time to detect any possible problems with leakage, distortion, or structural instability as well as to confirm that the structure can sustain the pressures applied by water.

2.8.2 Hydrostatic Flow Test

Zhang et al. (2024) conducted a comprehensive study on the properties of concrete under pressurized water. A water pressure of 0 MPa to 3 MPa was applied to cube concretes with grade C15, C20 and C30 using the constant water pressure loading system as shown in Figure 2.42. After hydrostatic test, CT scanning is conducted to examine the change in internal pore structure. Then, compressive and splitting tensile strength tests were conducted to determine the mechanical properties of the concrete after hydrostatic load test. In this experiment, there were a total of 12 test groups with 6 concrete cubes in each group. Every concrete cube had the same dimension which was 150 mm × 150 mm × 150 mm.

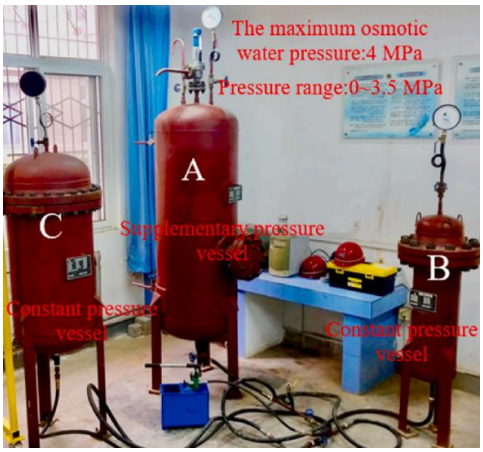

Figure 2.42: Constant Water Pressure Loading System (Zhang et al., 2024).

After hydrostatic load test, the moisture content of the cube concretes under 0, 1 MPa, 2 MPa and 3 MPa was recorded to determine the permeability of concrete under pressure. Figure 2.43 shows that the moisture content of concrete generally increased when the water pressure increased. It was observed that the moisture content in concrete increased drastically when the water pressure was in the range of 0 to 1 MPa. The rate of moisture gain slowly reduced when the water pressure was between 1 to 2 MPa. When low-strength grade concrete's tensile strength was exceeded by high pressure, micropores developed and this increased the internal porosity of the concrete under high water pressure. As a result, the concrete's capacity to withstand water infiltration was compromised. In contrast to low-strength concrete, high-strength grade concrete tends to have a lower moisture content, hence the extent of microcrack development in high-strength grade concrete was less important (Zhang et al., 2024).

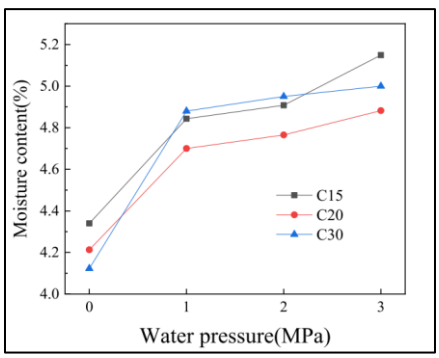

Figure 2.43: Graph of Moisture Content over Water Pressure (Zhang et al., 2024).

As illustrated in Figure 2.44 and Figure 2.45, both the compressive and splitting tensile strength of concrete decreased when the water pressure increased. For C30 concrete, when the water pressure increased from 0 to 3 MPa, the compressive strength showed a decrease of 4.78 %, 9.49 % and 13.22 % whereas the splitting tensile strength decreased by 4.23 %, 8.99% and 12.17 %. It can be concluded that concrete with lower grade suffered a greater strength loss under higher water pressure when compared to high-grade concrete.

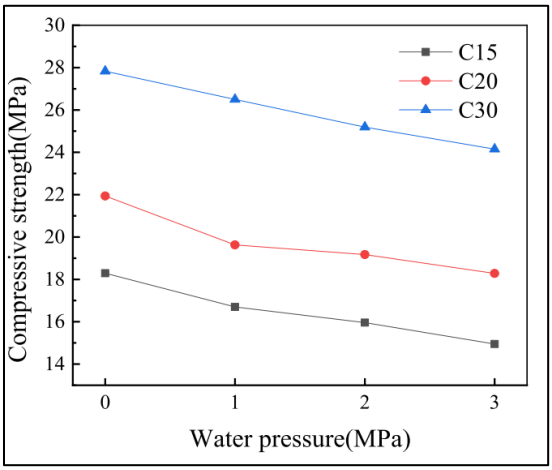

Figure 2.44: Graph of Compressive Strength over Water Pressure (Zhang et al., 2024).

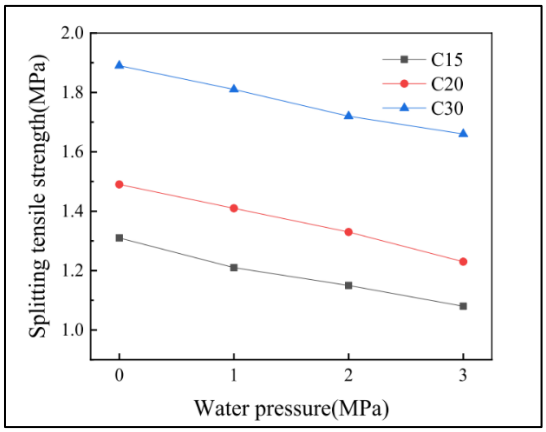

Figure 2.45: Graph of Splitting Tensile Strength over Water Pressure (Zhang et al., 2024).

2.9 Standards for Water-Retaining Structure

Storing and preserving huge amounts of water securely is the main function of water-retaining buildings, such as tanks, reservoirs, and water treatment plants. These structures need to be strong, durable, and water resistant for long-term use. The compressive strength of the concrete used in the construction is critical in assuring these qualities as it directly affects the structure's resistance to external and internal stresses, durability, and water seepage prevention.

The term "compressive strength" describes the concrete's capacity to withstand loads that are imposed on it. Acquiring the necessary compressive strength is important for water-retaining structures because the stored water constantly imposes pressure on the structure. The more concrete's compressive strength, the more pressure it can bear before breaking or failing. According to the JKR standard as well as internationally recognized codes such as BS 8007:1987 (Design of Structures for Retaining Aqueous Liquids) and Eurocode 2 (EN 1992-3:2006), the compressive strength required for concrete used in water-retaining structures should not be lower than 35 MPa at 28 days. In BS 8007:1987, the minimum cement content required for severe exposure conditions is 325 kg/m^3 whereas the water/cement ratio for the fly ash concrete should be at most 0.5 (Andrés, 2020). Concrete with insufficient compressive strength and inadequate mix proportion could result in poor performance, which raises the possibility of leaks, cracks, and even structural failure of water-retaining structures.

On top of that, crack control in water-retaining structures is also particularly emphasised in Eurocode 2-Part 3 and BS 8007:1987 standards. In most cases, the maximum permitted crack width is 0.2 mm to prevent the water-tightness of the structure from being compromised by the cracks. Limiting the size of cracks is crucial since wider fractures could let water soak through and possibly cause the steel reinforcement in the concrete to corrode, which would degrade the structure over time.

2.10 Summary

In a nutshell, incorporating fly ash into the concrete as cement replacement has significant impact on the properties of concrete. After research, fly ash concrete tends to have higher workability, denser concrete matrix, lower bleeding of

water and lower heat of hydration. On top of that, utilizing fly ash in concrete would decrease the initial strength of the concrete due to the pozzolanic reaction that occurred slower but resulted in higher ultimate strength. Based on most of the literature review, even though optimum amount of Class F fly ash replacement for Grade 35 concrete is estimated to fall in the range of 5 to 15 %, this value needs to be confirmed through local practical testing as the behaviour of fly ash concrete can differ greatly depending on several variables, including the quantity and quality of the materials used, chemical composition of fly ash, mix ratio, and the curing procedures. The concrete mix proportion is to be determine in this study using BS method prepared by Building Research Establishment.

For the waterproofing method, sheet membrane method, liquid membrane method and integral mixing method are the main methods used in the industry. Using crystalline waterproofing admixtures of integral mixing method is preferred in many water-retaining building projects since it is not only practical in terms of application but also more affordable than alternative method.

In addition, replacing Ordinary Portland Cement with fly ash significantly increased surface water resistivity, particularly in water-cured concrete with lower w/c ratio which demonstrated a significant ISAT improvement compared to plain cement concrete. ISAT value decreased with increasing concrete grade due to a more compact and denser concrete matrix. Similar results are obtained for the water absorption test and sorptivity test at which higher fly ash replacement showed lower water absorption.

The effect of hydrostatic pressure on concrete is also studied. Continuous exposure to water pressure can increase the risk of water ingress into the concrete matrix, especially through surface cracks and interconnected pores. Over time, this can alter the internal pore structure, leading to increased permeability and making the concrete more susceptible to chemical attacks such as sulphate or chloride penetration.

CHAPTER 3

METHODOLOGY AND WORK PLAN

3.1 Introduction

A thorough and systematic method was required for correlating sustainable fly ash concrete with a 35 MPa compressive strength that was specifically designed for water-retaining structures. Partially substituting some of the cement with fly ash ensured that the final concrete mix not only satisfied the structural requirements but also promoting environment sustainability by reducing the use of cement. The approach tackled the technical requirements of building a sustainable and long-lasting water-retaining structure. Compression test, water absorption test and sorptivity test were done according to ASTM standards as ASTM standards were widely accepted and dominant in concrete material testing, especially in research and industry applications. However, ISAT was done based on British Standard as ASTM did not provide equivalent guidelines for ISAT.

3.2 Operational Workflow

Proper material preparation was a crucial first step in any concrete research project. All necessary materials were weighed and prepared, including cement, coarse and fine aggregates, water, fly ash, and waterproofing admixture. The concrete mix was designed based on the British method prepared by Building Research Establishment. After determining the proportion of each material, the trial mix was performed and cast in three cylinder moulds and cured for 28 days. Compression test was conducted based on ASTM C39 (2023) to ensure that the designed concrete mix was able to achieve the targeted strength of 35 MPa. Three concrete cylinder samples were tested, and the average value was obtained. If the concrete samples fail the compression test, a new concrete mix is to be designed until the concrete produced can achieve the required strength of 35 MPa. Otherwise, the experiment proceeds.

The next step of the experiment was to determine the optimum amount of fly ash to replace cement while still maintaining the compressive strength of 35 MPa. The determination process started by replacing 5 %, 10 %, 15 % and

20 % of cement with fly ash. Three concrete cylinder samples were prepared for each fly ash replacement and tested under ASTM C39 (2023). The mix with specific fly ash replacement that produced the highest average compressive strength will be concluded as the optimum amount of fly ash for this study. If the compressive strength of all the fly ash concrete cannot achieve 35 MPa, the concrete mix was redesigned to ensure that the fly ash concrete can achieve at least 35 MPa at 28-days curing.

Following that, waterproofing additive was added to the fly ash concrete to increase its durability. The main objective of this stage was to assess the capability of the fly ash concrete to resist the water penetration, which was crucial to the long-term performance of water-retaining structures. The optimized fly ash concrete mix was combined with the waterproofing additive and cast into cube samples to undergo water absorption test (ASTM C642, 2022) and sorptivity test (ASTM C1585). Last but not least, ISAT was also conducted on cube samples according to BS 1881-Part 208 (British Standards Institution, 1996) to determine the surface water permeability of the fly ash concrete. All the tests were conducted on samples with and without the waterproofing admixture or fly ash to allow direct comparison. Each test was repeated with 3 concrete samples for each batch and the average results were obtained.

After all necessary data had been obtained, a comprehensive analysis was conducted whereby the compressive strength and durability of different batches of concrete samples were compared to examine the waterproofing capability of the fly ash concrete. Lastly, the conclusion and recommendations were provided to assist in the continuous development of long-lasting, environmentally friendly concrete mixtures that satisfy contemporary building requirements. The overall workflow is presented in Figure 3.1(a) and 3.1(b).

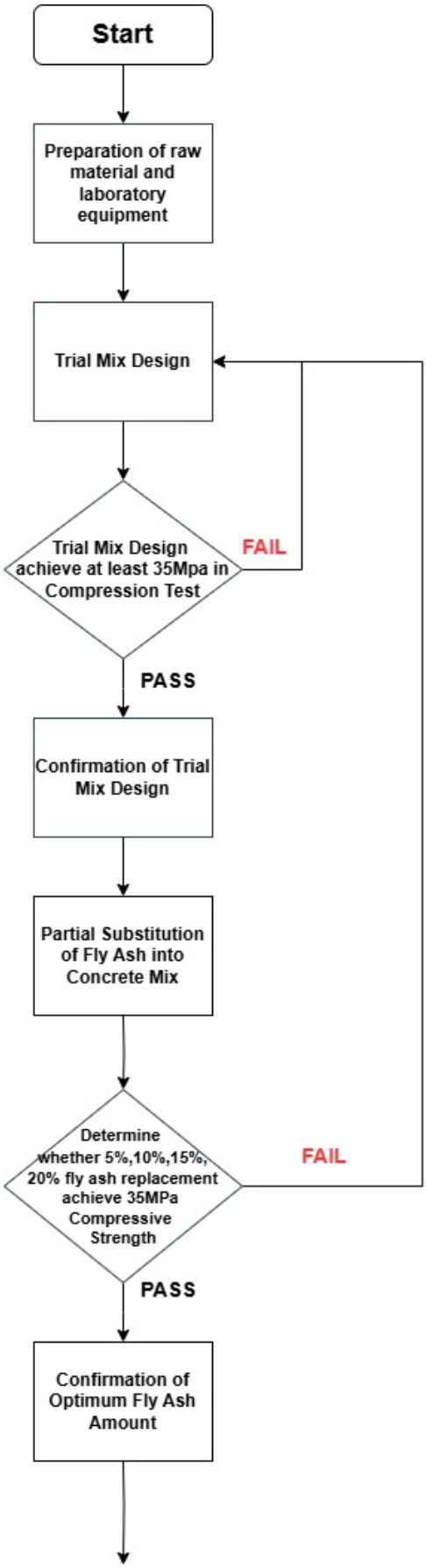
Start
Preparation of raw material and laboratory equipment
Trial Mix Design
Trial Mix Design achieve at least 35Mpa in Compression Test
FAIL
PASS
Confirmation of Trial Mix Design
Partial Substitution of Fly Ash into Concrete Mix
Determine whether 5%,10%,15%, 20% fly ash replacement achieve 35MPa Compressive Strength
FAIL
PASS
Confirmation of Optimum Fly Ash Amount

(a)

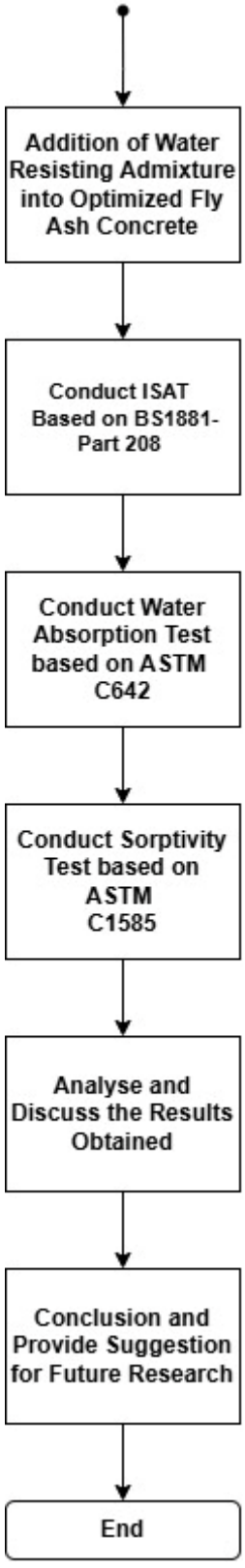

(b)

Figure 3.1: Overall Workflow (a) Part 1, (b) Part 2.

3.3 Raw Material

The materials used in producing the fly ash concrete in this study were stated below:

1. Cement
2. Aggregate
3. Water
4. Fly Ash
5. Waterproofing Admixture (Sika)

3.3.1 Cement

For this study, Type I Ordinary Portland Cement produced by YTL Cement was used. Type I OPC from YTL Cement, as shown in Figure 3.2, was named "Orang Kuat" and complied with MS EN 197-1:2014 CEM I 52.5N. Since there was no exposure to sulphate, Type I cement was suitable for producing fly ash concrete. For optimum performance of concrete, the cement was oven-dried if any moisture was found. This was because moisture in cement could cause premature hydration, which significantly reduced the effectiveness of the cement. Based on ASTM C150 (2022), concrete produced using Type I cement was required to have a minimum compressive strength of 7 MPa at 3 days of curing and 12 MPa at 7 days of curing. According to BS8007:1987 (Andrés, 2020), the cement content for water-retaining structures was to be at least 325 kg/m^3 for non-reinforced concrete.

Figure 3.2: Orang Kuat Type 1 OPC.

3.3.2 Aggregate

Crushed coarse and fine aggregates were used in this study to produce fly ash concrete. The aggregate was sieved to determine the percentage of fine and coarse aggregates used, as the size of aggregate had a major impact on concrete strength. According to ASTM C33 (2008), aggregates were classified based on their size. Particles greater than 4.75 mm were categorized as coarse aggregate (Figure 3.3 (a)), while those smaller were classified as fine aggregate (Figure 3.3 (b)). To maintain consistency and prevent variations in the water-cement ratio, the aggregates were oven-dried if moisture was detected. This step ensured that the water content in the mix remained controlled, preventing excess water that could negatively impact strength and durability. For this study, the aggregate used had a relative density of 2.7, and the maximum aggregate size allowed was 20 mm.

(a) (b)

Figure 3.3: (a) Coarse Aggregate, (b) Fine Aggregate.

3.3.3 Water

Water served as a lubricant in the concrete mix, and the amount of water in the mixture influenced the workability of the concrete. The long-term durability of the concrete could be impacted by contaminants that interfere with the cement hydration process. Therefore, as per ASTM 1602 (2022), tap water was accepted for use in this study.

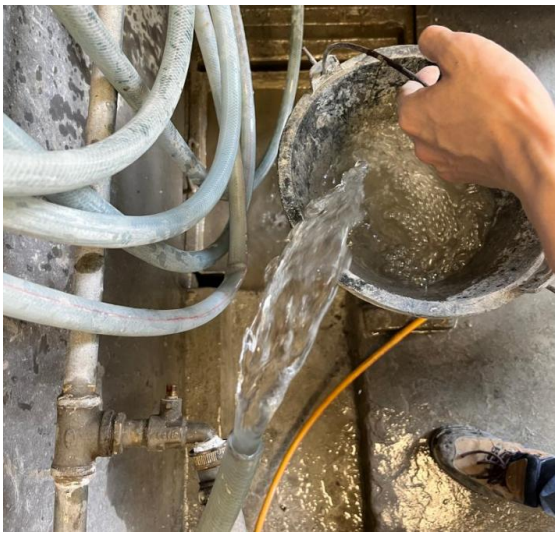

Figure 3.4: Tap Water.

3.3.4 Fly Ash

In this study, the fly ash used was produced by Sultan Abdul Aziz Power Plant located in Kapar as shown in Figure 3.5. The fly ash was dried in an oven at 100 °C for 24 hours to remove any moisture. The size range of the filler was 45 to 170 µm. Based on the XRF study presented in Table 3.2, the fly ash was categorised as Class F according to ASTM C618 as its total content of for SiO_2, Fe_2O_3 and Al_2O_3 was 83.09 %, which was greater than 70 %.

Figure 3.5: Fly Ash from Sultan Abdul Aziz Power Plant.

Table 3.1: Chemical Composition of Class F Fly Ash from Sultan Abdul Aziz Power Plant (Mustafa Al Bakri et al., 2013).

Chemical Composition	Percentage (%)
SiO_2	52.11
Al_2O_3	23.59
Fe_2O_3	7.39
TiO_2	0.88
CaO	2.61
MgO	0.78
Na_2O	0.42
K_2O	0.8
P_2O_5	1.31
SO_3	0.49
MnO	0.03

3.3.5 Waterproofing Admixture

The advanced concrete admixture Sika WT-220 PMY (Figure 3.6) was made up of a combination of cement, amino alcohols, and other active components that could improve the capability of concrete for self-healing and waterproofing. The active components produced non-soluble compounds in the pore and capillary structure of the concrete, permanently sealing it and preventing the entry of water. It was used in a wide range of construction applications such as manholes, tunnels, water tanks, swimming pools, canals, and culverts (Sika Malaysia, 2024).

Figure 3.6: Sika WT-220 PMY.

Sika WT-220 PMY is the waterproofing admixture that was used in this study. According to Sika Malaysia (2024), the density of cement used should be at least 350 kg/m^3 and the water/cement ratio should be at most 0.45 for the optimal performance of Sika® WT-220 PM. The recommended dosage of Sika WT-220 PMY depended on the concrete volume in which 3.5 kg of Sika WT-220 PMY was to be used for 1 m^3 of concrete. Curing methods such as water submerging method, ponding, water spraying, and polythene sheet was recommended.

3.4 Concrete Mix Design

In this study, the concrete mix proportion was designed based on the British Standard prepared by Building Research Establishment that was published with the title of "Design of Normal Concrete Mixes" as shown in Figure 3.7.

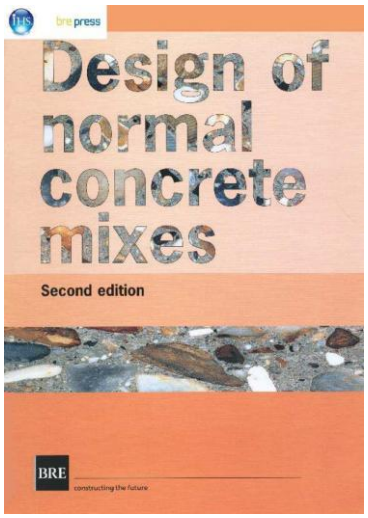

Figure 3.7: Design of Normal Concrete Mixes by BRE (Marsh, 1988).

In this study, a characteristic strength of 35 MPa was to be achieved at 28 days with 1 % of proportion defective. Based on Figure 3.8, the standard deviation of 8 MPa was obtained, and the target mean strength of 53.64 MPa was calculated by using Equation 3.1.

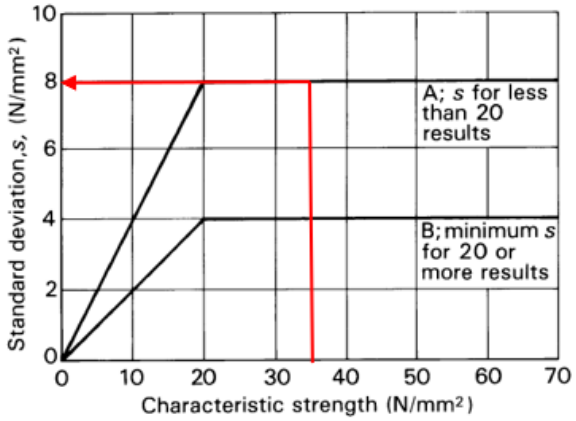

Figure 3.8: Standard Deviation Graph (Marsh, 1988).

$$F_m = f_c \times 1.64s \quad (3.1)$$

where

f_m = Target Mean Strength

f_c = Characteristic Strength

s = Standard Deviation

Since the cement used was of 52.5 strength class and the aggregate used was crushed aggregate, an approximate compressive strength of 55 MPa at 28 days based on 0.5 water/cement ratio was obtained from Table 3.2. Based on Figure 3.9, a water/cement ratio is of 0.51 was obtained. However, water cement ratio of 0.45 was used in the experiment due to the requirement of Sika® WT-220 PMY. The free water content was determined as 210 kg/m^3 from Table 3.3 with a design slump of 30 to 60 mm and a maximum aggregate size of 20 mm. The cement content of 466.7 kg/m^3 was found by dividing the free water content by the water/cement ratio while the wet concrete density of 2400 kg/m^3 was found in Figure 3.10 based on relative aggregate density of 2.7.

Table 3.2: Table of Approximate Compressive Strength Based on 0.5 W/C ratio (Marsh, 1988).

Cement strength class	Type of coarse aggregate	Compressive strengths (N/ mm²) Age (days) 3	7	28	91
42.5	Uncrushed	22	30	42	49
	Crushed	27	36	49	56
52.5	Uncrushed	29	37	48	54
	Crushed	34	43	55	61

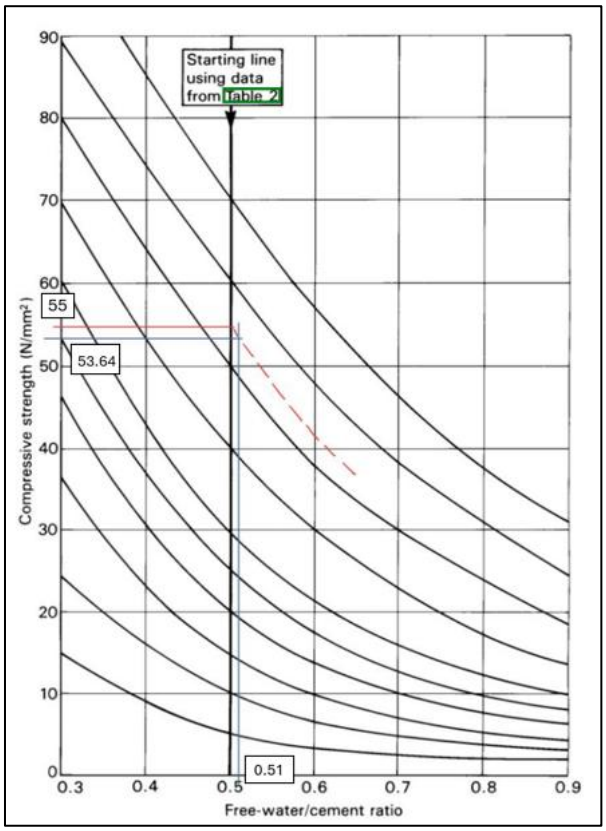

Figure 3.9: W/C Ratio Graph (Marsh, 1988).

Table 3.3: Free Water Content Table (Marsh, 1988).

Slump (mm) / Vebe time (s)		0–10 >12	10–30 6–12	30–60 3–6	60–180 0–3
Maximum size of aggregate (mm)	Type of aggregate				
10	Uncrushed	150	180	205	225
	Crushed	180	205	230	250
20	Uncrushed	135	160	180	195
	Crushed	170	190	210	225
40	Uncrushed	115	140	160	175
	Crushed	155	175	190	205

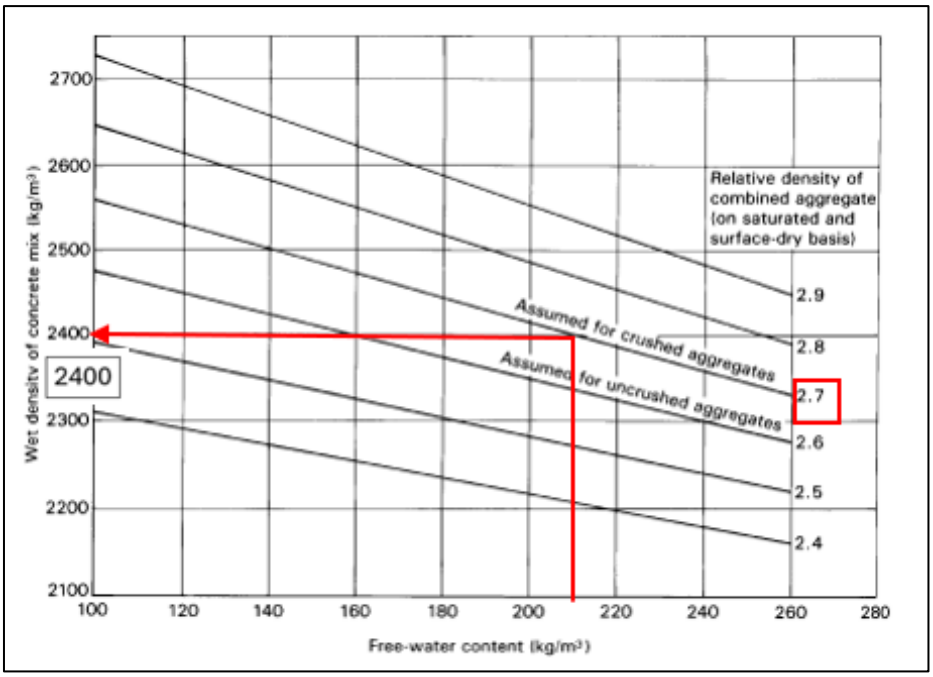

Figure 3.10: Wet Concrete Density Graph (Marsh, 1988).

After conducting the sieve test, it was found that 60 % of the fine aggregate had passed the 600 µm sieve. Therefore, 32 % of the fine aggregate was determined based on Figure 3.11. Fine and coarse aggregate content of 551.4 kg/m^3 and 1171.9 kg/m^3 were obtained respectively. Table 3.4 summarized the design parameters, and the concrete mix proportion is shown in Table 3.5.

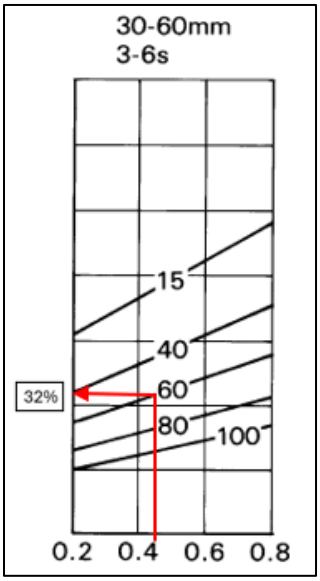

Figure 3.11: Fine Aggregate Percentage Graph (Marsh, 1988).

Table 3.4: Summary of Concrete Mix Design Parameter.

No.	Description	Results
1	Compressive Strength with 5% tolerance (K=1.64)	35 MPa at 28 days
2	Standard Deviation	8 MPa
3	Target Mean Strength	53.64 MPa
4	Cement Strength Class	52.5
5	Type of Aggregate	Crushed
6	Water/Cement Ratio	0.45
7	Slump	30-60 mm
8	Max Aggregate Size	20 mm
9	Free Water Content	210 kg/m^3
10	Cement Content	466.7 kg/m^3
11	Relative Density of Aggregate	2.7
12	Wet Concrete Density	2400 kg/m^3
13	Total Aggregate Content	1723.3 kg/m^3
14	% of Fine Aggregate	32 %
15	Fine Aggregate Content	551.4 kg/m^3
16	Coarse Aggregate Content	1171.9 kg/m^3

Table 3.5: Trial Mixture Proportion.

Mix Proportion	Cement (kg)	Water (kg)	Fine Aggregate (kg)	Coarse Aggregate (kg)
Per 1 m^3	466.7	210	551.4	1171.9
Ratio	1	0.45	1.18	2.51

3.5 Sample Specification

Three cylinder concrete samples with 100 mm diameter and 200 mm height were made using the mix proportion shown in Table 3.6 and Table 3.7. 15 % of wastage was taken into consideration since the concrete was prepared by hand mix due to the relatively small amount. The calculation of the required volume of concrete is shown below and the mix proportion to produce three concrete cubes and cylinders are shown in Table 3.6.

Table 3.6: Volume of Cylinder and Cube Concrete Sample.

	Cylinder	Cube
Dimension	100 mm (diameter) and 200 mm (height)	150 mm per side
Volume of One Concrete Sample	$\pi\ (0.05\ \text{m})^2 \times\ (0.2\ \text{m}) = 0.00157\ \text{m}^3$	$0.15m \times 0.15 \times 0.15m = 0.00338\ \text{m}^3$
Volume of Three Concrete Samples	$0.00157\ \text{m}^3 \times 3 = 0.00471\ \text{m}^3$	$0.00338\ \text{m}^3 \times 3 = 0.0101\ \text{m}^3$
Volume of Three Concrete Samples with 15 % Wastage	$0.00471\ \text{m}^3 \times 1.15 = 0.00542\ \text{m}^3$	$0.01014\ \text{m}^3 \times 1.15 = 0.0112\ \text{m}^3$

Table 3.7: Trial Mixture Proportion for 3 Concrete Cylinder and Cube.

Mixed Proportion	Cement (kg)	Water (kg)	Fine Aggregate (kg)	Coarse Aggregate (kg)
Per 1 m^3	466.7	210	551.4	1171.9
Per 0.00542 m^3 (3 Cylinder)	2.53	1.14	2.99	6.35
Per 0.0112 m^3 (3 Cube)	5.23	2.35	6.18	13.13

After the control concrete mix design proved to achieve the minimum compressive strength of 35 MPa at 28 days of curing, the substitution process started. According to BS8110-Part 1 (British Standards Institution, 1997), the targeted mean fly ash replacement should be less than 35% for water-retaining structures. Therefore, based on the literature review done by other researchers, Class F fly ash was set to replace 0 %, 5 %, 10 %, 15 % and 20 % of the cement content in the trial mix. Based on the recommendations from Sika Company, 3.5 kg of Sika® WT-220 PMY was used with 1 m^3 of cement. The fly ash content for each replacement percentage and the content of Sika® WT-220 PMY is shown in Table 3.8.

Table 3.8: Fly Ash and Sika Content for Cube and Cylinder Samples.

Cement Content (kg)	Fly Ash Replacement (%)	Fly Ash Content (kg)	Sika® WT-220 PMY Content (kg)
2.53 (3 Cylinder)	0	0	0.019
	5	0.127	
	10	0.253	
	15	0.380	
	20	0.506	
5.23 (3 Cube)	0	0	0.039
	5	0.262	
	10	0.523	
	15	0.785	
	20	1.046	

The average value of the concrete's compressive strength should be obtained by conducting three concrete cylinder samples for every percentage of fly ash substitution. The fly ash replacement that produced the highest average compressive strength results was concluded as the optimum amount of fly ash for this study and was used for the following experiment process.

3.6 Concrete Casting

All dry ingredients, such as aggregates, fly ash, and cement, were precisely weighed and stirred in dry condition to guarantee uniform material distribution before the mixing process began as shown in Figure 3.12. The purpose of this initial dry mixing was to make sure that the fly ash could be evenly distributed throughout the slurry and to prevent the formation of lumps.

Figure 3.12: Mixing of Dry Raw Materials.

After mixing the dry ingredients well, clean tap water was gradually added while the mixture was stirred constantly. Sika® WT-220 PMY was added to the mixture at the last step and was evenly dispersed throughout the concrete to produce the desired performance qualities. The amount of Sika® WT-220 PMY added was based on the calculated dosage of Sika for concrete cube and cylinder samples. After the mixing process, the concrete mixture was then poured into moulds. The moulds were coated with a layer of oil prior to the pouring of concrete to prevent the adhesion of concrete on the surface of the and to ensure the easy removal of concrete after setting. The concrete mixture was poured in three layers in which the concrete was tamped 25 times per layer to remove any air pockets, ensuring the concrete produced was dense and homogenous. The mixture was then cast into three concrete cylinder moulds with 200 mm height and 100 mm diameters as shown in Figure 3.13. A trowel was used to level the concrete surface in the moulds to ensure flat surface of concrete.

Figure 3.13: Concrete Casted into Cylinder Moulds.

3.7 Concrete Curing

After 24 hours of setting, the hardened concrete cylinders were carefully demoulded and labelled accordingly. The demoulded concrete cylinders are presented in Figure 3.14. Then, all concrete cylinders were put in a water tank as shown in Figure 3.15 to undergo curing process. The curing process lasted

for 28 days and the water temperature in the tank was in the range of $23 \pm 2°C$, as stated in ASTM 511 (2021).

Figure 3.14: Demoulded Concrete Cylinder Samples.

Figure 3.15: Concrete Curing in Water Tank.

After 28 days of curing, the concrete cylinder samples were taken out from the water tank and dried using an air compressor as shown in Figure 3.16

to ensure the concrete cylinder samples were in saturated surface dry condition before proceeding for testing.

Figure 3.16: Concrete Samples Dried Using Air Compressor.

3.8 Test Method

3.8.1 Compressive Strength Test

After being prepared to a saturated surface dry (SSD) condition, the concrete cylinder samples were carefully placed on the compression testing machine's plate, as illustrated in Figure 3.17. The compression machine was calibrated to match the dimensions of the concrete cylinders being tested. This ensured that the equipment applied pressure consistently and accordingly to the standards. The compression rate was precisely set at 2 kN/s to provide a controlled and gradual application of force, reducing the likelihood of sudden failure or inaccuracies due to shock loading. The entire test was done based on ASTM C39 (2023) and ended when the concrete cylinder samples failed. The maximum load sustained by each cylinder at the point of failure was recorded. The test was repeated for three concrete cylinder samples from the same batch and the average compressive load sustained by these three samples was calculated.

Figure 3.17: Setup of Compressive Strength Test.

3.8.2 Initial Surface Absorption Test (ISAT)

The Initial Surface Absorption Test (ISAT) was designed to evaluate the surface permeability of concrete, which was a critical factor for water-retaining structures. According to BS 1881-208 (British Standards Institution, 1996), concrete cube samples that had been cured for 28 days were used in this ISAT and the dimension of the concrete cube samples was $150\ \text{mm} \times 150\ \text{mm} \times 150\ \text{mm}$. Before conducting the test, the concrete cube sample was oven-dried at a temperature of $105\ °C \pm 5°C$ for at least 24 hours (Figure 3.18) until a constant weight to remove the moisture inside the concrete.

Figure 3.18: Concrete Samples in Oven.

Then, the concrete cube sample was left in a dry environment to cool down to room temperature. The concrete surface that was tested was ensured to be flat and clean to avoid any external factors affecting water absorption. A specially designed ISAT apparatus, consisting of a graduated capillary tube connected to a rubber sealing ring, was attached to the concrete surface using a watertight seal. Water was introduced into the apparatus and maintained at a constant pressure of 200 mm $\pm$ 20mm of water. The rate of water absorption was measured at different time intervals, typically 10 minutes, 30 minutes, 1 hour, and 2 hours. The complete setup of the ISAT is shown in Figure 3.19.

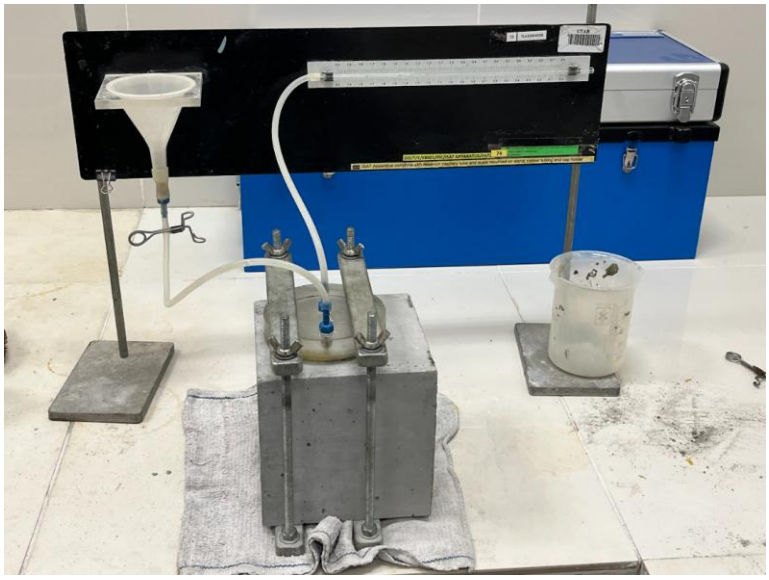

Figure 3.19: Setup of ISAT.

During the Initial Surface Absorption Test, the procedure for recording measurements required careful handling of the capillary tube to ensure accurate readings. Just before each specified interval (10 minutes, 30 minutes, 1 hour, and 2 hours), the capillary tube was slightly lowered to allow water to completely fill it, ensuring that the meniscus reached zero on the division scale. This step was crucial for maintaining consistency in measurements and ensuring that the test began with a full column of water in the capillary tube.

Once the exact time of the specified interval was reached, the capillary tube was clamped back to stop additional water from flowing from the reservoir into the concrete sample. At that moment, the movement of the meniscus within the division scale of the capillary tube was observed and recorded for 5 seconds.

Each division on the scale corresponded to 0.01 units, providing a fine level of precision in measuring water absorption. The amount of water absorbed in this short period helped determine the recommended recording time for the permeability of the concrete sample, as outlined in Table 3.9.

Table 3.9: Determination of Period of Movement (British Standards Institution, 1996).

No. of Scale Division Moved in 5 seconds	**Period during which Movement is Measured**
< 3	2 minutes
3 to 9	1 minute
10 to 30	30 seconds
> 30	Record initial surface absorption as more than $3.60ml/m2/s$

The number of scale divisions moved during the recommended recording time was noted, and if the reading was taken over a 2-minute or 30-second period, it was adjusted by multiplying the divisions by 0.5 or 2 respectively. This ensured that all results were standardized to a 1-minute period, providing consistency in permeability assessment. The initial surface absorption rate (ISAR) was then determined by multiplying the number of scale divisions by 0.01 and the final value was expressed in ml/m²/s. This calculated value represented the rate at which water was absorbed into the concrete surface under controlled conditions.

A key evaluation point occurred at the 10-minute interval. If the recorded absorption rate at this stage is below 0.05 mL/m²/s, the test should be stopped, and the result should be recorded as “concrete too impermeable to be sensitive to a longer-term test.” This indicated that the concrete has very low permeability, making further measurements unnecessary. On the other hand, if the 10-minute reading exceeds 3.60 mL/m²/s, the test should also be stopped, with the result recorded as “concrete too permeable to be within the sensitivity of the test method.” This suggested that the material has excessively high absorption, falling outside the reliable range of the ISAT.

3.8.3 Sorptivity Test

The sorptivity test, as described in ASTM C1585 (2020), was a standardized method used to measure the rate of water absorption by capillary action in hydraulic-cement concrete under unsaturated conditions. The test involved preparing cylindrical or prismatic concrete specimens, typically $100\ \text{mm} \pm 6\text{mm}$ in diameter and 50 mm in height which were cured for at least 28 days. Before testing, the specimens were oven-dried at 50°C (±2°C) until they reached a constant mass, ensuring that internal moisture does not interfere with absorption measurements. After cooling, the specimen's bottom surface was exposed to a shallow layer of water (1–3 mm deep). The complete setup is illustrated in Figure 3.20.

Figure 3.20: Setup of Sorptivity Test.

The mass of the specimen was recorded at predetermined time intervals, such as 1, 5, 10, 20, 30, 60, and 120 minutes. Water absorption was calculated as the mass of water absorbed using Equation 3.2. A graph of water absorption versus the square root of time was plotted. Data points corresponding to times where the plot showed a clear deviation or change in slope were omitted to ensure a linear relationship. The sorptivity coefficient ($\text{mm}/\text{min}^{0.5}$) was obtained as the slope of the best-fit straight line through the remaining linear portion of the plot.

$$I = \frac{M}{A \times \rho} \tag{3.2}$$

where

$I = \text{Absorption (mm)}$

$M = \text{Mass of Water Absorbed (g)}$

$A = \text{Exposed Surface Area } (mm^2)$

$\rho = \text{Density of Water } (g/mm^3)$

3.8.4 Water Absorption Test

According to ASTM C642 (2022), water absorption test was conducted on cube samples with a side dimension of 150 mm which needed to be cured for 28 days. This test aimed to assess the total porosity and overall permeability of concrete under fully submerged conditions. After curing, the samples were taken out and oven-dried at a temperature of approximately 105°C for 24 hours or until they reached a constant weight to remove all free water from the pores of the concrete, ensuring that subsequent measurements reflect only the absorption of water during the test. Once dried, the samples were cooled to room temperature. The dried concrete samples were then fully submerged in water as shown in Figure 3.21 for a period of time, commonly 24 or 48 hours, depending on the testing standard. The water temperature was maintained at a controlled level, typically around 20°C to 25°C, to ensure consistency.

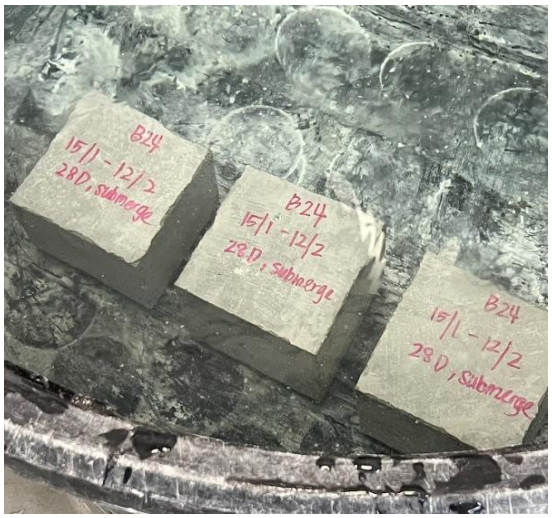

Figure 3.21: Immersion of Concrete during Water Absorption Test.

After the submersion period, the samples were carefully removed from the water. Excess surface water was gently wiped off with a damp cloth to avoid inaccuracies caused by external water droplets. The weight of the saturated samples was then measured immediately to identify the total water absorbed by the concrete. The water absorption of the concrete samples was calculated using Equation 3.3:

$$\text{Water Absorption (\%)} = \frac{\text{Saturated Weight} - \text{Dry Weight}}{\text{Dry Weight}} \times 100\% \qquad (3.3)$$

3.9 Sustainability and Cost Saving

To evaluate the environmental and economic benefits of partially replacing cement with fly ash in concrete production, a comprehensive assessment of CO_2 emissions and material costs was conducted. The methodology involved a step-by-step calculation based on the concrete mix design, emission factors of materials involved, and prevailing market prices for cement and fly ash.

After the confirmation of cement content in trial mix proportion and optimum fly ash replacement for this study, mission factors were applied to quantify the amount of carbon dioxide emitted per kilogram of cement manufactured. Based on research from Bakhtyar, Kacemi and Nawaz (2017), approximately 900 kg of CO_2 is emitted per ton of cement produced. Using these values, the total percentage of CO_2 emissions can be estimated using Equation 3.4.

$$CO_2 \text{ Emissions (kg)} = \frac{m_c \times (100\% - R)}{100\%} \times \frac{900}{1000} \qquad (3.4)$$

where

m_c = Mass of Cement per m^3 in Trial Mix (kg)

R = Optimum Fly Ash Replacement Level (%)

In parallel with the environmental analysis, a cost-saving evaluation was also conducted. This requires identifying the market price of OPC and fly ash. Based on Department of Statistic Malaysia (2025), the cost of OPC is

approximately RM 23.65 per 50 kilogram which equivalent to RM 0.47 per kilogram, while fly ash is significantly cheaper at around RM 0.11 per kilogram (IMARC Group, 2025). Using these rates, the binder material cost can be calculated using Equation 3.5.

$$\text{Binder Cost (RM)} = \left(\frac{m_c \times (100\% - R)}{100\%} \times 0.47\right) + \left(\frac{m_c \times R}{100\%} \times 0.11\right) \quad (3.5)$$

where

m_c = Mass of Cement per m^3 in Trial Mix(kg)

R = Optimum Fly Ash Replacement Level (%)

CHAPTER 4

RESULTS AND DISCUSSIONS

4.1 Introduction

This research investigated the performance of various concrete mixes to determine the optimal fly ash substitution and assess the durability of fly ash concrete. The study began with the establishment of a control mix (0 % FA) to ensure compliance with the minimum compressive strength requirement of 35 MPa for water-retaining structures, as specified in BS 8007:1987 and EN 1992-3:2006. The concrete mix design followed a predetermined proportion of 1:0.45:1.18:2.51 (cement : water : fine aggregate : coarse aggregate), formulated based on the British standard developed by the Building Research Establishment.

Once the control mix was verified to achieve a minimum compressive strength of 35 MPa, fly ash was introduced as a partial replacement for cement at incremental levels of 5 %, 10 %, 15 %, and 20 % by weight. This phase of the study aimed to evaluate the influence of fly ash on the mechanical properties of concrete, with a particular focus on compressive strength development. The optimal fly ash content was determined based on the highest 28-day compressive strength above 35 MPa , ensuring that the replacement enhances the durability without compromising structural integrity.

After identifying the optimal fly ash replacement, additional testing was conducted by incorporating Sika WT-220 PMY into the modified concrete mix. The durability of the optimized mix was assessed through water resistance evaluations, including ISAT, water absorption test, and sorptivity test. These tests provided valuable insights into the permeability characteristics of the fly ash concrete with or without Sika WT-220 PMY, determining its suitability for water-retaining structures and other applications requiring enhanced durability.

4.2 Workability and Density

The results presented in Table 4.1 and Figure 4.1 indicated a clear trend of increasing slump values with higher fly ash replacement levels. The slump value for the control mix (0 % FA) was recorded at 32 mm, and as the fly ash content increased to 5 %, 10 %, 15 %, and 20 %, the slump values progressively rose to

35 mm, 40 mm, 46 mm, and 51 mm, respectively. Highest slump value of 51 mm was achieved at 20 % fly ash replacement, representing a significant 59.38 % increase compared to the control mix.

Table 4.1: Slump Value for 0 %, 5 %, 10 %, 15 % and 20 % Fly Ash Replacement.

Fly Ash Replacement	Slump Value (mm)
0%	32
5%	35
10%	40
15%	46
20%	51

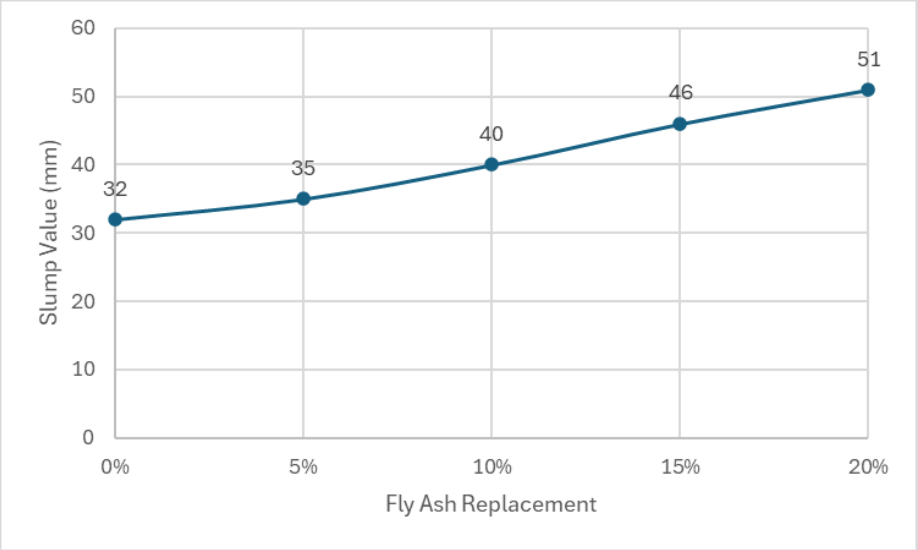

Figure 4.1: Graph of Slump Value against Fly Ash Replacement.

The observed trend aligns with the previous research findings by Nath and Sarker (2011), which indicated that the incorporation of fly ash generally enhances the workability of fresh concrete. This improvement in workability is primarily attributed to the physical properties of fly ash. The spherical shape of fly ash particles functions as tiny ball bearings between cement grains and aggregates, reducing internal friction and facilitating smoother movement within the concrete mix (Yurdakul et al., 2014). This effect enhances the overall flowability of the mix, making it easier to handle, place, and compact.

Additionally, fly ash has a lower water demand compared to cement, which allows a greater portion of the mixing water to remain unbound and available within the concrete matrix (Yurdakul et al., 2014). This surplus water further enhances the workability of the concrete mix, ensuring better cohesion and minimizing the likelihood of harsh or dry mixes.

Next, the results illustrated in Figure 4.2 indicated a clear trend in the variation of saturated surface-dry (SSD) density with different percentages of fly ash replacement in concrete. Initially, the SSD density showed a steady increase from 2367 kg/m^3 at 0 % fly ash to 2392 kg/m^3 at 5 % and continued rising to 2411 kg/m^3 at 10 %, reaching the highest value of 2415 kg/m^3 at 15 % replacement. This progressive increase in density is attributed to the filler effect of fly ash, where its fine particles occupy the voids between larger cement and aggregate particles, leading to a denser and more compact concrete matrix (Elrahman and Hillemeier, 2014). Supporting this observation, the scanning electron microscope (SEM) analysis presented in Figure 4.3 confirmed that concrete containing fly ash exhibited a denser microstructure compared to the control sample without fly ash. Additionally, the pozzolanic reaction of fly ash enhances the packing and reduces the porosity within the concrete, contributing to a higher SSD density.

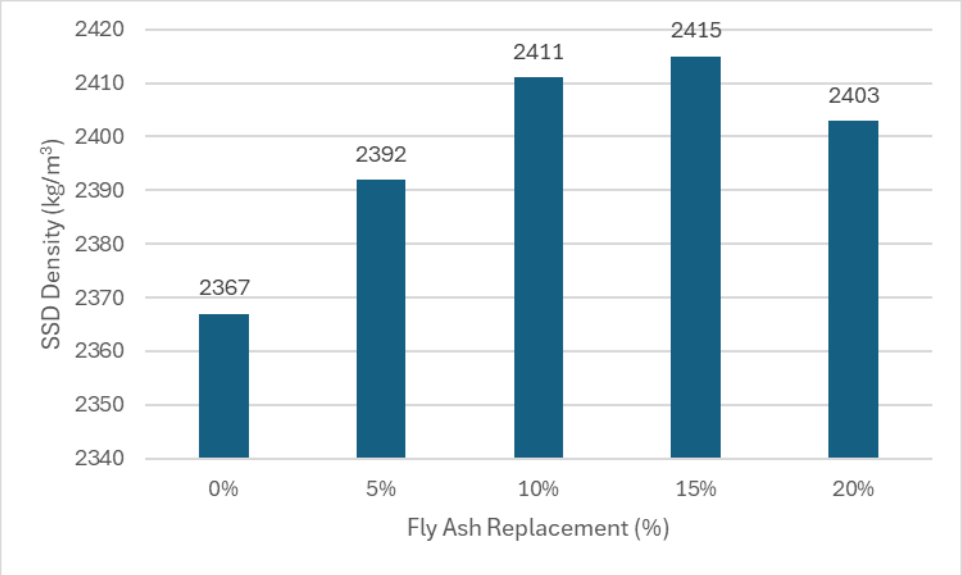

Figure 4.2: Graph of SSD Density against Fly Ash Replacement.

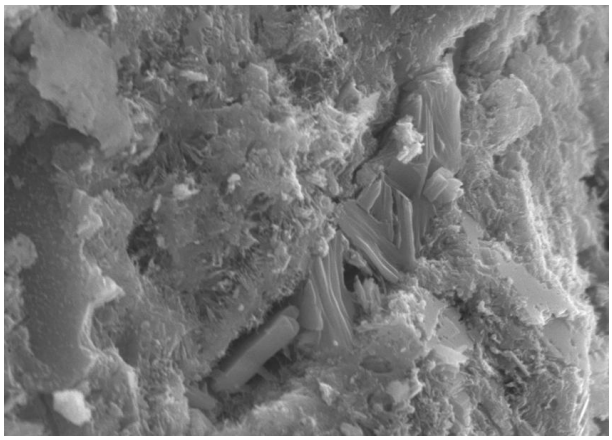

(a)

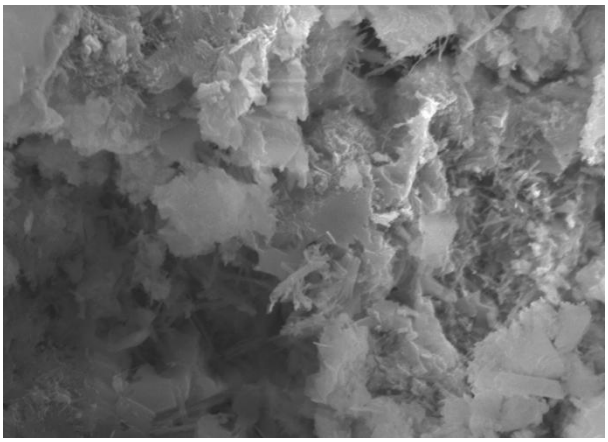

(b)

Figure 4.3: SEM of Concrete (a) Without Fly Ash, (b) With Fly Ash.

However, at 20 % replacement, the SSD density slightly dropped to 2403 kg/m^3 . This reduction, though minor, suggested that excessive replacement of cement with fly ash begin to negatively affect the mix's compactness. At higher replacement levels, the reduced availability of cement for hydration and the slower reactivity of fly ash can lead to incomplete densification and a slight increase in internal porosity. Hence, while moderate incorporation of fly ash improved the SSD density of concrete, excessive amounts may counteract these benefits. Overall, 15 % fly ash replacement appeared to be the most effective proportion for maximizing SSD density without compromising material compactness.

4.3 Compressive Strength Test

The compressive strength test results of the trial mix (Table 4.2) confirmed that the designed concrete mix ratio of 1:0.45:1.18:2.51 successfully met and exceeded the expected strength requirements. The 7-day average compressive strength of 26.17 MPa surpassed the anticipated early strength of 23.33 MPa, which was two-thirds of the targeted 28-day strength of 35 MPa as per ACI Committee 301. This indicated that the concrete had achieved a 12.17 % higher early strength than expected. This early strength gain suggested that the hydration process of cement was efficient and that the concrete developed sufficient early-age strength for handling, demoulding, and potential early load applications. Furthermore, the 28-day compressive strength of 36.91 MPa was 5.46 % higher than the target strength of 35 MPa. When compared, 28-day strength was 41.04% higher than that of 7-day strength. This result confirmed that the mix design not only met but exceeded the required performance standards for water-retaining structures as per BS 8007:1987 and EN 1992-3:2006 (Andrés, 2020).

Table 4.2: Compression Strength Results For Trial Mix (0% Fly Ash).

Trial Mix Sample	**Compressive Strength (MPa)**	
	7-day	28-day
1	26.01	36.63
2	26.17	36.97
3	26.32	37.14
Average	26.17	36.91

After the concrete mix is confirmed, Class F fly ash sourced from Sultan Abdul Aziz Power Plant was then incorporated into the mix design as a partial replacement for cement. The compressive strength test results (Table 4.3 and Figure 4.4) showed the impact of fly ash replacement on the compressive strength of concrete at 7-day and 28-day curing periods. The findings indicated that increasing the percentage of Class F fly ash replacement leads to a gradual reduction in compressive strength at both early and later stages of curing.

Table 4.3: 7-day and 28-day Compression Strength Results For Different Fly Ash Replacement.

Fly Ash Replacement	Average Compressive Strength (MPa)	
	7-day	28-day
0%	26.17	36.91
5%	24.56	35.86
10%	23.93	32.97
15%	23.33	30.56
20%	22.49	29.31

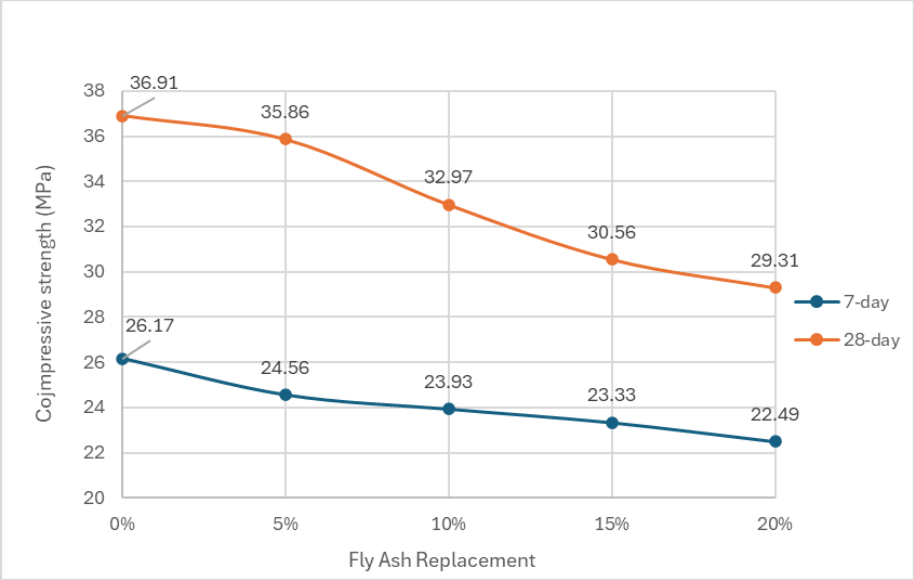

Figure 4.4: Graph of Compressive Strength against Fly Ash Replacement.

The 7-day compressive strength results showed a consistent decline in strength as the percentage of fly ash increased. The control mix (0 % fly ash) achieved a 7-day compressive strength of 26.17 MPa, which was higher than all fly ash-modified mixes. When 5 % fly ash was incorporated, the strength reduced to 24.56 MPa, marking a 6.1 % decrease. This trend continued as the fly ash content increased. At 10 % fly ash, the strength further declined to 23.93 MPa, while the 15 % and 20 % fly ash mixes showed a lower compressive strength of 23.33 MPa and 22.49 MPa, respectively. The highest fly ash replacement level (20 % FA) resulted in a 14.1 % reduction in 7-day strength compared to the control mix, which was the lowest among all mixes.

Despite lower early-age strength, fly ash concrete continued to gain strength over time. However, the 28-day compressive strength results still showed a declining trend as the fly ash content increased. When 5 % fly ash was introduced, the 28-day compressive strength slightly decreased to 35.86 MPa, which was only 2.8 % lower than the control mix. This suggests that at low replacement levels, Class F fly ash can be incorporated without significantly compromising strength performance. However, as the replacement percentage increased, the strength reductions became more pronounced. The 10 % fly ash mix achieved 32.97 MPa, showing a 10.7 % reduction compared to the control mix, while the 15 % and 20 % fly ash mixes exhibited even lower strength of 30.56 MPa and 29.31 MPa.

The observed decline in 7-day and 28-day strength can be attributed to the slow pozzolanic reaction of Class F fly ash over time. Unlike cement that can undergo direct hydration, fly ash relies on the availability of calcium hydroxide (a byproduct of cement hydration) to initiate the pozzolanic reactions and produce secondary calcium silicate hydrate (C-S-H) gel for strength development (Hemalatha and Ramaswamy, 2017). Some fly ash particles were observed to be partially enveloped by hydration products as shown in Figure 4.4, indicating that the pozzolanic reaction had initiated and hydration was occurring around them. However, as illustrated in Figure 4.5, a significant portion of the fly ash particles still remained unreacted even after 28 days of curing. These unreacted particles did not contribute to the strength development and only acted as inert fillers within the matrix, which explained the decline in compressive strength at both 7 and 28-day.

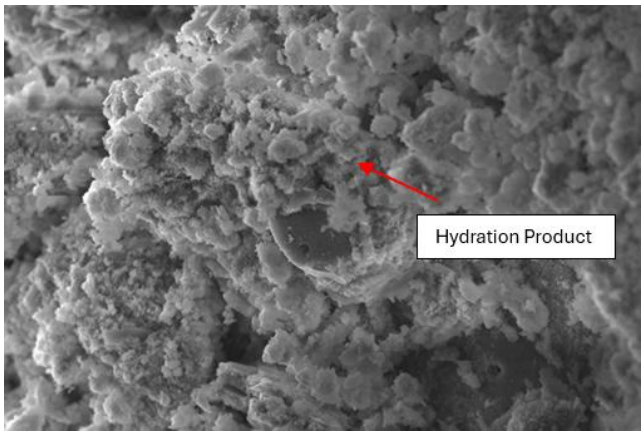

Figure 4.4: SEM Image of Fly Ash Particle Covered with Hydration Product.

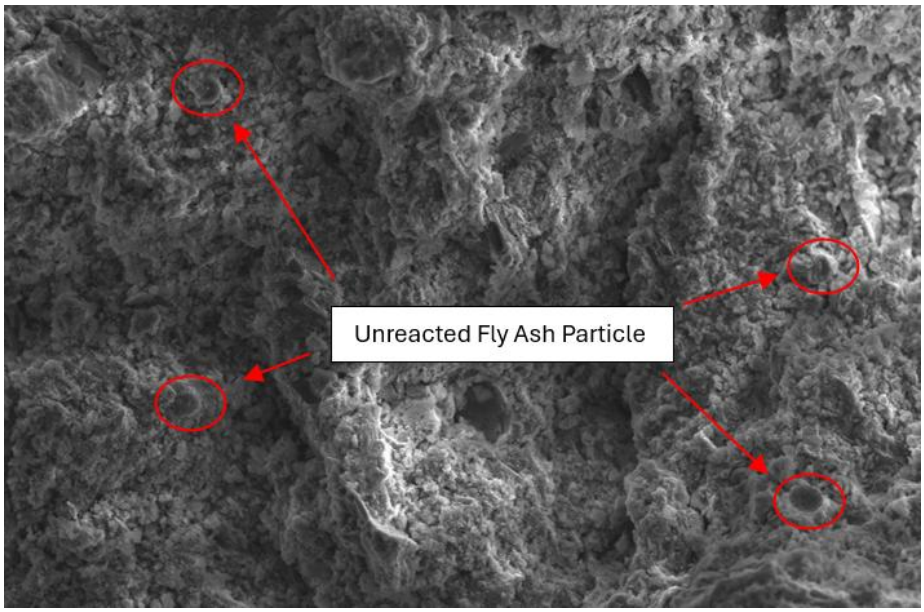

Figure 4.5: SEM Image of Unreacted Fly Ash Particle.

This observation aligns with the SEM analysis by Chindaprasirt, Jaturapitakkul, and Sinsiri (2007), who concluded that pozzolanic reactions in Class F fly ash progress significantly slower than the primary hydration of cement as some fly ash particles still remained unreacted even after 28 days of curing, thus acting merely as inert fillers. The results are also consistent with the findings of Misra, Ramteke, and Bairwa (2007), who reported that concrete incorporating fly ash generally exhibits lower compressive strength than the control mix at 7-day and 28-day curing.

Although high-density concrete typically exhibits higher compressive strength, the results obtained in this study revealed a different trend. Despite the 20 % fly ash concrete achieving a higher density than the control mix, its 28-day compressive strength was 20.6% lower. This is because the strength development in concrete is primarily governed by the content and quality of C-S-H gel rather than density and porosity (Saha, 2018). Therefore, the increase of density due to the filler effect of Class F fly ash particles is not sufficient to compensate for the loss of compressive strength due to reduced cement hydration (Tasdemir, 2003).

Based on the compressive strength test results, it can be concluded that a 5 % replacement of cement with Class F fly ash sourced from the Sultan Abdul Aziz Power Plant represented the optimum level for the concrete mix design in

this study. At 5 % replacement level, the concrete achieved a 28-day compressive strength of 35.86 MPa, which was only marginally lower than that of the control mix (36.91 MPa). This indicates that Class F fly ash sourced from Sultan Abdul Aziz Power Plant requires a longer curing period than 28 days to surpass or match the compressive strength of the control concrete. Despite the slight reduction, the achieved strength still surpassed the minimum target of 35 MPa, as stipulated for water-retaining structures. This indicates that incorporating 5 % fly ash not only maintains structural performance but also offers the added environmental and economic advantages associated with partial cement replacement. Therefore, subsequent experiments were proceeded using this optimal 5 % fly ash replacement in combination with the addition of Sika WT-220 PMY to evaluate the concrete's durability characteristics.

4.4 Effect of Sika® WT-220 PMY

The data presented in Table 4.4 illustrated the influence of Sika WT-220 PMY, a crystalline waterproofing admixture, on the saturated surface dry (SSD) density of concrete, both with and without the inclusion of fly ash. In the control mix without fly ash (0 % replacement), the SSD density was 2367 kg/m^3. When Sika WT-220 PMY was introduced into the same mix, the density rose to 2404 kg/m^3, indicating an increase of 37 kg/m^3. This increase can be attributed to the chemical nature of the crystalline waterproofing admixture. Sika WT-220 PMY reacts with free lime (calcium hydroxide) in the cement matrix to form an insoluble crystalline C-S-H compound that blocks capillary pores (Gojević et al., 2021). This leads to a denser and more impermeable concrete microstructure, which in turn contributes to an increase in SSD density.

Table 4.4: SSD Density of Samples With and Without Sika.

Concrete Samples	**SSD Density (Kg/m^3)**
0%	2367
0%+Sika	2404
5%	2392
5%+Sika	2419

The trend remained consistent even with the incorporation of fly ash at a 5 % replacement level. The SSD density of the 5 % fly ash mix without Sika was recorded at 2392 kg/m^3. When the waterproofing admixture was added, the density further increased to 2419 kg/m^3. Although the increase in this case was slightly smaller (27 kg/m^3 compared to the 37 kg/m^3 increase in the control mix), it still confirmed the admixture's ability to enhance the concrete's density even when supplementary cementitious materials like fly ash were present. The SEM analysis (Figure 4.6) also revealed that concrete incorporating Sika WT-220 PMY contained a greater amount of insoluble C-S-H compound and lesser pores within the matrix than plain OPC concrete. Even though Class F fly ash is known to reduce the calcium hydroxide content due to its pozzolanic reaction (Hemalatha and Ramaswamy, 2017) which may slightly moderate the admixture's effect, the combination of Class F fly ash and Sika WT-220 PMY still yielded a net positive effect on SSD density of concrete.

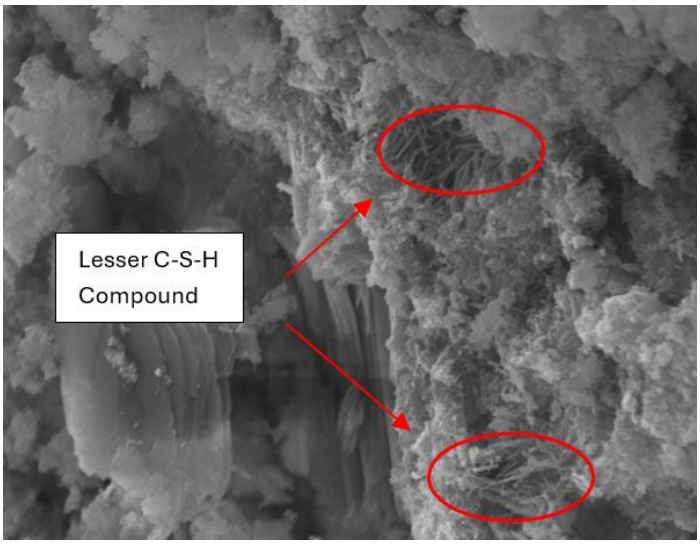

(a)

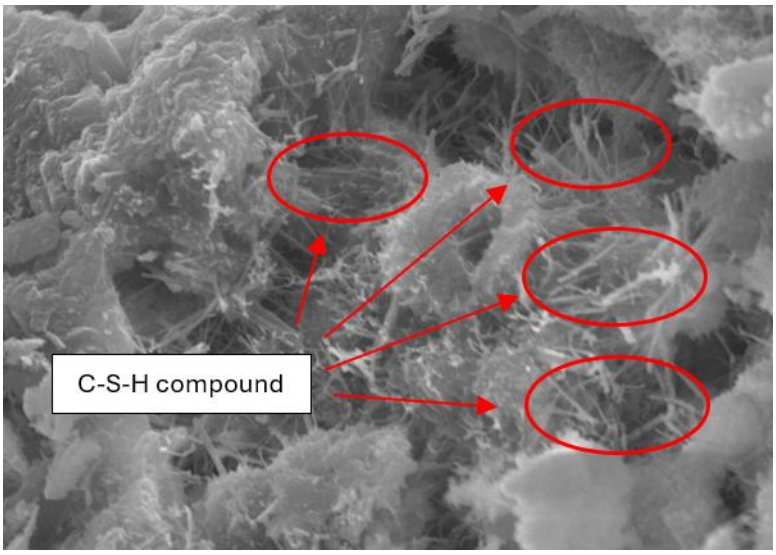

(b)

Figure 4.6: SEM Image of Concrete (a) Without WT-220 PMY, (b) With WT-220 PMY.

The effect of Sika WT-220 PMY on the 28-day compressive strength of concrete was also evaluated on concrete samples with and without the addition of the admixture. The results are shown in Table 4.5. For concrete without fly ash, the average compressive strength of the control samples was 36.91 MPa, whereas the samples containing Sika WT-220 PMY achieved a slightly higher average strength of 36.98 MPa. In the case of concrete with 5 % fly ash replacement, the 5 % FA mix recorded an average compressive strength of 35.86 MPa, while the sample with added Sika WT-220 PMY showed a slightly improved strength of 35.92 MPa. The minor increase of 0.07 MPa and 0.06 MPa respectively indicated that the incorporation of the waterproofing admixture does not compromise the compressive strength of concrete but contributes minorly to strength gain. This can be attributed to the admixture's mechanism of action, which involves the formation of insoluble crystalline structures within the concrete matrix. These crystals effectively fill capillary pores and microcracks, resulting in a denser and less permeable microstructure (Gojević et al., 2021).

Table 4.5: 28-d Compression Results of Samples With and Without Sika.

Concrete Samples	28-d Compressive Strength (MPa)			
	Sample 1	Sample 2	Sample 3	Average
0%	36.63	36.97	37.14	36.91
0%+Sika	36.95	36.90	37.07	36.98
5%	35.98	35.34	35.82	35.86
5%+Sika	35.93	36.07	35.77	35.92

Overall, Sika WT-220 PMY can be considered an effective admixture for improving the durability and waterproofing performance of fly ash concrete without negatively impacting its density and compressive strength. This makes it particularly suitable for the use in water-retaining structures where both impermeability and strength are critical performance requirements. Even though Sika WT-220 PMY can contribute to the compressive strength of concrete due to the formation of insoluble C-S-H compound within the concrete matrix, it cannot be used as the primary strength-enhancing agent as the strength gain is relatively minor and is considered negligible in structural terms.

4.5 Initial Surface Absorption Test (ISAT)

The data presented in Figure 4.7 shows the ISAT results of all four mixes which are 0 % FA, 0 % FA + Sika, 5 % FA and 5 % FA + Sika. All four mixes showed the highest surface absorption at 10-minutes intervals. One clear trend observed across all mixes was that the surface water absorption was highest at the 10-minute interval. This is a common phenomenon in ISAT results mainly due to dry concrete surface and the rapid water absorption at the early stage (Balakrishna et al., 2018).

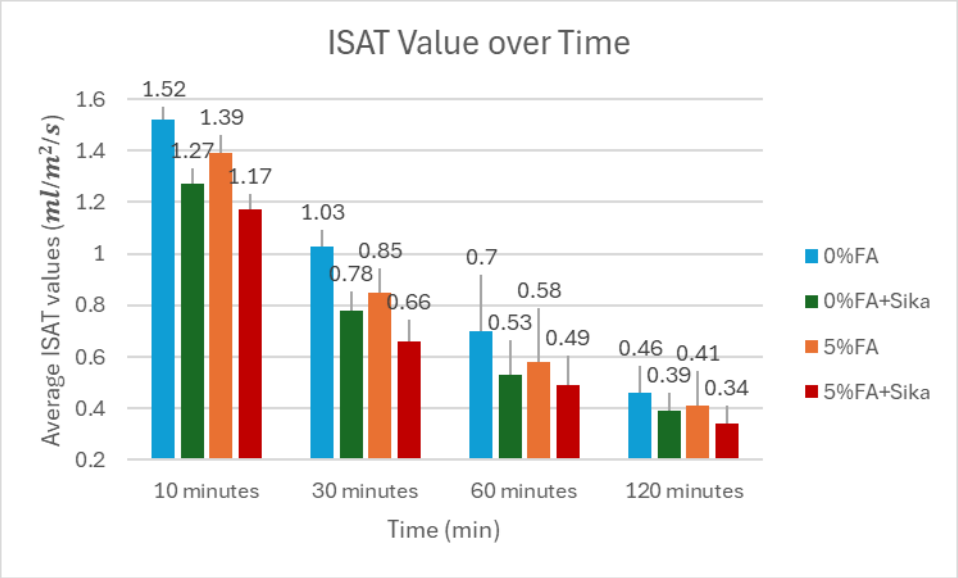

Figure 4.7: Graph of ISAT Results over Time.

Among all mixes, the control sample (0 % FA) exhibited the highest ISAT values across all time intervals, starting at 1.52 $ml/m^2/s$ at 10 minutes and gradually reducing to 0.46 $ml/m^2/s$ at 120 minutes. This trend demonstrates that plain OPC concrete has higher surface permeability, making it more susceptible to surface water ingress. In contrast, the incorporation of Sika WT-220 PMY into the control mix resulted in a noticeable reduction in ISAT values, particularly at early time intervals. The ISAT value at 10 minutes decreased to 1.27 $ml/m^2/s$ and further reduced to 0.39 $ml/m^2/s$ at 120 minutes. Notably, the ISAT results of control mix with Sika WT-220 PMY were even lower than those reported for Grade 40 plain OPC concrete by Balakrishna et al. (2018). This improvement highlights the role of the crystalline waterproofing admixture in reducing surface water absorption through the formation of insoluble C-S-H compounds that block micro-pores and capillaries, thus enhancing the waterproofing of the concrete surface (Gojević et al., 2021).

Similarly, the partial replacement of cement with 5 % Class F fly ash (5 % FA) also contributed to a lower surface absorption than the control mix, with ISAT values ranging from 1.39 $ml/m^2/s$ at 10 minutes to 0.41 $ml/m^2/s$ at 120 minutes. The improvement can be attributed to the pozzolanic activity of Class F fly ash, which reacts with calcium hydroxide to form additional calcium silicate hydrate (C-S-H) gel (Hemalatha and Ramaswamy, 2017). This gel

enhances particle packing and refines the pore structure, thereby reducing permeability and improving surface resistance to water ingress over time.

The ISAT values of the 5 % FA mix were found to be higher than those of the control mix containing Sika WT-220 PMY, despite the well-documented benefits of fly ash in enhancing concrete durability. This is because Class F fly ash improves durability primarily through a pozzolanic reaction which is relatively slow and typically requires an extended curing period to fully develop (Chindaprasirt, Jaturapitakkul and Sinsiri, 2007) while Sika WT-220 PMY acts more rapidly by chemically reducing permeability after mixing. As a result, the control mix with Sika WT-220 PMY benefits from an early-age reduction in surface absorption, which explains the lower ISAT values compared to the 5 % FA mix.

The most significant improvement was observed in the sample containing both 5 % fly ash and Sika WT-220 PMY. This mix demonstrated the lowest ISAT values throughout the test duration, decreasing from 1.17 $\mathrm{ml/m^2/s}$ at 10 minutes to 0.34 $\mathrm{ml/m^2/s}$ at 120 minutes. This represented reductions of 26.09 % compared to the control mix, 12.82 % compared to the control mix with Sika WT-220 PMY, and 17.95 % compared to the 5 % fly ash mix at the 120-minute mark. The synergistic effect of using both the Class F fly ash and Sika WT-220 PMY proved to have produced a denser and more refined concrete surface with significantly lower surface absorption. This finding is consistent with the SSD density results obtained previously in Table 4.4, which indicates that the mix containing 5 % fly ash and Sika WT-220 PMY achieved the highest SSD density among all tested samples.

Overall, the ISAT results clearly demonstrated that the incorporation of Class F fly ash and Sika WT-220 PMY significantly enhanced the surface impermeability of concrete. The trend observed in this study is also consistent with the findings of Fonseka and Nanayakkara (2022) where ISAT values decrease with increasing Class F fly ash replacement. Among all the mixes tested, the combination of 5 % fly ash with Sika WT-220 PMY exhibited the lowest surface absorption values, indicating the most refined and compact concrete surface. This optimized mix design is especially well-suited for water-retaining structures and environments exposed to moisture, where minimizing

water ingress through the concrete surface is critical to ensuring long-term durability and service performance.

4.6 Sorptivity Test

The data presented in Table 4.6 showed the mass of water absorbed by the concrete specimens at various time intervals, ranging from 1 minute to 120 minutes. This mass gain represents the water absorption mass through capillary suction. Subsequently, a graph of water absorption versus the square root of time was plotted in Figure 4.8. The initial linear portion of the graph was fitted with the best-fit straight lines for each mix. The sorptivity coefficient was determined as the slope of the best-fit straight lines, quantifying the rate of water ingress into the concrete via capillary action under unsaturated condition. The results for the sorptivity coefficient for each mix are summarized in Figure 4.9.

Table 4.6: Mass of Water Absorbed (g) in Sorptivity Test.

Time Interval (min)	**Mass of Water Absorbed (g)**			
	0%FA	0%FA+Sika	5%FA	5%FA+Sika
1	3.6	3.2	3.4	2.7
5	1.6	1.1	1.4	0.8
10	1.9	1.3	1.5	1.1
20	2.2	1.7	1.9	1.5
30	2.6	2	2.3	1.8
60	3.2	2.5	2.8	2.3
120	3.9	3.1	3.4	2.8

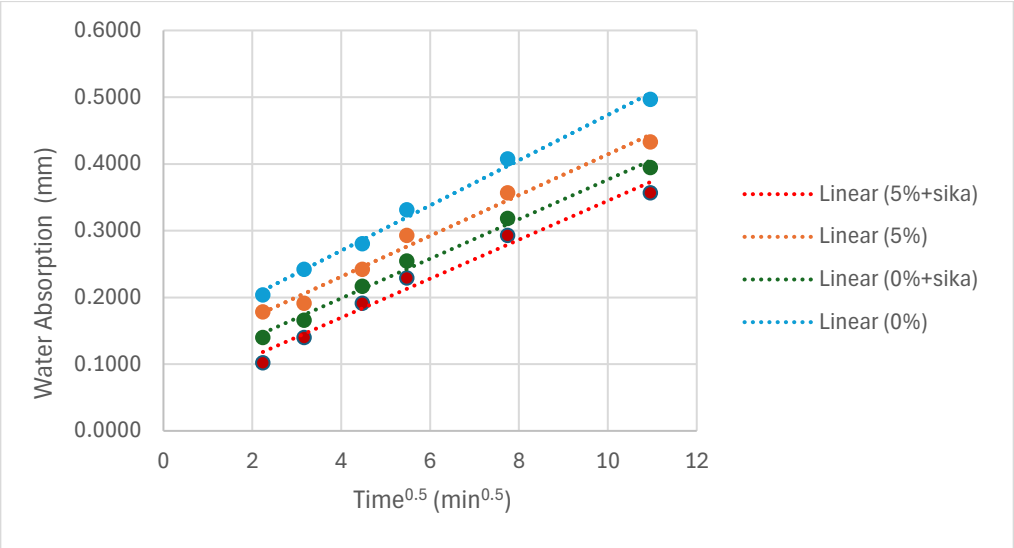

Figure 4.8: Graph of Cumulative Water Absorption (mm) over Square Root of Time.

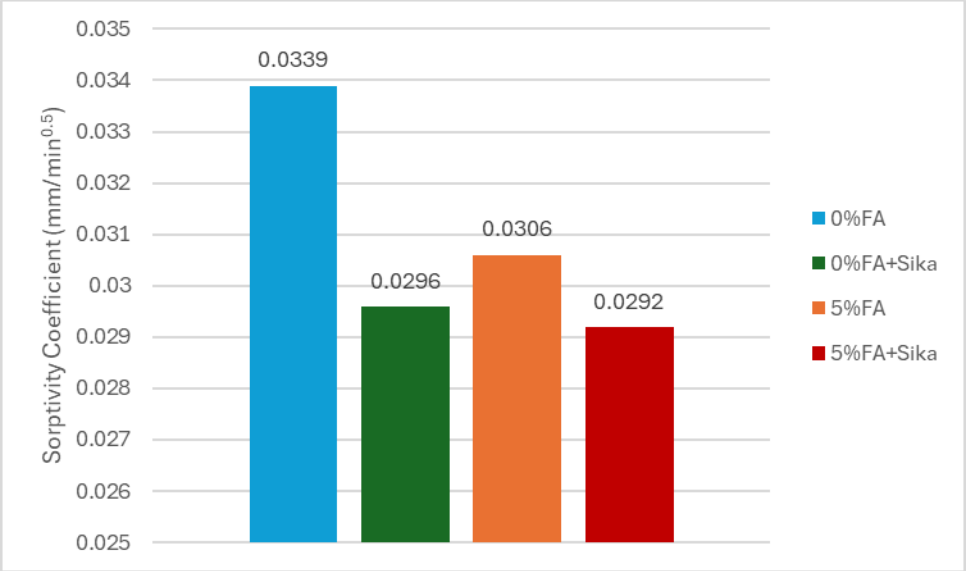

Figure 4.9: Results of Sorptivity Coefficient.

The sorptivity results obtained in this study clearly demonstrated the positive impact of incorporating Class F fly ash and Sika WT-220 PMY on the capillary absorption properties of concrete. Among all the mixes tested, the control sample (0 % FA) exhibited the highest sorptivity coefficient of 0.0339 $mm/min^{0.5}$. This relatively high value is attributed to the porous microstructure of plain OPC concrete (Elrahman and Hillemeier, 2014) which allows easier capillary suction of water through interconnected pores. The high rate of capillary water absorption indicates a greater vulnerability to moisture ingress,

which can adversely affect the long-term durability of the water-retaining structures.

The addition of Sika WT-220 PMY to the control mix (0 % FA + Sika) resulted in a noticeable reduction in sorptivity, lowering the coefficient to 0.0296 $mm/min^{0.5}$. This represented a significant reduction of approximately 12.67 % compared to the control mix. The improvement is attributed to the action of Sika WT-220 PMY which reacts with calcium hydroxide and moisture to form additional insoluble calcium silicate hydrate (C-S-H) compounds (Gojević et al., 2021). These compounds block micro-pores and disrupt the continuity of pores within the concrete matrix, thus preventing the movement of water through the concrete.

Similarly, the use of 5 % fly ash replacement without Sika (5 % FA mix) also improved the capillary absorption properties of the concrete compared to the plain control mix, achieving a sorptivity coefficient of 0.0306 $mm/min^{0.5}$. The enhancement is primarily due to the physical and chemical effects of fly ash. As a finely divided material, unreacted fly ash particle fills the voids between larger cement particles, leading to a denser packing of the concrete mix (Elrahman and Hillemeier, 2014). Additionally, the pozzolanic reaction between fly ash and calcium hydroxide generates more secondary C-S-H gel, which further refines the pore structure by reducing pore size and connectivity (Hemalatha and Ramaswamy, 2017).

Among all the mixes, the combination of 5 % fly ash and Sika WT-220 PMY (5 % FA + Sika) exhibited the most significant improvement, with the lowest sorptivity coefficient of 0.0292 $mm/min^{0.5}$. This represents a reduction of about 13.86 % compared to the control mix (0 % FA). The results suggest a synergistic interaction between fly ash and Sika WT-220 PMY, where the dense packing effect and pore refinement provided by fly ash complement the pore-blocking action of the crystalline admixture. Together, these effects lead to a more refined and compact concrete microstructure with significantly reduced pore connectivity.

Overall, the sorptivity test results confirmed that the combination of 5 % cement replacement with Class F fly ash and the incorporation of Sika WT-220 PMY is highly effective in reducing the volume of interconnected pores. The results are also in good agreement with the findings of Saha (2018) who

reported that increasing fly ash replacement levels leads to a lower sorptivity coefficient at both 28-day curing periods. This reduction in pore connectivity significantly improves the concrete durability and reduces the rate of water transfer within the concrete matrix via capillary action under unsaturated conditions.

4.7 Water Absorption Test

The results of the water absorption test as presented in Table 4.7 provide valuable insights into the pore structure characteristics and overall permeability of the different concrete mixtures. Water absorption is a critical durability indicator as it directly reflects the overall volume of pores that allows moisture ingress into the concrete matrix.

Table 4.7: Results of Water Absorption Test.

Concrete Samples	Dry Mass (kg)	Average Mass of Water Absorbed (kg)	Average Mass of Water Absorbed (%)
0%FA	7.726	0.338	4.37
0%FA+Sika	7.792	0.317	4.07
5%FA	7.763	0.322	4.15
5%FA+Sika	7.846	0.255	3.25

From the results, the control sample (0 % FA) exhibited the highest average mass of water absorbed, recorded at 4.37 %. This indicates that the control concrete possesses a relatively more porous microstructure with a greater volume of pores that facilitate the ingress and retention of water (Elrahman and Hillemeier, 2014). Such a high level of water absorption is unacceptable for water-retaining structures, as it increases the risk of deterioration mechanisms such as corrosion of embedded reinforcement, sulphate attack, freeze-thaw damage, and alkali-silica reaction. However, the incorporation of Sika WT-220 PMY into the control mix (0 % FA + Sika) led to a noticeable reduction in overall water absorption, with an average value of 4.07 %. The decrease in water absorption confirms the effectiveness of the crystalline waterproofing admixture in improving the concrete's resistance to

moisture ingress. Sika WT-220 PMY reacts chemically with free lime produced during cement hydration, forming an insoluble crystalline compound that grows within the capillaries and micro-cracks of the concrete matrix (Gojević et al., 2021). These compounds block water pathways into the concrete and reduce the overall bulk porosity.

Replacing 5 % of the cement content with Class F fly ash (5 % FA) also had a positive influence on the water absorption properties, with the average value recorded at 4.15 %. While the improvement was less pronounced compared to the addition of Sika WT-220 PMY, it still indicates densification of the concrete microstructure. The contribution of Class F fly ash stems primarily from its pozzolanic activity. Upon reacting with calcium hydroxide liberated during cement hydration, fly ash produces additional calcium silicate hydrate gel which fills capillary pores and refines the overall pore structure (Hemalatha and Ramaswamy, 2017). Furthermore, the spherical shape of fly ash particles also aids in improving workability and packing density, leading to fewer voids throughout the concrete matrix (Wang, Zhang, and Sun, 2003). This secondary hydration reaction and improved microstructure collectively contributed to reduced overall water absorption and enhanced durability characteristics.

The most substantial improvement was observed when both 5 % fly ash replacement and Sika WT-220 PMY were combined (5 % FA + Sika), resulting in an average water absorption of only 3.25 %. This represents a 24.56 % reduction compared to the control mix, clearly highlighting the synergistic effect achieved by combining fly ash with waterproofing admixtures. In this case, the pozzolanic reaction from the fly ash contributed to further refinement of the pore structure while the crystalline admixture provided an additional barrier by physically blocking residual capillaries. The dual mechanism of microstructure densification and crystalline pore blocking significantly reduces the ability of water to penetrate and be absorbed by the concrete, thus making it highly resistant to water ingress.

Overall, the water absorption test results strongly validated the effectiveness of both 5 % Class F fly ash and Sika WT-220 PMY in reducing the bulk porosity and the water absorption under fully submerged conditions. These findings are also consistent with previous research by Kurda, Brito, and

Silvestre (2019), and Zhuang, Wang, and Zhang (2022), who concluded that replacing cement with fly ash leads to a lower water absorption rate compared to plain OPC concrete due to refinement of the pore structure.

4.8 Sustainability and Cost Saving

Incorporating 5 % Class F fly ash as a partial cement replacement in the concrete mix design demonstrated both economic and environmental benefits, supporting the broader goals of sustainable construction. Based on the mix proportions used in this study, the binder content per cubic meter of concrete is 466.7 kg. In the control mix, where 100 % of the binder comprises Ordinary Portland Cement, the binder material cost is approximately RM 220.75 per cubic meter, applying the cement market price of RM 23.65 per 50 kilogram (Department of Statistic Malaysia, 2025).

However, in the optimized mix where 5 % of the cement was replaced with Class F fly ash, the total cement content was reduced to 443.4 kg and fly ash was added at 23.3 kg per cubic meter. Given the average market price of China Class F fly ash at approximately RM 0.11 per kilogram (IMARC Group, 2025), the revised material cost becomes RM 209 .73 for cement and RM 2.56 for fly ash, totalling RM212.29 per cubic meter. This results in a direct material cost saving of RM 8.46 per cubic meter of fly ash concrete, which equates to roughly 3.83 % in binder cost savings. For large-scale water-retaining structure construction projects, such savings can significantly reduce overall expenditure without compromising structural strength while improving the durability performance.

Beyond cost efficiency, the substitution of fly ash also contributed to a notable reduction in the embodied carbon footprint of the concrete. Cement production is energy-intensive and is associated with substantial CO_2 emissions, estimated at around 900 kg CO_2 exhibited per tonne of cement produced (Bakhtyar, Kacemi and Nawaz, 2017). By replacing 5 % of cement (23.3 kg) per cubic meter with Class F fly ash, approximately 20.97 kg of CO_2 emissions were avoided for every cubic meter of concrete. This represents a 4.99 % reduction in CO_2 emissions compared to concrete made with 100 % OPC. When scaled over 1,000 cubic meters of concrete, this corresponds to a reduction of approximately 20.97 tonnes of CO_2. The saving of binder cost and carbon

emission is presented in Figure 4.10(a) and Figure 4.10(b). Moreover, since fly ash is an industrial by-product obtained from coal-fired power stations, the reuse of fly ash in concrete also prevents landfill disposal, further enhancing the environmental credentials.

(a)

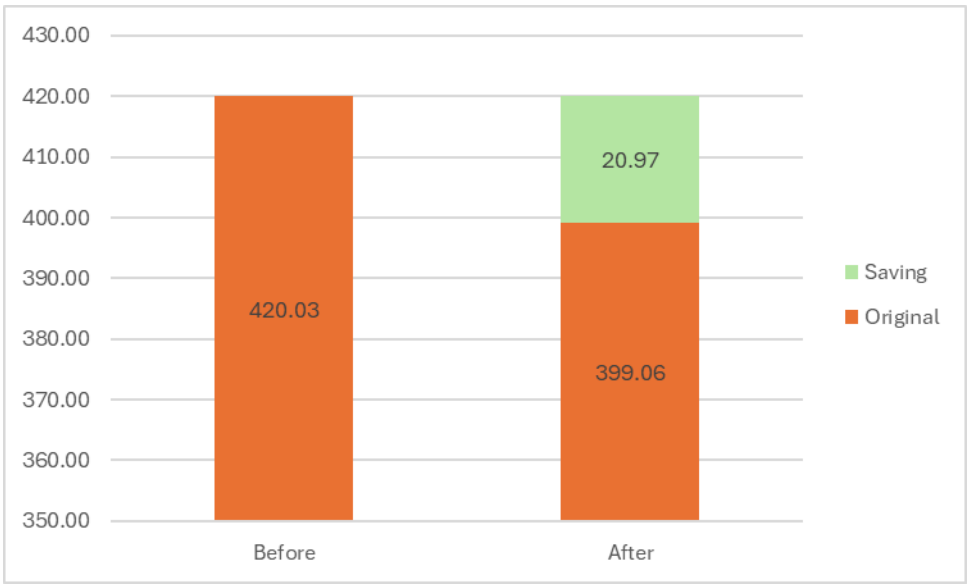

(b)

Figure 4.10: Comparison per meter cube Before and After using 5 % Class F Fly Ash Replacement in terms of (a) Binder Price, (b) CO_2 Emissions.

4.9 Summary

The summary of the results of this study is presented in Table 4.8. Although the 28-day compressive strength of the 5 % FA + Sika mix (35.92 MPa) was slightly lower than the control mix (36.91 MPa), it still exceeded the 35 MPa minimum strength requirement for water-retaining structures as stated in BS 8007:1987 and EN 1992-3:2006. It can be concluded that the combination of 5 % Class F fly ash sourced from Sultan Abdul Aziz Power Plant and the crystalline waterproofing admixture Sika WT-220 PMY showed the best performance in all Initial Surface Absorption Test, Sorptivity Test and Water Absorption Test. This optimized mix achieved a 26.09 % reduction in Initial Surface Absorption Test (ISAT) values, a 13.86 % decrease in the sorptivity coefficient, and a 24.56 % lower water absorption compared to the control sample, indicating significantly improved resistance to surface moisture ingress, capillary suction and reduced permeability.

Table 4.8: Summary Results of Each Test.

Concrete Samples	**28d Compressive Strength (MPa)**	**2hr ISAT Value ($ml/m^2/s$)**	**Water Absorption (%)**	**Sorptivity Coefficient ($mm/min^{0.5}$)**
0%FA	36.91	0.46	4.37	0.0339
0%FA+Sika	36.98	0.39	4.07	0.0296
5%FA	35.86	0.41	4.15	0.0306
5%FA+Sika	35.92	0.34	3.25	0.0292

From a sustainability and economic perspective, the partial replacement of cement with 5 % Class F fly ash contributed to a 3.83 % reduction in binder cost per cubic meter of concrete. In addition, 5 % Class F replacement also resulted in an estimated reduction of 20.97 kg of CO_2 emissions per cubic meter, thereby lowering 4.99 % carbon footprint associated per meter cube of concrete in this study. These outcomes align with the objectives of the United Nations Sustainable Development Goal 13 (SDG 13) which focuses on combating climate action, and the Twelfth Malaysia Plan's strategies to reduce carbon emissions and promote sustainable construction practices (Devan, 2023).

CHAPTER 5

CONCLUSION AND RECOMMENDATIONS

5.1 Conclusion

The incorporation of fly ash as a partial replacement for Ordinary Portland Cement (OPC) has been extensively studied and found to enhance workability, reduced water bleeding, denser microstructure, and lower heat of hydration. Experimental results from this study confirmed the literature findings on the beneficial effects of fly ash in concrete. Using British Standard prepared by Building Research Establishment, the concrete mix proportion for 35 MPa strength was obtained as 1:0.45:1.18:2.51 (cement : water : fine aggregate : coarse aggregate). After the trial mix proved to obtain 28-day compressive strength of 36.91 MPa, the OPC of the trial mix was then partially replaced by Class F fly ash by replacing 5 %, 10 %, 15 % and 20 % by weight. The result demonstrated that concrete mix incorporating 5 % Class F fly ash sourced from Sultan Abdul Aziz Power Plant proved to be the optimal replacement level among all tested variations, achieving an average 28-day compressive strength of 35.86 MPa that was slightly lower than the control mix but still remained above the minimum requirement of 35 MPa for water-retaining structures as per BS 8007:1987 and EN 1992-3:2006. The inclusion of Sika WT-220 PMY further improved the strength to 35.92 MPa, reaffirming the positive synergistic effect of this combined approach for producing strong concrete.

In terms of durability, the 5 % FA + Sika mix outperformed all other mixes. Compared to the control mix, the optimized mix achieved a 26.09 % reduction in Initial Surface Absorption Test (ISAT) values, a 13.86 % reduction in sorptivity coefficient, and a 24.56 % decrease in overall water absorption. These reductions indicated a significantly lower porosity, denser microstructure, and greater resistance to water ingress. From a sustainability and economic perspective, the replacement of 5 % OPC with Class F fly ash achieved a 3.83 % saving in binder cost per cubic meter of concrete, offering direct material cost efficiency. Additionally, fly ash substitution also avoided approximately 20.97 kg of CO_2 emissions per cubic meter of concrete.

In conclusion, this study confirms that incorporating 5 % Class F fly ash sourced from Sultan Abdul Aziz Power Plant with Sika WT-220 PMY not only met the strength and durability requirements for water-retaining concrete but also offered measurable sustainability and cost advantages. These outcomes align with the objectives of the United Nations Sustainable Development Goal 13 (SDG 13) and the Twelfth Malaysia Plan's strategies to combat climate change, reduce carbon emissions and promote sustainable construction practices.

5.2 Recommendations for Future Work

It is recommended that future studies extend the curing period beyond the conventional 28 days to fully examine the long-term pozzolanic reaction and full performance benefits of Class F fly ash in concrete. Evaluating compressive strength, sorptivity, surface absorption, and water absorption at 56 and 90 days would provide a more comprehensive understanding of the long-term durability enhancements offered by fly ash. This is particularly relevant for water-retaining structures or big infrastructure designed with a service life of several decades, where long-term performance outweighs early-age strength gains. By extending the curing duration and testing period in future research, the full potential of fly ash as a sustainable cement replacement can be more accurately assessed, thereby supporting its broader application in durable and environmentally conscious construction.

Based on the findings of this study, it is recommended that further investigation be conducted into the use of pulverized Class F fly ash as a cement replacement in concrete. Although the results of this study showed a reduction in 28-day compressive strength with increasing Class F fly ash content, this limitation could be addressed by refining the physical properties of the fly ash. Specifically, reducing the particle size through mechanical pulverization can significantly enhance its pozzolanic activity and packing ability, leading to improved strength development and a denser concrete matrix. Consequently, this may allow for higher replacement levels beyond 5 %. This recommendation is supported by previous studies conducted by Moghaddam, Sirivivatnanon, and Vessalas (2019) and Jamkar, Ghugal, and Patankar (2013) which concluded that pulverized Class F fly ash contributes to higher 28-day compressive strength and increased concrete density when compared to unpulverized fly ash.

REFERENCES

Abd Elrahman, M. and Hillemeier, B., 2014. Combined effect of fine fly ash and packing density on the properties of high performance concrete: An experimental approach. *Construction and Building Materials*, *58*, pp.225-233.

ACI Committee 212, 2016. *212.3R-16 Report on Chemical Admixtures for Concrete*. pp.43–48.

Adlina, 2024. *CREAM dan ACE Greencemt Rakan Kongsi untuk Merintis Penyelesaian Konkrit Mampan di Malaysia*. [online] CIDB HQ. Available at: <https://www.cidb.gov.my/eng/cream-and-ace-greencemt-partner> [Accessed 2 August 2024].

Aïtcin, P.C., 2016. Portland cement. In *Science and Technology of Concrete Admixtures* (pp. 27-51). Woodhead Publishing.

Akbulut, Z.F., Yavuz, D., Tawfik, T.A., Smarzewski, P. and Guler, S., 2024. Enhancing Concrete Performance through Sustainable Utilization of Class-C and Class-F Fly Ash: A Comprehensive Review. *Sustainability*, [e-journal] 16(12), p.4905. https://doi.org/10.3390/su16124905.

Akinwumi, I. I., & Gbadamosi, Z. O., 2014. Effects of curing condition and curing period on the compressive strength development of plain concrete. *International Journal of Civil and Environmental Research*, 1(2), 83–99.

Andrés, P., 2020. BS 8007 1987 British Standard Design of Concrete structures for retaining aqueous liquids. *Academia.edu*.

AnkeshS, B., Malla, B. and Gowda, C., 2016. Study on compressive strength of concrete by using fly ash and nanosilica. *International Research Journal of Engineering and Technology*, *7*(7), pp.5173-5179.

ASTM C33, 2008. *Standard Specification for Concrete Aggregates*. ASTM International. https://doi.org/10.1520/c0033-07.

ASTM C511, 2021. *Specification for Mixing Rooms, Moist Cabinets, Moist Rooms, and Water Storage Tanks Used in the Testing of Hydraulic Cements and Concretes*. ASTM International. https://doi.org/10.1520/c0511-21.

ASTM C1602, 2022. *Specification for Mixing Water Used in the Production of Hydraulic Cement Concrete*. ASTM International. https://doi.org/10.1520/c1602_c1602m-22.

ASTM C150, 2012. *Standard Specification for Portland Cement.* West Conshohocken: ASTM International.

ASTM C642, 2022. *Test Method for Density, Absorption, and Voids in Hardened Concrete*. ASTM International. https://doi.org/10.1520/c0642-21.

Bakhtyar, B., Kacemi, T. and Nawaz, M.A., 2017. A review on carbon emissions in Malaysian cement industry. *International Journal of Energy Economics and Policy*, *7*(3), pp.282-286.

Balakrishna MN, Fouad Mohamad, Robert Evans, Rahman MM. Assessment of water absorption of concrete by Initial surface absorption test. *Indian Journal of Engineering*, 2018, 15, 57-65.

Belaid, F., 2022. How does concrete and cement industry transformation contribute to mitigating climate change challenges? *Resources, Conservation & Recycling Advances*, [e-journal] 15(1), p.200084. https://doi.org/10.1016/j.rcradv.2022.200084.

Bergin, B.M.D., 2018. The Innovative Genius of Herod at Caesarea Maritima. *Journal of Cultural and Religious Studies*, [e-journal] 6(7). doi:https://doi.org/10.17265/2328-2177.

Borle, S. and Ghadge, A.N., 2016. Comparative study of conventional and modern waterproofing techniques. *International Journal of Engineering Research*, *5*(1), pp.32-36.

British Standards Institution, 1996. *Testing concrete - Part 208: Recommendations for the determination of the initial surface absorption of concrete.* London: BSI.

British Standards Institution, 1997. *Structural use of concrete - Part 1: Code of practice for design and construction.* London: BSI.

Camarasa, V., 2014. *SEÑOR DEL BIOMBO: EL OPUS CAEMENTICIUM ROMANO*. [online] SEÑOR DEL BIOMBO. Available at: https://seordelbiombo.blogspot.com/2014/10/el-opus-caementicium-romano.html [Accessed 26 Jun. 2024].

Chandini, S. and Nusari, M.S., 2021. Experimental investigation on compressive strength of high strength concrete using fly ash and silica fume. *Webology (ISSN: 1735-188X)*, 18(6).

Chindaprasirt, P., Jaturapitakkul, C. and Sinsiri, T., 2007. Effect of fly ash fineness on microstructure of blended cement paste. *Construction and Building Materials*, [e-journal] 21(7), pp.1534–1541. https://doi.org/10.1016/j.conbuildmat.2005.12.024.

Choi, S.J., Lee, S.S. and Monteiro, P.J.M., 2012. Effect of Fly Ash Fineness on Temperature Rise, Setting, and Strength Development of Mortar. *Journal of Materials in Civil Engineering*, [e-journal] 24(5), pp.499–505. https://doi.org/10.1061/(asce)mt.1943-5533.0000411.

CivilDigital., 2013. *Cement Manufacturing Process Simplified Flow Chart | CivilDigital |*. [online] Available at: https://civildigital.com/cement-manufacturing-process-simplified-flow-chart/ [Accessed 17 Jul. 2024].

Claisse, P.A., Elsayad, H.I. and Shaaban, I.G., 1997. Absorption and Sorptivity of Cover Concrete. *Journal of Materials in Civil Engineering*, [e-journal] 9(3), pp.105–110. https://doi.org/10.1061/(asce)0899-1561(1997)9:3(105).
Constro Facilitator, 2020. *A guide to different types of materials used in waterproofing*. [online] constrofacilitator.com. Available at: <https://constrofacilitator.com/a-guide-to-different-types-of-materials-used-in-waterproofing/> [Accessed 27 July 2024].

Dale, T., 2023. *Uses, Benefits, and Drawbacks of Fly Ash in Construction*. [online] The Spruce. Available at: https://www.thespruce.com/fly-ash-applications-844761 [Accessed 29 Jun. 2024].

Demissew, A., 2022. Comparative Analysis of Selected Concrete Mix Design Methods Based on Cost-Effectiveness. *Advances in Civil Engineering*, 2022, [e-journal] pp.1–8. https://doi.org/10.1155/2022/4240774.

Department of Statistic Malaysia, 2025. *The Unit Price Index of Building Materials*. [online] Available at: <https://www.dosm.gov.my/portal-main/release-content/special-release----for-building-and-structural-works-march-2025> [Accessed 29 April 2025].

De Schutter, G., 2002. Finite element simulation of thermal cracking in massive hardening concrete elements using degree of hydration based material laws. *Computers & Structures*, [e-journal] 80(27-30), pp.2035–2042. https://doi.org/10.1016/s0045-7949(02)00270-5.

Devan, P., 2023. *YTL Cement inks MOU with CREAM to support country's transition to sustainable construction*. [online] The Edge Malaysia. Available at: https://theedgemalaysia.com/node/662937 [Accessed 30 Jun. 2024].

Du, S., Zhao, Q. and Shi, X., 2021. High-Volume Fly Ash-Based Cementitious Composites as Sustainable Materials: An Overview of Recent Advances. *Advances in Civil Engineering*, [e-journal] 2021, pp.1–22. https://doi.org/10.1155/2021/4976169.

E. Davis, R., Carlson, R.W., Kelly, J.W. and Davis, H.E., 1937. Properties Of Cements And Concretes Containing Fly Ash. *ACI Journal Proceedings*, [e-journal] 33(5), pp.577–612. doi:https://doi.org/10.14359/8435.

Fantu, T., Alemayehu, G., Kebede, G., Abebe, Y., Selvaraj, S.K. and Paramasivam, V., 2021. Experimental investigation of compressive strength for fly ash on high strength concrete C-55 grade. *Materials Today: Proceedings*, [e-journal] 46, pp.7507–7517. doi:https://doi.org/10.1016/j.matpr.2021.01.213.

Fonseka, I. and Nanayakkara, A., 2022. Assessment of Concrete Durability by Surface Resistivity and Initial Surface Absorption. *Lecture notes in civil*

engineering, [e-journal] pp.603–620. https://doi.org/10.1007/978-981-19-2886-4_43.

García-Vera, V., Tenza-Abril, A., Saval, J. and Lanzón, M., 2018. Influence of Crystalline Admixtures on the Short-Term Behaviour of Mortars Exposed to Sulphuric Acid. *Materials*, [e-journal] 12(1), p.82. https://doi.org/10.3390/ma12010082.

Gojević, A., Ducman, V., Netinger Grubeša, I., Baričević, A. and Banjad Pečur, I., 2021. The Effect of Crystalline Waterproofing Admixtures on the Self-Healing and Permeability of Concrete. *Materials*, [e-journal] 14(8), p.1860. https://doi.org/10.3390/ma14081860.

Gromicko, N. and Shepard, K., 2011. *The History of Concrete - InterNACHI*. [online] Nachi.org. Available at: https://www.nachi.org/history-of-concrete.htm [Accessed 26 Jun. 2024].

Gull, S., Wani, S.B. and Amin, I., 2020. Exploring optimum percentage of fly-ash as a replacement of cement for enhancement of concrete properties. *Challenge Journal of Concrete Research Letters*, [e-journal] 11(1), p.16. https://doi.org/10.20528/cjcrl.2020.01.003.

Haque, M.N. and Kayali, O., 1998. Properties of high-strength concrete using a fine fly ash. *Cement and Concrete Research*, [e-journal] 28(10), pp.1445–1452. https://doi.org/10.1016/s0008-8846(98)00125-2.

Hemalatha, T. and Ramaswamy, A., 2017. A review on fly ash characteristics – Towards promoting high volume utilization in developing sustainable concrete. *Journal of Cleaner Production*, [e-journal] 147, pp.546–559. https://doi.org/10.1016/j.jclepro.2017.01.114.

IMARC Group, 2025. Fly Ash Price Trend, Chart, Index, News, Demand & Forecast. [online] Imarcgroup.com. Available at: <https://www.imarcgroup.com/fly-ash-pricing-report> [Accessed 2 May 2025].

Jamkar, S.S., Ghugal, Y.M. and Patankar, A.S., 2013. Effect of fly ash fineness on workability and compressive strength of geopolymer concrete. *The Indian Concrete Journal*, 87(4), pp.57-61.

Jiao, D., Shi, C., Yuan, Q., An, X., Liu, Y. and Li, H., 2017. Effect of constituents on rheological properties of fresh concrete-A review. *Cement and Concrete Composites*, [e-journal] 83, pp.146–159. doi:https://doi.org/10.1016/j.cemconcomp.2017.07.016.

Kim, S.G., 2010. Effect of heat generation from cement hydration on mass concrete placement.

Kiran, T.G.S. and Ratnam, M.K.M.V., 2014. Fly ash as a partial replacement of cement in concrete and durability study of fly ash in acidic (H2SO4) environment. *International Journal of Engineering Research and Development*, *10*(12), pp.01-13.

Kosmatka, S.H., 2006. Bleed water. *Significance of tests and properties of concrete and concrete-making materials*, pp.99-122.

Koui, M & Ftikos, Ch.. 1998. The ancient Kamirian water storage tank: A proof of concrete technology and durability for three millenniums. *Materials and Structures*, Vol. 31, pp. 623-627.

Kurda, R., de Brito, J. and Silvestre, J.D., 2019. Water absorption and electrical resistivity of concrete with recycled concrete aggregates and fly ash. *Cement and Concrete Composites*, [e-journal] 95, pp.169–182. https://doi.org/10.1016/j.cemconcomp.2018.10.004.

Lavagna, L. and Nisticò, R., 2022. An Insight into the Chemistry of Cement—A Review. *Applied Sciences*, [e-journal] 13(1), p.203. doi:https://doi.org/10.3390/app13010203.

Levitt, M., 1970. Non-destructive testing of concrete by the initial surface absorption method. In *Non-destructive testing of concrete and timber* (pp. 23-26). Thomas Telford Publishing.

Limited, A., 2010. *Stone water supply reservoir, Ancient Kamiros, Rhodes, Greece Stock Photo - Alamy*. [online] www.alamy.com. Available at: https://www.alamy.com/stock-photo-stone-water-supply-reservoir-ancient-kamiros-rhodes-greece-30564317.html [Accessed 25 Jun. 2024].

Lockard, C.A. and Zakaria Bin Ahmad, 2019. Malaysia - Climate. In: *Encyclopædia Britannica*. [online] Available at: <https://www.britannica.com/place/Malaysia/Climate> [Accessed 3 August 2024].

Lößlein, S.M., Merz, R., Müller, D.W., Kopnarski, M. and Mücklich, F., 2022. An in-depth evaluation of sample and measurement induced influences on static contact angle measurements. *Scientific Reports*, [e-journal] 12(1), p.19389. https://doi.org/10.1038/s41598-022-23341-3.

Lymm Construction., 2023. *The History and Evolution of Concrete as a Building Material*. [online] Available at: https://www.lymmconstruction.com/blog/evolution-of-concrete [Accessed 26 Jun. 2024].

MacLaren, D.C. and White, M.A., 2003. Cement: Its Chemistry and Properties. *Journal of Chemical Education*, [e-journal] 80(6), p.623. doi:https://doi.org/10.1021/ed080p623.

Mac, M.J., Yio, M.H.N., Wong, H.S. and Buenfeld, N.R., 2021. Analysis of autogenous shrinkage-induced microcracks in concrete from 3D images. *Cement and Concrete Research*, [e-journal] 144, p.106416. https://doi.org/10.1016/j.cemconres.2021.106416.

Madhumitha Jaganmohan, M., 2024. *Cement production global 2019*. [online] Statista. Available at: https://www.statista.com/statistics/1087115/global-cement-production-volume/ [Accessed 30 Jun. 2024].

Mardiaman, M. and Dewita, H., 2022. Effect of Adding Fly Ash and Rice Husk Ash on Compressive Strength to Meet the fc'35 MPa Concrete Quality. *Civilla : Jurnal Teknik Sipil Universitas Islam Lamongan*, [e-journal] 7(1), p.35. https://doi.org/10.30736/cvl.v7i1.778.
Marsh, B., 1988. *Design of normal concrete mixes Second edition Building Research Establishment*.

McCarthy, M.J. and Dyer, T.D., 2019. Pozzolanas and pozzolanic materials. *Lea's Chemistry of Cement and Concrete*, *5*, pp.363-467.
Macrotrends (2024). *World Population 1950-2024*.

Misra, A., Ramteke, R. and Bairwa, M.L., 2007. Study on strength and sorptivity characteristics of fly ash concrete. *ARPN Journal of Engineering and Applied Sciences*, 2(5), pp.54-59.

Moghaddam, F., Sirivivatnanon, V. and Vessalas, K., 2019. The effect of fly ash fineness on heat of hydration, microstructure, flow and compressive strength of blended cement pastes. *Case Studies in Construction Materials*, [e-journal] 10, p.e00218. https://doi.org/10.1016/j.cscm.2019.e00218.

Montgomery, A., Mahipal Kasaniya, Zhao, P., Thomas, M. and Peterson, K., 2023. The dam that fly ash built. *Journal of microscopy*, [e-journal] 294(2), pp.117–127. doi:https://doi.org/10.1111/jmi.13248.

Muhammad, N.Z., Keyvanfar, A., Abd. Majid, M.Z., Shafaghat, A. and Mirza, J., 2015. Waterproof performance of concrete: A critical review on implemented approaches. *Construction and Building Materials*, [e-jounal] 101, pp.80–90. https://doi.org/10.1016/j.conbuildmat.2015.10.048.

Mustafa Al Bakri, A.M., Abdulkareem, O.A., Kamarudin, H., Khairul Nizar, I., Rafiza, A.R., Zarina, Y. and Alida, A., 2013. Microstructure Studies on the Effect of the Alkaline Activators of Fly Ash-Based Geopolymer at Elevated Heat Treatment Temperature. *Applied Mechanics and Materials*, [e-journal] 421, pp.342–348. https://doi.org/10.4028/www.scientific.net/amm.421.342.

Nath, P. and Sarker, P., 2011. Effect of Fly Ash on the Durability Properties of High Strength Concrete. *Procedia Engineering*, [e-journal] 14, pp.1149–1156. doi:https://doi.org/10.1016/j.proeng.2011.07.144.

Nele De Belie, Marios Soutsos and Gruyaert, E., 2018. *Properties of Fresh and Hardened Concrete Containing Supplementary Cementitious Materials*.[e-journal] *RILEM state-of-the-art reports*. Springer Nature (Netherlands). https://doi.org/10.1007/978-3-319-70606-1.

Nelson, E.B., 1990. *Well cementing*. Amsterdam ; New York: Elsevier ; New York, Ny, Usa.

Nwakire, U., 2013. INFLUENCE OF MIX DESIGN METHODS ON THE COMPRESSIVE SRENGTH OF CONCRETE. *ARPN Journal of Engineering and Applied Sciences*, 8(6).

Oner, A.D.N.A.N., Akyuz, S. and Yildiz, R., 2005. An experimental study on strength development of concrete containing fly ash and optimum usage of fly ash in concrete. *Cement and Concrete Research*, 35(6), pp.1165-1171.
Our World in Data., 2024. *Share of electricity production from coal*. [online] Available at: https://ourworldindata.org/grapher/share-electricity-coal?tab=table&time=latest [Accessed 6 Jul. 2024].

Rahimi, M.Z., Zhao, R., Sadozai, S., Zhu, F., Ji, N. and Xu, L., 2023. Research on the influence of curing strategies on the compressive strength and hardening behaviour of concrete prepared with Ordinary Portland Cement. *Case Studies in Construction Materials*, [e-journal] 18, p.e02045. doi:https://doi.org/10.1016/j.cscm.2023.e02045.

Ravindrarajah, R.S., 2003, December. Bleeding of fresh concrete containing cement supplementary materials. In *Proceedings of 9th East Asia-Pacific Conference on Structural Engineering and Construction* (pp. 16-18).

Ruiz-Agudo, E., Kudłacz, K., Putnis, C.V., Putnis, A. and Rodriguez-Navarro, C., 2013. Dissolution and Carbonation of Portlandite [Ca(OH)2] Single Crystals. *Environmental Science & Technology*, [e-journal] 47(19), pp.11342–11349. https://doi.org/10.1021/es402061c.

Saha, A.K., 2018. Effect of class F fly ash on the durability properties of concrete. *Sustainable Environment Research*, [e-journal] 28(1), pp.25–31. https://doi.org/10.1016/j.serj.2017.09.001.

Salah, M., Mohammadreza Izadifar, Neven Ukrainczyk, Eduardus Koenders and Middendorf, B., 2022. Dissolution of Portlandite in Pure Water: Part 1 Molecular Dynamics (MD) Approach. *Materials*, [e-journal] 15(4), pp.1404–1404. https://doi.org/10.3390/ma15041404.

Santhosh, R. and Shivananda, P., 2017. A review of Concrete Mix Designs. *International Journal for Research in Applied Science and Engineering Technology*, [e-journal] V(XI), pp.586–590. https://doi.org/10.22214/ijraset.2017.11091.

Slowik, V. and Saouma, V.E., 2000. Water Pressure in Propagating Concrete Cracks. *Journal of Structural Engineering*, [e-journal] 126(2), pp.235–242. https://doi.org/10.1061/(asce)0733-9445(2000)126:2(235).

Sousa, V. and Bogas, J.A., 2021. Comparison of energy consumption and carbon emissions from clinker and recycled cement production. *Journal of Cleaner Production*, [e-journal] 306, p.127277. https://doi.org/10.1016/j.jclepro.2021.127277.

Tennis, P.D. and Jennings, H.M., 2000. A model for two types of calcium silicate hydrate in the microstructure of Portland cement pastes. *Cement and Concrete Research*, [e-journal] 30(6), pp.855–863. doi:https://doi.org/10.1016/s0008-8846(00)00257-x.

The Constructor, 2018. *How to Estimate Concrete Costs*? [online] The Constructor. Available at: <https://theconstructor.org/concrete/estimate-concrete-costs/27668/> [Accessed 13 September 2024].
The Constructor., 2022. *What is Ashcrete?* [online] Available at: https://theconstructor.org/building/ashcrete/565323/#goog_rewarded [Accessed 24 Jul. 2024].

Thomas, M., 2013. Supplementary Cementing Materials in Concrete. CRC Press.
Threlfall, T., 2003. *Concrete construction for liquid-retaining structures*. Elsevier eBooks, 4, pp.1–17. https://doi.org/10.1016/b978-075065686-3/50302-5.

Trong Lam, N., 2020. Assessment of the compressive strength and strength activity index of cement incorporating fly ash. *IOP Conference Series: Materials Science and Engineering*, [e-journal] 869(3), p.032052. https://doi.org/10.1088/1757-899x/869/3/032052.

Uysal, M. and Akyuncu, V., 2012. Durability performance of concrete incorporating Class F and Class C fly ashes. *Construction and Building Materials*, [e-journal] 34, pp.170–178. https://doi.org/10.1016/j.conbuildmat.2012.02.075.

Vipin Kant Singh, 2023. *Hydration and setting of Portland cement*. *Elsevier eBooks*, Elsevier BV. pp.423–466. https://doi.org/10.1016/b978-0-323-95080-0.00012-1.

Wang, A., Zhang, C. and Sun, W., 2003. Fly ash effects: I. The morphological effect of fly ash. *Cement and Concrete Research*, [e-journal] 33(12), pp.2023–2029. https://doi.org/10.1016/s0008-8846(03)00217-5.

Wang, M., Chen, D., Wang, H. and Gao, W., 2024. A review on fly ash high-value synthesis utilization and its prospect. *Green energy and resources*, [e-journal] 2(1), pp.100062–100062. doi:https://doi.org/10.1016/j.gerr.2024.100062.

Xie, S., Cheng, Z. and Wan, L., 2019. Hydration And Microstructure Of Astm Type I Cement Paste. *Science and Engineering of Composite Materials*, [e-journal] 26(1), pp.215–220. https://doi.org/10.1515/secm-2019-0004.

Xu, O., Han, S., Liu, Y. and Li, C., 2020. Experimental investigation surface abrasion resistance and surface frost resistance of concrete pavement incorporating fly ash and slag. *International Journal of Pavement Engineering*, [e-journal] pp.1–9. https://doi.org/10.1080/10298436.2020.1726348.

Yao, Z.T., Ji, X.S., Sarker, P.K., Tang, J.H., Ge, L.Q., Xia, M.S. and Xi, Y.Q., 2015. A comprehensive review on the applications of coal fly ash. *Earth-Science Reviews*, [e-journal] 141, pp.105–121. https://doi.org/10.1016/j.earscirev.2014.11.016.

Yousuf, A., Manzoor, S. O., & Youssouf, M., 2020. Fly ash: production and utilization in India-an overview. *Journal of Materials and Environmental Science*, [e-journal] 11(6), 911–921.

Yurdakul, E., Taylor, P.C., Ceylan, H. and Bektas, F., 2014. Effect of Water-to-Binder Ratio, Air Content, and Type of Cementitious Materials on Fresh and Hardened Properties of Binary and Ternary Blended Concrete. *Journal of Materials in Civil Engineering*, [e-journal] 26(6), p.04014002. https://doi.org/10.1061/(asce)mt.1943-5533.0000900.

Zemajtis, J.Z., 2018. *Role of Concrete Curing*. [online] Cement.org. Available at: https://www.cement.org/learn/concrete-technology/concrete-construction/curing-in-construction [Accessed 21 Jul. 2024].

Zhang, G., Zheng, H., Wei, X., Li, Z., Yan, Z. and Chen, X., 2024. Concrete mechanical properties and pore structure influenced by high permeability water pressure. *Developments in the Built Environment*, [e-journal] 17, pp.100385–100385. https://doi.org/10.1016/j.dibe.2024.100385.

Zhao, Z., Wang, Q., Zhao, J., Zhao, B., Ma, Z. and Zhang, C., 2021. Adhesion of Teeth. *Frontiers in Materials*, [e-journal] 7. https://doi.org/10.3389/fmats.2020.615225.